The PHILOSOPHICAL MAGAZINE

FIRST PUBLISHED IN 1798

1 Eighth Series No. 5 May 1956

A Journal of Theoretical Experimental and Applied Physics

PRICE 15s. 0d.
Annual Subscription £8 0s. 0d. payable in advance

ALERE FLAMMAM.
Printed and Published by
TAYLOR & FRANCIS LTD.
RED LION COURT, FLEET STREET, LONDON, E.C.4

CONTENTS OF No. 5.

**All communications for the Philosophical Magazine should be addressed, post-paid, to the Editors, c/o Messrs. Taylor and Francis, Ltd., Red Lion Court, Fleet Street, London, England.

XXXVII. *Isotopic Spin Selection Rules VII : Breakdown of the Rules and the Situation in* ^{16}O

By D. H. Wilkinson
Cavendish Laboratory, Cambridge†

[Received January 26, 1956]

Abstract

Factors governing the breakdown of the isotopic spin selection rules are discussed. Two energy ranges exist within which we expect the rules to be obeyed ; at low excitation individual excited states are well separated in energy and have good isotopic spin purity so that the rules are obeyed in reactions passing through such states only ; at high excitation individual states no longer have a well-defined isotopic spin but the rules are obeyed because many overlapping levels are simultaneously excited in a total state of initially well-defined isotopic spin which breaks up before the Coulomb forces have had time to cause much isotopic spin mixing. In between these regions where the rules are obeyed (although for very different reasons) severe breakdown is to be expected. The approximate extent of these reasons is discussed. The experimental situation as regards the operation of the rules and other consequences of charge independence is examined in ^{16}O where we have knowledge relating to the effective isotopic spin purity of ten energy levels or energy ranges between 6 and 30 MeV excitation. Good correspondence with theoretical expectation is found in the above-described general trend of effective impurity versus excitation. It is concluded that the situation is adequately described by the Coulomb perturbation of an otherwise charge independent (symmetric) Hamiltonian.

§ 1. Introduction

During the past few years a body of data has built up concerning the validity of the concept of isotopic spin as applied to the classification of states of light nuclei. Attention has focused on the one hand on the comparison in mass between members of isotopic spin multiplets (see paper VIII of this series) and on the other on the operation of the selection rules associated with the isotopic spin quantum number. The first type of study is of chief interest in attempting to get a measure of the charge-independence of nuclear forces, in particular the relationship between n–n and n–p forces. The effect of the Coulomb perturbation in disturbing

† Communicated by the Author.

the results to be expected under complete specifically nuclear charge independence is here a second order one : the first order effect is the mixing by the Coulomb forces of the isotopic spins of states of different primitive isotopic spin but of the same ordinary spin and parity ; this is followed by the ordinary configuration mixing of the components of the same isotopic spin in the various sets of states of different primitive isotopic spin with attendant displacement in energy in the usual way. We may therefore hope that the Coulomb perturbation will not interfere drastically with investigations of charge-independence through the comparison of multiplets. On the contrary in the study of the selection rules we see the relaxation of the rules as a first order consequence of the Coulomb perturbation which is consequently much easier to pick out.

We have in this series of papers been chiefly concerned with determining the degree to which the selection rules hold and with attempting to assess in each case whether or not the result was consistent with the expected effects of the perturbation of a completely charge-independent (symmetric) Hamiltonian by Coulomb forces alone. This is a difficult procedure because it is only for especially simple and usually experimentally inaccessible states that one can compute the isotopic spin mixing with any degree of confidence. The matrix element of the Coulomb perturbation between states of different primitive isotopic spin varies by more than a factor of ten from case to case so the theoretical relaxation of the selection rules which is proportional to the square of the mixing is often unsure to two orders of magnitude. However sufficient data are now becoming available in a few cases for us to begin to survey the situation as regards the relaxation of the rules—the isotopic spin impurity—over a wide range of excitation in a single nucleus and to see whether the general trend of impurity versus excitation that we observe is consistent with what we expect from the Coulomb perturbation.

In this paper we attempt such an examination of ^{16}O. Before we do this we discuss in general terms the way in which we might expect the breakdown of the selection rules to depend on energy of excitation.

§ 2. Effective Isotopic Spin Impurity

In discussing the degree to which we expect the isotopic spin selection rules to be obeyed we must distinguish two extreme classes of experimentation :

(i) Experiments in which *all* the states that are involved from the isotopic spin point of view, including those of the intermediate compound system, are *well-isolated and discrete.*

(ii) Experiments in which the states of the intermediate compound system whose isotopic spin is relevant to the selection rules are in the *continuum region of strongly overlapping levels.*

And of course we shall in practice be interested in all intermediate cases. We first discuss these extreme classes :

(i) In this class are experiments such as those on the forbidden emission of $E1$ radiation with which we have chiefly dealt in this series. We deal only with well-isolated levels and so are concerned only with essentially static descriptions of those states such as a unique spin and parity and a time-independent isotopic spin make-up. In such cases in order to assess the severity of the expected breakdown of the rules we ask for $\alpha_T(T')$, the relative amplitude of the state of isotopic spin T' that the Coulomb forces mix with our state of primitive isotopic spin T.† If the process which we study is forbidden for isotopic spin T and allowed for T' we then expect it to proceed at a rate of order $\alpha_T^2(T')$ of that which we should have anticipated but for the isotopic spin inhibition (more properly the breakdown will depend on the appropriate combination of the α's of the initial and final states between which the forbidden transition is made). Now $\alpha_T(T')=H^c_{TT'}/\Delta E_{TT'}$ where $\Delta E_{TT'}$ is the separation in energy of the state of T and those of T' of the same J, π whose mixing by H^c we consider (we sum over all states T'). Radicati (1953) and MacDonald (1954, 1955) have estimated H^c in several cases in light nuclei. The treatment of MacDonald is rather the more detailed and we now make our discussion chiefly in the light of his results. $\alpha_T(T')$ may be very roughly broken down into two parts, one associated with the isotopic spin impurity arising from excitation of the core and the other from the mixing of the valence nucleons either with other configurations or with other states of their own configuration or mixed configuration. In the first part H^c is large but so is ΔE and α^2 due to core excitation of 1s- or 1p-shell nuclei for example is about 2 to 4×10^{-3}. In the second part, when the contaminated state belongs to a pure configuration, the only case that MacDonald considers, H^c is rather small as a rule, typically 0·1 MeV or less. Larger values up to nearly 1 MeV are to be found but only between states in which one of the particles changes its total quantum number without changing its orbital quantum number and such states are expected to be separated by 10–30 MeV so the large H^c does not bring a large α^2. For the more usual cases we may take $H^c=0{\cdot}1$ MeV as a fairly safe upper limit although of course here ΔE may perhaps be very small. We should also consider contamination arising in mixed configurations of valence nucleons. It seems that here we may expect both H^c to be large and ΔE perhaps to be small on occasion. It is well known (e.g. Lane 1954) that the interaction of an s- or d-wave nucleon with p-shell nuclei tends to be weak, giving rise to states whose parentage description in respect of that nucleon is rather simple. When, say, an s-wave nucleon interacts with the p-shell nucleus

---

† The $E1$ selection rule may also be violated by virtue of higher-order terms in the $E1$ Hamiltonian (Gell-Mann and Telegdi 1953) or of the inadequacy of the assumption that the charge resides on the protons–mesonic effects (Morpurgo 1954). Both these effects are small and are negligible for the following discussions.

(ground or excited state) J, π, T we may expect them to form the closely-related states $J \pm \frac{1}{2}, \pi, T \pm \frac{1}{2}$ with not very great separation which are able strongly to contaminate one another.†

So for the experiments of class (i) we should not expect to find the isotopic spin selection rules affording factors of discouragement greater than 500 or so since we always have an impurity of order 2 to 4×10^{-3} from core excitation. When states of the same J, π and different T approach within 500 kev or so of each other we must anticipate that valence nucleon contamination with $H^c \sim 0{\cdot}1$ Mev may have taken over. Indeed at considerably greater spacing contamination of the mixed configuration type last discussed may have become considerable; by the time $\Delta E = 1$ Mev has been reached the mixing may be almost complete and isotopic spin may have largely lost its meaning as a label for this state. This appears to have happened for ^{10}B at 6·88 Mev (Wilkinson and Clegg 1956). It will probably start happening for light ($A \leqslant 20$) 4n+2-type nuclei at an excitation of 6 to 10 Mev, for light 4n-type nuclei at 14 to 22 Mev and at 11 to 17 Mev for light nuclei of odd mass.

(ii) In this second class are experiments of the (d, d′), (d, α) and other types in which, although the initial and final states are well isolated and so receive descriptions of the time-independent type discussed above, the intermediate state may be at an excitation of perhaps 30 or 40 Mev in the continuum region of strongly overlapping levels. It was in such types of experiments as this that the applicability of the isotopic spin rules (straightforward conservation between initial and final states) was first established. However, at the high excitations of the intermediate state through which the reaction must pass and through which isotopic spin must be conserved, the considerations of (i) above would lead us to suppose that the mixing of isotopic spins of individual states should be so complete that isotopic spin should no longer have any significance. Why then is it that the simple conservation rules seem to work under these conditions? The answer is that we are no longer dealing, as in (i), with single states in the intermediate compound system but with the simultaneous excitation of a great number of overlapping states of comparable amplitude. The correct picture is therefore no longer a time-independent one but one that involves the changing phase relationships between the many excited states. In particular the total state of the compound system as originally formed will approximate itself as closely as possible to the isotopic spin of the initial system. This is possible, despite the fact that the time-independent description of each individual state contains a mixture of several isotopic spins in comparable proportions, because we simultaneously excite many such states and a suitable choice of their phase relationships can result in an initially

† Although it seems reasonable that large values of H^c should be generated in this way they have not yet been found by direct calculation (J. P. Elliott—private communication).

more or less well-defined isotopic spin for the total state. The Coulomb forces perturb this total state and cause the growth of the other isotopic spins with a characteristic time of order $\hbar/H^c$. If they had an indefinite time in which to act they would cause complete mixing and the system would forget the isotopic spin of the initial system from which it was made up. The final break-up would then lead to states violating the simple isotopic spin conservation rules as readily as to those obeying the rule. However, an indefinite time is not available and the underlying individual states have a finite width Γ which may be several MEV at the excitations we now discuss, so the break-up occurs with a characteristic time of order $\hbar/\Gamma$. If now $\Gamma \gg H^c$ the system breaks up before the Coulomb forces have had time to cause forgetting of the isotopic spin of the initial system and the conservation rules are obeyed. The degree to which they are obeyed will now be determined by H^c/Γ rather than by $H^c/\Delta E$.† So as we tend to higher and higher excitation the selection rules should be better and better obeyed as Γ becomes bigger and bigger and more and more overlapping states are involved. A similar argument applies to reactions whose mechanisms are referred to as ' direct ' : again it is the short time scale that enables the conservation to hold. This class (ii) situation is characterized by a smooth excitation function with no clear remaining resonance structure. It will probably have set in by about 14–18 MEV in light 4n+2-nuclei, by 22–30 MEV in light 4n-nuclei and by 15–25 MEV in light nuclei of odd mass.

Between these two extremes, at intermediate excitations, we shall find situations where levels are dense and overlapping but where a sufficiently large number is not yet involved for the considerations of class (ii) to apply. Here we should expect to find severe breakdown of the selection rules. This intermediate situation will be characterized by an excitation function which although it is not one of well-separated resonances yet retains some bumps telling of traces of single level structure ; the total state is one of many overlapping levels but not of such a mixture that a few do not retain some individual importance ; we do not yet excite so great a mass that we can arrange for the intermediate compound state to start off closely approximating the isotopic spin conditions of the initial system.

At low excitation (class (i)), the operation of the selection rules is characterized by α^2 the isotopic spin impurity of the individual states concerned. At high excitation (class (ii)) we have seen that the operation of selection rules is no longer determined by the properties of individual states, all of which are very impure, but rather by the properties of the assembly of overlapping states and by the way in which it is excited. We can still define an effective isotopic spin impurity α_{eff}^2 as the reciprocal

† This is a rather picturesque way of describing the situation. A proper treatment would not split up the process into ' contamination ' and ' decay ' but treat them together—with the same result.

of the factor by which the forbidden transition is inhibited remembering that it has nothing to do with α^2 of the individual states at that excitation but that it depends on many states and also on the way in which the assembly is excited.

In general terms then we expect the operation of the selection rules to get worse with increasing excitation as α^2 increases, to pass through a region of more or less complete breakdown with values of α^2 ranging up to unity and finally to get better again as α_{eff}^2 takes over from α^2 in the continuum region.

§ 3. States of ^{16}O

We have no direct information relating to the isotopic spin purity of the ground state of ^{16}O and for purposes of discussion of transitions involving it we adopt the theoretical figure of MacDonald, namely $\alpha_0^2(1) \sim 4 \times 10^{-3}$.

We now take the states in turn about which we have information relating to the purity of their isotopic spin and follow them with a discussion of the regions for which we can say something about α_{eff}^2.

(i) 6·14 *and* 6·91 Mev

The observed mode of decay of the 6·91 Mev $2+T=0$ state† is by $E2$ radiation to the ground state rather than by $E1$ radiation to the 6·14 Mev $3-T=0$ state. The systematics of gamma-ray transitions in light nuclei (Wilkinson 1953 a, 1955 a) suggest $|M|^2=0{\cdot}032$ in Weisskopf units as the most probable *a priori* strength to expect for $E1$ transitions that do not violate the isotopic spin selection rule.‡ If we take $|M|^2=1$ for the competing $E2$ transition§ we should then have expected the relative strengths of the $E1$ and $E2$ transitions to have been 0·13 : 1 but for the violation of the isotopic spin selection rules. In (I) of this series Wilkinson and Jones (1953) reported that in fact this ratio is

† For the general assignments see Ajzenberg and Lauritsen (1955).

‡ It is observed that 85% of all allowed $E1$ transitions in light nuclei have speeds within a factor of 7 of $|M|^2=0{\cdot}032$. We shall use this figure when we wish to guess uninhibited transition strengths. Its reliability is then presumably rather better than an order of magnitude.

§ There is little to guide us in guessing the strengths of $E2$ transitions Several examples of $|M|^2>1$ are known in light nuclei but so are some considerably lower values. It is unlikely that this particular $E2$ transition is very considerably enhanced since a very strong $E2$ transition, representing most of the available collective strength from the ground state, is known to the 14·7 Mev state (Wilkinson 1955 b). On the other hand Devons *et al.* (1955) have shown that the $E2$ lifetime is less than $1{\cdot}2 \times 10^{-14}$ seconds or $|M|^2>0{\cdot}5$. An upper limit is provided by the appropriate sum rule relating to $E2$ transitions that do not change the isotopic spin (Gell-Mann and Telegdi 1953). This limit is $|M|^2 \sim 10$ for this transition but is unlikely to be approached for the reasons just given. It therefore seems that $|M|^2=1$ is probably not too bad a guess.

$<5\times10^{-3}:1$. Since then the 770 kev $E1$ transition has been sought by an independent (coincidence) method by the writer and Dr. B. J. Toppel at Brookhaven National Laboratory. This work confirms the earlier result and shows that the ratio is $<2\times10^{-3}:1$. We therefore conclude, within the limits given by the uncertainty of our guesses about uninhibited widths, that the isotopic spin rule is imposing an inhibition factor of at least 65 on this transition and so $\alpha_0^2(1)$ for both of these levels is $<0{\cdot}015$.

(ii) 7·12 MEV

Devons, Manning and Bunbury (1955) report that the lifetime of the $1-T=0$ level for E_1 transition to the ground state is less than 8×10^{-15} seconds. This means $|M|^2>2{\cdot}3\times10^{-4}$. Since the ground state $T=1$ impurity alone would produce $|M|^2\sim10^{-4}$ we conclude that probably for the excited state $\alpha_0^2(1)>4\times10^{-3}$ (neglecting interference effects).

(iii) 8·87 MEV

This $2-T=0$ state was observed by Toppel, Wilkinson and Alburger (1955) to decay to the $2+T=0$ state at 6·91 MEV with about one-third the intensity of its decay to the $1-T=0$ state at 7·12 MEV. This would appear to suggest the high $T=1$ impurity for the 2− state of $\alpha_0^2(1)\sim0{\cdot}03$† or a little less if allowance has to be made for the impurity of the 6·91 MEV state—see (i) above. However, it was also observed indirectly that the $M1$ competing transition is very probably rather slow and it was concluded that in fact this forbidden $E1$ transition is more probably inhibited by a factor of about 900 (see Toppel *et al.* 1955 for the detailed argument). So we say $10^{-3}<\alpha_0^2(1)<0{\cdot}03$ with the lower figure favoured.

(iv) 12·95 MEV

This 2− state is probably the first $T=1$ state of ^{16}O (see VIII of this series). However it decays by alpha-particle emission to the 2+ 4·43 MEV $T=0$ state of ^{12}C with a reduced width of 4·2% (alternatively 11·2%) of the single-particle value.‡ Although the single-particle value is not an absolute upper limit it has never been surpassed with certainty. It is of course practically the same as the Wigner sum-rule limit. An alpha-particle reduced width of 4% is quite a large one even for an allowed transition; we can therefore say $\alpha_1^2(0)>0{\cdot}04$ with the likelihood that it may be considerably larger. The 2− $T=0$ state at 12·51 MEV resembles this present one in having a very large reduced width for d-wave proton emission to the ground state of ^{15}N (75% of the

† In making this estimate we use the result from the systematics that the most probable $|M|^2$ value for $M1$ transition in light nuclei is about 0·15 (an uncertainty of roughly an order of magnitude either way covering most of the transitions).

‡ We use $a=1{\cdot}45(A_1^{1/3}+A_2^{1/3})\times10^{-13}$ cm, a recipe found suitable for the analysis of alpha-particle scattering by ^{12}C (Hill 1953).

single-particle value against 45% for the present state). It is therefore possible that these two states are the 2− $T=0$ and 1 linkages of a $1d_{5/2}$ proton to the ground state of ^{15}N as unique parent. They would then contaminate each other rather effectively in the manner discussed in § 2 for mixed configurations. In this case our alpha-particle emission from the $T=1$ state is due to the admixture of the $T=0$ character from the other, whose reduced alpha-particle width is 80% of the single-particle value. If this interpretation is correct we obtain the value $\alpha_1^2(0)\sim 0{\cdot}05$ for the present state ; in case it is not correct we must continue to use 0·04 as a lower limit.

(v) 13·05 MeV

This 1− state behaves like $T=1$ in that its $E1$ transition to the ground state shows $|M|^2\sim 0{\cdot}1$, a large value. But it also decays by alpha-particle emission to the 0+ ground state and 2+ 4·43 MeV state of ^{12}C, both $T=0$, with reduced widths of 2·8 and 5·5% (alternatively 5·6 and 11·0%) of the single-particle value respectively. So we say $\alpha_1^2(0)>0{\cdot}05$ with the probability that this is a low figure. The $E1$ radiative width for the ground state transition is 150 ev (Schardt, Fowler and Lauritsen 1952). The large s-wave reduced proton width to the ground state of ^{15}N agrees well with that theoretically expected if the ground state is the unique parent. In this case we can with some confidence compute the expected radiative width in either extreme coupling scheme under the assumption of charge independence (a pure $T=1$ state). We find theoretical widths of 150 ev in LS coupling and 50 ev in jj coupling. The good agreement with experiment found in LS coupling which is expected to be the better approximation suggests that in fact the $T=0$ contamination cannot be complete. $\alpha_1^2(0)=0{\cdot}5$† would reduce the theoretical radiative width to about 100 ev or less which begins to conflict with experiment. We therefore say $0{\cdot}06<\alpha_1^2(0)<0{\cdot}5$. The relevant spin and parity assignments have been made earlier (see Wilkinson 1953 b) ; since then the work of Kraus (1954) has confirmed them.

(vi) 16–19 MeV

In this region resonance structure has been observed and measured in the reaction $^{16}O(\gamma, n)^{15}O$ by Katz, Haslam, Horsley, Cameron and Montalbetti (1954) and by B. M. Spicer and A. Penfold (unpublished work at the University of Illinois—see also Ajzenberg and Lauritsen 1955). Resonance structure in the same region has been observed in $^{16}O(\gamma, p)^{15}N$ by Johansson and Forkman (1955). This region of excitation is low enough to make it very likely that only the ground state of ^{15}N is involved in the (γ, p) reaction and only the ground state of ^{15}O is energetically accessible in the (γ, n) reaction. If the isotopic spin is well defined we

† Such large values of α^2 are of course no longer relevant to any perturbation expansion but merely indicate relative intensities for the components of different isotopic spin.

then expect the neutron and proton yields to bear calculable ratios to each other; these ratios do not depend critically on the (unknown) multipolarity and type of transition. In general the (γ, p) resonances are found at the same positions as the (γ, n) and there is also a quite good general correspondence between the experimental relative intensities and those expected under charge independence. This leads to the conclusion that in this region isotopic spin is a fairly good quantum number. If we take α^2 as a measure of the fractional deviation from the expected intensity ratios we say $\alpha^2 < 0{\cdot}3$. This figure is obtained by clumping the observations in units of 1 MeV. If we compare individual transitions some deviations from expectation are apparent that would lead us to say $\alpha^2 > 0{\cdot}1$ or more for some levels but the statistical accuracy is very low and there are discrepancies between the various measurements of the level strengths in the (γ, n) process used for the comparison so we do not feel safe in concluding that even this small amount of impurity is definitely established.

(vii) 20–23 MeV

This is the region of the 'giant resonance' seen in $^{16}O(\gamma, n)^{15}O$ at 22·2 MeV and $^{16}O(\gamma, p)^{15}N$ at 22·3 MeV. The structure of these resonances has been investigated by Katz *et al.* and by Spicer and Penfold in the first reaction, and by Stephens, Mann, Patton and Winhold (1955) in the second. There is good general agreement as to position and gross features of the resonance seen in the two reactions and this we should expect whether the isotopic spin were well-defined or not. There appear, however, to be some features not consistent with well-defined $T=1$ (the resonance is $E1$). For example, the ratio of the integrated cross sections in the ranges 21–22 MeV and 20–21 MeV is about 1 : 1 for (γ, n) and 2·5 : 1 for (γ, p). (Since the binding energy of a neutron in ^{16}O is 16·0 MeV and the first excited state of ^{15}O is at 5·27 MeV we can ignore transitions to all but the ground state of ^{15}O in the giant resonance region.) The figures given above for (γ, p) refer to emission to the ground state of ^{15}N only. Again the integrated cross section to the peak of the resonance in (γ, n) is about 20 MeV-mb whereas in (γ, p) it is only about 14 Mev-mb (again to the ground state only). This is despite the fact that the proton energies are well above the Coulomb barrier and nearly 4 MeV more energy is available to the protons than to the neutrons; this would lead us to expect roughly 30% more protons than neutrons. On the basis of these observations we should suppose that the requirements of charge-independence were no longer being fulfilled even though no actual selection rule was being broken. This degree of difference of behaviour for neutrons and protons would seem to imply at least $\alpha_1^2(0) > 0{\cdot}1$.

We must also consider, however, the behaviour of the (γ, α) and allied reactions in this region. These have been analysed by Gell-Mann and Telegdi (1953) and by Hsiao and Telegdi (1953) as suggesting that the

$E1$ cross section for $^{16}O(\gamma, \alpha)^{12}C$ is suppressed in the region of the giant resonance because the resonance state is of $T=1$ while a $T=1$ state in ^{12}C is not yet energetically available (allowance being made for the Coulomb barrier). $T=1$ states in ^{12}C become available above $E_\gamma \sim 25$ MeV. Above this energy the cross section for (γ, α) remains at more or less the same level as in the giant resonance region and transitions are made chiefly to the $T=1$ region in ^{12}C. It has been supposed that this indicates a considerable degree of isotopic spin purity in the giant resonance region around 22 MeV since if the total absorption cross section were dropping rapidly from the resonance peak as we move to higher energies the constancy of the (γ, α) cross section would indicate that mechanisms suppressed in the giant resonance region ($E1$ absorptions) were coming into play above the effective threshold for transition to $T=1$ states in ^{12}C. However, we do not believe that this inference can necessarily be made since in fact the total absorption cross section at $E_\gamma = 25$ MeV seems to be fully a third of its peak value according to Stephens *et al.* (compare the 'long tails' observed in $^{12}C(\gamma, n)^{11}C$ and $^{16}O(\gamma, n)^{15}O$ by Sagane (1951) and in more detail by Barber, George and Reagan (1955) in $^{12}C(\gamma, n)^{11}C$). The cross section for $^{16}O(\gamma, 4\alpha)$ has also fallen somewhat from 22·6 MeV (where it too has a resonance) to 25 MeV (Goward and Wilkins 1952) and so it has not changed its form dramatically relative to the total absorption cross section. Indeed the very rapid rise in the $^{16}O(\gamma, 4\alpha)$ cross section above 20 MeV which coincides with the rapid rise in the total cross section and the coincidence of its strongest resonance with the giant resonance suggest that in fact $E1$ absorption is taking place for the (γ, α) processes in the giant resonance region and that $E2$, $M1$ and other mechanisms are relatively unimportant there. We therefore believe that the evidence from the (γ, α) reactions is quite consistent with our conclusion that in the giant resonance region there is considerable isotopic spin impurity. On the other hand if we go to somewhat higher energies ($E_\gamma > 30$ MeV) the (γ, α) processes have increased by a factor of 4 or 5 in strength relative to the (γ, n) and this suggests that they are here enjoying some freedom denied them at the lower excitation where therefore $\alpha^2 = 1$ is presumably not attained. It seems then that all evidence is consistent with a value of $\alpha_1^2(0)$ of about 0·1–0·5 in the giant resonance region.

(viii) 25–35 MeV

Above 25 MeV we continue the argument based on the $^{16}O(\gamma, \alpha)^{12}C$ reaction. Hsiao and Telegdi find that here the mechanism is one that appears to imply a fair degree of effective purity to the isotopic spin states. This they see because transitions to a ($T=0$) state in ^{12}C at about 13 MeV which were strongly favoured at lower energies give place to transitions chiefly (by a factor of 5 or more) to the $T=1$ region of ^{12}C around 16 MeV. This then suggests $\alpha^2(0)_{\text{eff}} < 0{\cdot}1$ in this region. Consistent with this improvement in effective isotopic spin purity that has taken

place above the giant resonance region is our observation in (vi) above on the trends of relative (γ, α) and total absorption cross sections.

(ix) 26·8 MeV

This is the energy of the compound system when the first $T=1$ state of ^{14}N at 2·31 MeV fails to show up in ^{14}N(d, d′)^{14}N at $E_d=6{\cdot}98$ MeV (Bockelman, Browne, Buechner and Sperduto 1953). The $T=1$ state is excited at least 20 times less strongly than the $T=0$ state at 3·95 MeV so we say for the highly excited ^{16}O state $\alpha_0^2(1)_{\text{eff}}<0{\cdot}05$. We must note in caution, however, that although this $T=1$ state is strongly excited in ^{14}N(p, p′)^{14}N at $E_p=6{\cdot}92$ MeV—half as strongly as the 3·95 MeV state (Bockelman *et al.*)—it is only weakly excited at $E_p=9{\cdot}6$ MeV (Freemantle, Gibson, Prowse and Rotblat 1953).

§ 4. Discussion

We will first of all decide in the light of § 2 what values of α^2 or α_{eff}^2 we should expect in this range of excitation in ^{16}O. Before levels begin to overlap very strongly we have three types of contamination to consider :

(i) that due to core impurity ;

(ii) that due to mixing of valence nucleon states when the contaminated state is of a pure configuration ;

(iii) as (ii) when the contaminated state is not of a pure configuration.

Type (i) contamination persists throughout and may be presumed to lie between 10^{-3} and 10^{-2}. Type (ii) contamination we also find everywhere and it may be dominant when we are remote from the rather special levels which may have very heavy contamination of type (iii). But in the present case there is no type (ii) contamination proper because ^{16}O is a closed-shell nucleus. However we may anticipate that type (iii) contamination will also show two forms : the first belongs to the special states of unique parentage discussed in § 2 where H^c may be large ; the second belongs to the everyday states with complicated parentage relationships where smaller values of H^c similar to those of type (ii) contamination will be found.

The first $T=1$ state in ^{16}O is probably that at 12·95 MeV so until we approach within a few times H^c of this energy the impurity will remain at the type (i) level of 10^{-3} to 10^{-2}. We must then expect that type (iii) configuration may make itself felt above about 9 MeV since it is long range. For example the $2-$ $T=0$ state at 8·87 MeV may be contaminated by the $2-$ first $T=1$ state at 12·95 MeV. In fact we know that these two states are quite closely related because ^{16}N shows an allowed beta-transition of $\log ft=4{\cdot}4$ to the 8·87 MeV state (Toppel *et al.* 1955) and so H^c may well be quite large. So above an energy of 9 MeV or so

α^2 may begin to rise rather sharply and reach a value of order unity by about 12 Mev (complete isotopic spin mixing). On the low side we anticipate a rise due to the ' type (ii) ' aspect of type (iii) contamination. At 13 Mev states of the same spin and parity are separated by about 1 Mev. Taking $H^c \sim 0{\cdot}05$ Mev as a reasonable lowish figure for this type of mixing we see that we may anticipate $\alpha^2 \sim 3$ or 4×10^{-3} at 13 Mev due to this mixing and core impurity combined. As the excitation increases above the onset of $T=1$ states the level spacing diminishes until at 22 Mev it is down to about 200 kev or less with a corresponding lower limit to likely α^2 values of about 0·05.

At about 22 Mev, although some levels are still sharp, broad levels are common and we approach the region of complete overlap where α^2 is replaced by $\alpha_{\text{eff}}{}^2$ as we discussed in § 2. By the time an energy of 30 Mev is reached it seems likely that good overlap will be taking place with $\Gamma \sim 1$ Mev or more. The larger values for H^c are no longer relevant since we deal with the properties of the large numbers of levels into which single-particle motions will now be broken. On the other hand the smallest values of H^c need no longer be considered since their effects will be swamped by the stronger perturbations. $H^c \sim 0{\cdot}1$ Mev now seems a reasonable value giving $\alpha_{\text{eff}}{}^2 \sim 0{\cdot}01$. The upper and lower limits will converge as the excitation energy increases and we tend to a completely statistical description (which will, however, depend on the mechanism of excitation).

We can now compare these theoretical expectations with the results of experiment summarized in § 3. On the figure we display as the two full lines the theoretical rough upper and lower limits to the effective isotopic spin impurity that we have just derived following § 2. We also show the experimental results. The meanings of the various ways of entering the results will be clear from the discussion in § 3. The three lowest energy entries are ' limits ' (within the uncertainties involved in guessing the uninhibited radiative widths). The next entry, at 8·87 Mev, has an upper limit (in the same sense) but we have evidence that the true impurity is much lower so we enter the point at the low value and indicate by the downwards pointing arrow that we attach more weight to the location of the point than to the upper limit. The next entry has a fairly strict though not inviolable lower limit given by the single-particle value and which we indicate, but we enter the point at the value suggested by the identification of the contaminating state as that at 12·51 Mev, and indicate by the broken arrow that we think this identification a likely one (i.e. that we probably have here an actual value for α^2 rather than a limit only). For the next entry we have a fairly firm lower limit at which we place the point, indicating by the upwards pointing arrow that the impurity could run as high as shown but probably not all the way to $\alpha^2=1$. The next entry is at 16–19 Mev and is an upper limit, a lower limit being shown dashed because we do not regard it as well established. The next entry has both upper and lower limits that

seem equally well established so we place the point midway between them. The entries at 27 MEV and 25–35 MEV are again upper limits only.

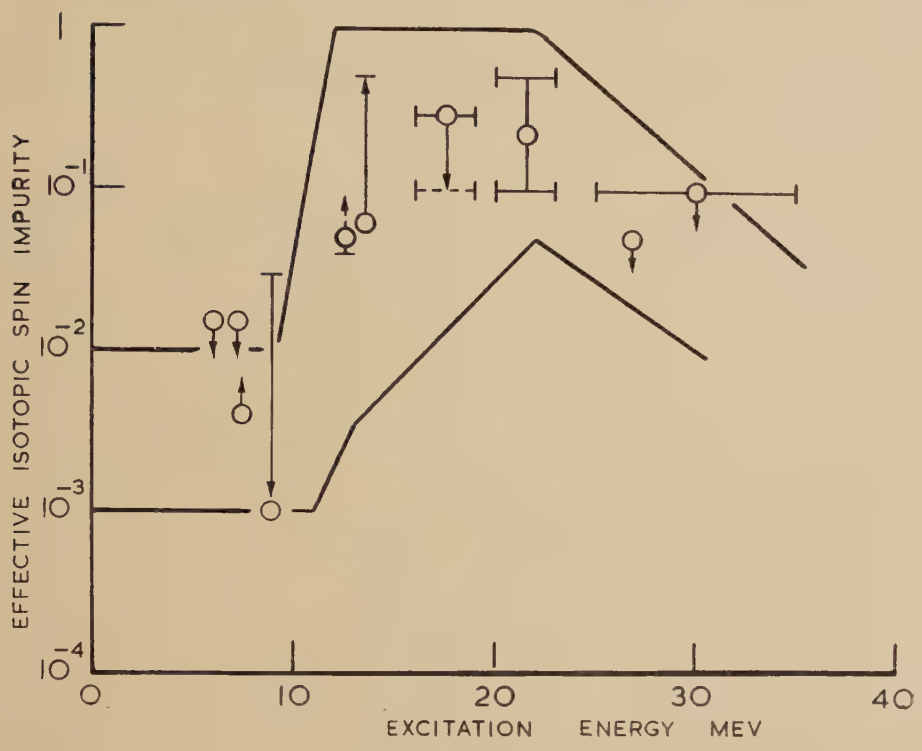

The theoretical and experimental isotopic spin impurities in ^{16}O as a function of excitation. The two full lines are the upper and lower limits theoretically expected for the impurity (defined as α^2 or α_{eff}^2 as is appropriate). The experimental points have the significance discussed in the text. Those around 7 MEV and 13 MEV have been shifted sideways a little to avoid overlapping.

Although the theoretical estimates and the extractions of the impurity from the experimental data are both admittedly rough it is clear from the figure that there is a very good agreement in general terms between the two. In particular we see in the experimental situation the expected high purity at low excitation followed by very substantial impurity at medium excitation and then by a return to a good effective purity at high excitation (for very different reasons) as α_{eff}^2 takes over from α^2.

§ 5. Conclusion

We conclude that the isotopic spin properties of ^{16}O over a wide range of energy show considerable changes with excitation but are in good agreement with theoretical expectation based on the Coulomb perturbation of an otherwise charge-independent (symmetric) Hamiltonian.

Acknowledgments

I should like to thank Dr. B. J. Toppel for his participation in the measurement described in § 3 (i). The discussion in § 2 of the operation of the selection rules in class (ii) experiments has benefited from conversations with many people particularly Dr. A. M. Lane, Dr. J. Weneser, Professor D. C. Peaslee and Professor R. F. Christy. To all these gentlemen I am pleasurably indebted.

References

Ajzenberg, F., and Lauritsen, T., 1955, *Rev. Mod. Phys.*, **27**, 77.
Barber, W. C., George, W. D., and Reagan, D. D., 1955, *Phys. Rev.*, **98**, 73.
Bockelman, C. K., Browne, C. P., Buechner, W. W., and Sperduto, A., 1953, *Phys. Rev.*, **92**, 665.
Devons, S., Manning, G., and Bunbury, D. St. P., 1955, *Proc. Phys. Soc.* A, **68**, 18.
Freemantle, R. G., Gibson, W. M., Prowse, D. J., and Rotblat, J., 1953, *Phys. Rev.*, **92**, 1268.
Gell-Mann, M., and Telegdi, V. L., 1953, *Phys. Rev.*, **91**, 169.
Goward, F. K., and Wilkins, J. J., 1952, *Proc. Phys. Soc.* A, **65**, 671.
Hill, R. W., 1953, *Phys. Rev.*, **90**, 845.
Hsiao, C. A., and Telegdi, V. L., 1953, *Phys. Rev.*, **90**, 494.
Johansson, S. A. E., and Forkman, B., 1955, *Phys. Rev.*, **99**, 1031.
Katz, L., Haslam, R. N. H., Horsley, R. J., Cameron, A. G. W., and Montalbetti, R., 1954, *Phys. Rev.*, **95**, 464.
Kraus, A. A., 1954, *Phys. Rev.*, **94**, 975.
Lane, A. M., 1954, *A.E.R.E., Document* T/R 1289.
MacDonald, W. M., 1954, *Thesis*, Princeton ; 1955, *Phys. Rev.*, **100**, 51.
Morpurgo, G., 1954, *Nuovo Cim.*, **12**, 60.
Radicati, L. A., 1953, *Proc. Phys. Soc.* A, **66**, 139 ; 1954, *Ibid.* A, **67**, 39.
Sagane, R., 1951, *Phys. Rev.*, **84**, 587.
Schardt, A., Fowler, W. A., and Lauritsen, C. C., 1952, *Phys. Rev.*, **86**, 527.
Stephens, W. E., Mann, A. K., Patton, B. J., and Winhold, E. J., 1955, *Phys. Rev.*, **98**, 839.
Toppel, B. J., Wilkinson, D. H., and Alburger, D. E., 1955, *Phys. Rev.*, **99**, 632 (and in press).
Wilkinson, D. H., 1953 a, *Phil. Mag.*, **44**, 450 ; 1953 b, *Phys. Rev.*, **90**, 721 ; 1955 a, *Phil. Mag.* (in press), *A.E.C.L. Chalk River Document* PD-260 ; 1955 b, *Phys. Rev.*, **99**, 1347.
Wilkinson, D. H., and Clegg, A. B., 1956, *Phil. Mag.* (in press).
Wilkinson, D. H., and Jones, G. A., 1953, *Phil. Mag.*, **44**, 542.

XXXVIII. *Diffusion of the Chloride Ion in* NaCl

By D. Patterson,† G. S. Rose,† and J. A. Morrison
Division of Pure Chemistry, National Research Laboratories, Ottawa, Canada

[Received July 27, 1955]

The rate of diffusion of ^{24}Na in NaCl has been measured (Mapother, Crooks and Maurer 1950) by evaporating a film of $^{24}NaCl$ on to the surface of a crystal of NaCl and subsequently determining the concentration of ^{24}Na as a function of the distance from the surface. Two diffusion processes have been found—diffusion by vacancies created thermally at higher temperatures (intrinsic range) and by vacancies produced by positive divalent impurities at lower temperatures (structure sensitive range). Some problems of interpretation raised by the experiments have been discussed by the above authors and by Seitz (1954). The study of the diffusion of the chloride ion using the same technique with the isotope ^{36}Cl (Chemla 1952) has been limited to temperatures exceeding 650°c by the low mobility of the chloride ion. The present note describes a different tracer method which allows diffusion of the chloride ion to be studied at much lower temperatures. Preliminary results for the diffusion coefficient and activation energy of chloride ion diffusion at 510°c and below are compared with data from the above mentioned papers.

The method is based on the observation that a rapid isotopic exchange takes place between chlorine gas and the surface of small NaCl particles (specific surface ≈ 30 m^2/gm) even at room temperature. A similar observation on the exchange between HCl and KCl was reported by Clusius and Haimerl (1942). It is unlikely that chlorine will dissolve in NaCl at temperatures considered here (Mollwo 1937). Therefore, if particles of NaCl of any size containing ^{36}Cl are surrounded by non-radioactive chlorine gas, the ^{36}Cl diffuses to the surface and appears in the gas due to the rapid exchange. Assuming that the concentration of ^{36}Cl at the surface is zero (i.e. that the rate of exchange is rapid compared with the rate of diffusion) and that the particles are semi-infinite, the number of ^{36}Cl atoms in the gas at time t is given by

$$N(t)=2AC_0\sqrt{(Dt/\pi)} \text{ (Carslaw and Jaeger 1947)} \quad . \quad . \quad (1)$$

where A is the area exposed to the chlorine, C_0 is the original number of ^{36}Cl atoms/cm^3 in the NaCl and the diffusion coefficient $D=D_0\exp(-E/kT)$. The condition that $C=0$ at the surface is only strictly true when the number of chlorine atoms in the gas is very large compared with that in the solid. For small amounts of exchange both conditions required by (1) are fulfilled experimentally. For large amounts

† National Research Laboratories Postdoctorate Research Fellow.

(or small ratios of gas to solid) an appropriate treatment can be given following the method of March and Weaver (1928).

If a portion of the gas is scanned by a Geiger counter, a counting rate R proportional to N is observed. The following 'calibration' makes it unnecessary to know explicitly the counter efficiency, the actual volume of gas scanned by the counter, or C_0. HCl, prepared from a known mass m of NaCl containing a concentration C_0 of ^{36}Cl, is condensed into the system where it produces a counting rate R_0. It may then be seen using (1) that the counting rate R is given by

$$R=2\left(\frac{\rho R_0}{m}\right)A\sqrt{\left(\frac{Dt}{\pi}\right)} \quad . \quad . \quad . \quad . \quad . \quad . \quad . \quad (2)$$

where ρ is the density of the NaCl. Obviously the calibration requires a quantitative separation of the HCl. The method used—treatment of NaCl with concentrated H_2SO_4—gave consistent yields of HCl in excess of 98%.

The apparatus used for the exchange experiments requires only a brief description. The detailed results given below were obtained for NaCl (Merck reagent grade) which had been fused in a platinum crucible and to which had been added a small amount of NaCl containing the radioisotope ^{36}Cl. Samples for the diffusion experiments (approximately 0·2 gm each) consisting of pieces about 0·2 mm in dimension were sealed in a Pyrex apparatus with about 50 cm^3 s.t.p. of chlorine which had been twice distilled from trap to trap. Before sealing, the apparatus was evacuated to a pressure of 1×10^{-6} mm Hg. A part of the sealed system was the jacketed volume of a Geiger counter and the chlorine was circulated through this volume by convection. The level of activity was read from a counting rate meter connected to a chart recorder. The NaCl samples were contained in a Pyrex bucket in a part of the apparatus which could be heated by an external furnace. Temperatures were determined with a chrome–alumel thermocouple placed on the wall of the part of the apparatus inside the furnace.

The results are given in figs. 1 and 2. In one experiment (fig. 1) the NaCl was held successively at 358°, 435° and 495° and in the second (fig. 2) at 467° and 510°. R^2 has been plotted against t for both sets of results and the linear relation required by eqn. (2) has been found although C and D both show a break after 10 to 15 hours.

The logarithm of the various slopes is plotted against the reciprocal of the absolute temperature in fig. 3. It is evident that the initial reaction at all temperatures is the same and the activation energy E derived from the slope of the solid line is 1·67±0·05 ev. Within the experimental uncertainty the later stages of C and D give the same activation energy (dashed line of fig. 3). It must be concluded, therefore, that a different diffusion process such as diffusion down grain boundaries is not proceeding here, but rather a slight change of D_0 has taken place. Various physical explanations of the break have been considered, viz. lack of

Fig. 1

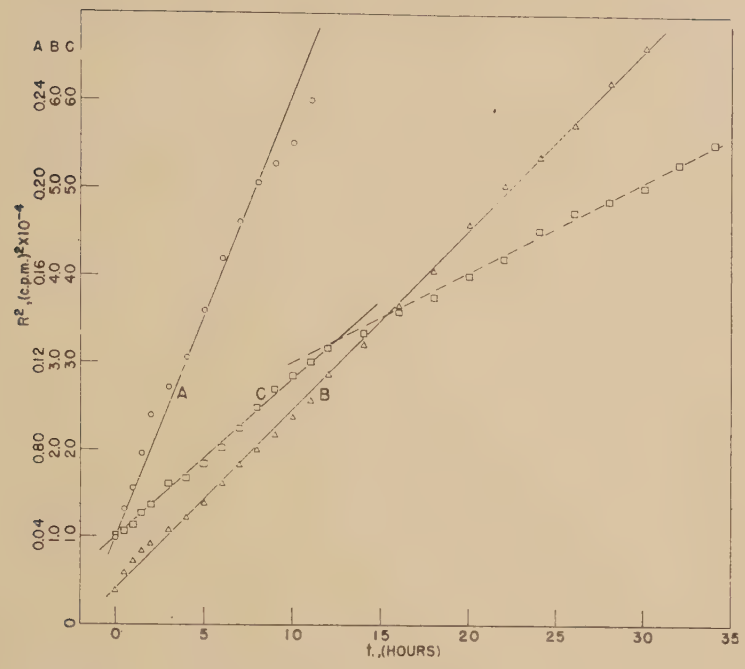

The diffusion of ^{36}Cl out of NaCl at 358°c(A), 435°c(B) and 495°c(C).

Fig. 2

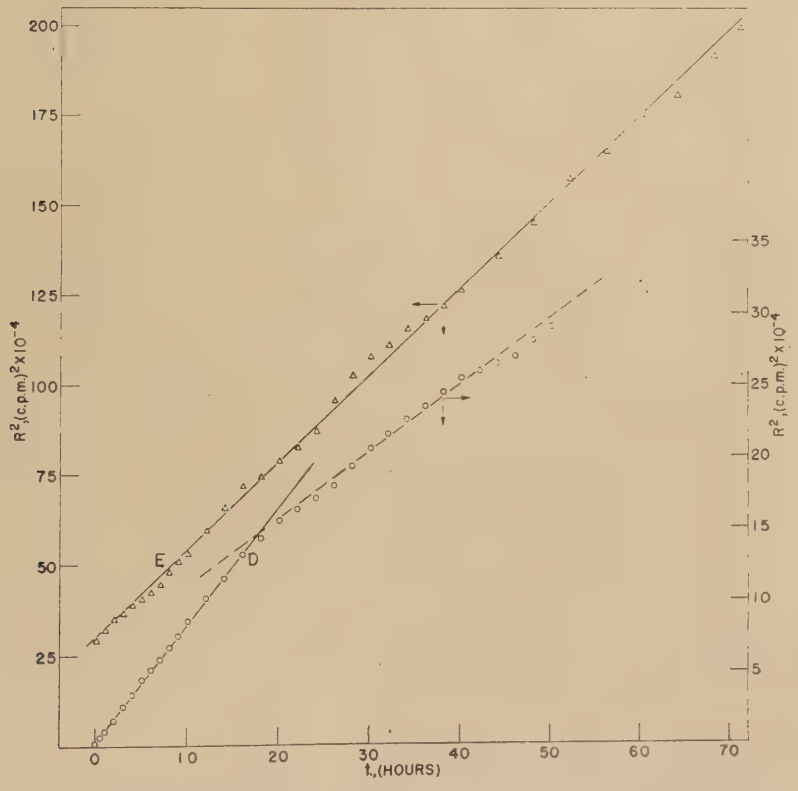

The diffusion of ^{36}Cl out of NaCl at 467°c(D) and 510°c(E).

equilibrium of thermally created vacancies, evaporation of NaCl from the surface at high temperatures, recrystallization of the surface, but none has been fully satisfactory.

Fig. 3

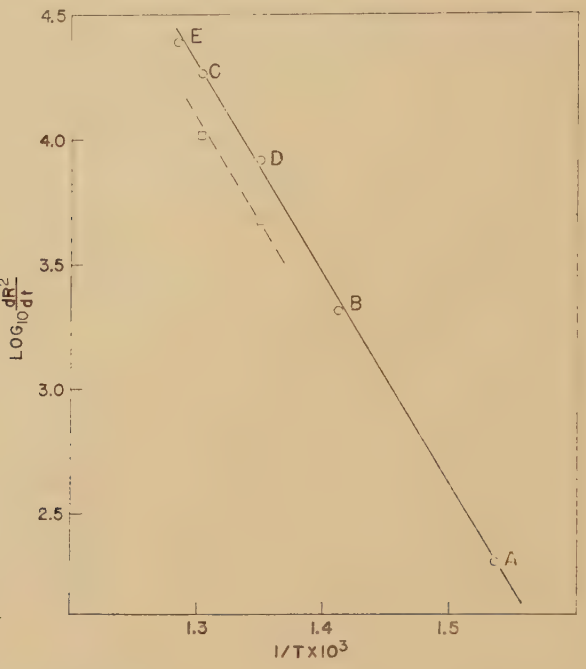

Activation energy plot. A, B, C, D and E as in figs. 1 and 2.

Using the geometrical area of the NaCl samples (25 ± 6 cm^2) with eqn. (2) the solid and dashed lines of fig. 3 lead to the values 0·10 and 0·03 cm^2/sec for D_0. The effective area of the samples as regards diffusion might be larger due to grain structure, but could hardly be larger by orders of magnitude. The present results are compared with those of Chemla (1952) for Cl^- diffusion, and those of Mapother, Crooks and Maurer (1950) for Na^+ diffusion in the table.

	Chloride Ion		Sodium Ion	
	Present work[1]	Chemla[2]	M–C–M[1]	M–C–M[2]
D_0—cm^2/sec	0·10	3×10^4	$1{\cdot}6\times10^{-6}$	3
E—electron volts	1·67	2·70	0·77	1·80
E—electron volts	1·03		1·03	
$(D_0)_2/(D_0)_1$	3×10^5		2×10^6	

[1] Structure sensitive range.
[2] Intrinsic range.

The low values of E and D_0 found in the present experiments places the diffusion process in the structure sensitive range where the concentration of vacancies no longer depends upon the temperature. Hence, the activation energy is presumed to be that for diffusion of a negative vacancy or of a complex whose rate of diffusion is determined by the diffusion of vacancies as assumed by Mapother *et al.* (1950) for positive ion diffusion. The diffusion coefficient may be given more explicitly by

$$\left.\begin{aligned} D&=(D_0)_2 \exp(-E/kT)=\nu_- d^2 \exp[-(U+W/2)kT] \text{ (intrinsic range)} \\ D&=(D_0)_1 \exp(-E/kT)=\nu_- C_- d^2 \exp(-U/kT) \text{ (structure-sensitive range)} \end{aligned}\right\} \quad . \quad . \quad . \quad (3)$$

for the negative ion with similar expressions for the positive ion. Here ν_- is the frequency of vibration of a negative ion, d the interionic distance, U the activation energy for motion of a vacancy and W the energy of formation of a pair of separated vacancies. C_- is the proportion of lattice sites which are vacant in the structure sensitive region.

ΔE in the table is, therefore $W/2$ and, as should be expected, the same value results from chloride and sodium ion diffusion experiments. The ratios of the diffusion coefficients, $(D_0)_2/(D_0)_1$, are also roughly the same for both types of sites. Since $(D_0)_2/(D_0)_1=1/C_-$ for negative ions and $(D_0)_2/(D_0)_1=1/C_+$ for positive ions, then the concentrations of negative and positive ion vacancies are approximately equal in the structure sensitive region. According to the expressions (3), $(D_0)_+/(D_0)_-=\nu_+/\nu_-$ in the intrinsic range. For NaCl, $\nu_+/\nu_-=10^{-4}$, which may be compared with 10^{-5} for KCl (Seitz 1954) and 10^{-2} for NaBr (Schamp and Katz 1954, Mapother, Crooks and Maurer 1950). The large difference between ν_+ and ν_- may be expressed in another way using the transition state theory :

$$\frac{(D_0)_+}{(D_0)_-}=\exp\frac{(\Delta S_+-\Delta S_-)}{k} \quad . \quad . \quad . \quad . \quad . \quad . \quad (4)$$

where ΔS_+ and ΔS_- are the entropies of activation for the motion of positive and negative ions. The ratio $\nu_+/\nu_-=10^{-4}$ leads to $\Delta S_- - \Delta S_+ = 18{\cdot}3$ cal/mol deg. Possibly this difference may be accounted for by the different polarizabilities of the ions.

Additional information may be had from the transference numbers of Cl^- and Na^+ measured by Tubandt *et al.* (1931) and quoted by Jacobs and Tompkins (1952). These presumably are for the structure-sensitive range. The ratio of the transference numbers gives

$$\frac{t_-}{t_+}=\exp\left[\frac{(\Delta S_- - \Delta S_+)}{k}\right]\exp\left[\frac{-(U_- - U_+)}{kT}\right].$$

For Tubandt's results $U_- - U_+ = 0{\cdot}72$ ev as compared with $0{\cdot}90$ ev from the data of the table. Furthermore, $(\Delta S_- - \Delta S_+)$ is approximately

13·7 cal/mol deg. which agrees reasonably well with the value found from the data in the table.

As has been pointed out, the cause of the structure sensitive region for positive ion diffusion lies in the presence of an extremely small concentration of divalent positive impurities (Mapother, Crooks and Maurer 1950). The foregoing discussion suggests that these might also affect the negative ion diffusion. However, purification of the NaCl by growth of crystals from the melt led to no significant change in E and D_0 for the structure sensitive range. Spectrographic analysis of this recrystallized NaCl showed a content of less than 0·005% of each of nine metallic impurities. Further, the addition of 0·3% of Cd^{++} ions (in the form of $CdCl_2$) produced no appreciable change in E and D_0. One is obliged to say, therefore, that chloride ion diffusion in the structure sensitive region proceeds by a mechanism independent of positive ion impurities. Elucidation of the mechanism must await further experiments. The possible existence of multivalent negative ions (e.g. O^{--}, S^{--}) in the lattice has not been investigated yet. In analogy with positive ion diffusion, it might be anticipated that multivalent negative ion impurities could affect the chloride ion diffusion.

Finally, brief mention should be made of the exchange between chlorine gas and the small particles of NaCl. The particles were prepared as described by Thomson *et al.* (1955) and from electron micrographs appeared to be cubes presumably bounded by {100} faces. At room temperature a rapid exchange reaction involving about 50% of the surface chloride ions was observed. A much slower, apparently diffusive reaction followed. Between room temperature and 80°C the activation energy for the slow process was about 0·3 ev. The measurements at higher temperatures were complicated by the occurrence of sintering and hence estimates of D_0 were quite unreliable. The low activation energy suggests surface rather than bulk diffusion. The fact that not all of the surface chloride ions entered into the rapid exchange is to be expected since perfect {100} faces would exchange only very slowly with adsorbed chlorine molecules. The rapidly exchanging portion of the surface may then be associated with disorder of the surface producing 'exposed' NaCl molecules which are easily exchangeable.

Acknowledgment

We should like to thank Mr. G. Ensell for assistance in the development of the apparatus and Dr. W. M. Gray of the Department of Mines and Technical Surveys for the spectrographic analyses.

References

Carslaw, H. S., and Jaeger, J. C., 1947, *Conduction of Heat in Solids* (Oxford: The Clarendon Press), p. 40 *et seq.*

Chemla, M., 1952, *Comptes Rendus*, **234**, 2601.

Clusius, K., and Haimerl, H., 1942, *Zeit. f. Phys. Chem.* **51B**, 347.

Jacobs, P. W. M., and Tompkins, F. C., 1952, *Quart. Rev.*, **6**, 238.

Mapother, D., Crooks, H. N., and Maurer, R., 1950, *J. Chem. Phys.*, **18,** 1231.
March, H. W., and Weaver, W., 1928, *Phys. Rev.*, **31,** 1072.
Mollwo, E., 1937, *Ann. Physik*, **29,** 394.
Schamp, H. W., and Katz, E., 1954, *Phys. Rev.*, **94,** 828.
Seitz, F., 1951, *Phys. Rev.*, **83,** 134 ; 1954, *Rev. Mod. Phys.*, **26,** 7.
Thompson, F. W., Rose, G. S., and Morrison, J. A., 1955, *J. Sci. Instruments*, **32,** 325.
Tubandt, C., Reinhold, H., and Liebold, G., 1931, *Z. anorg. Chem.*, **197,** 225.

XXXIX. *The Creep of Cadmium Crystals at Liquid Helium Temperatures*

By J. W. Glen
Royal Society Mond Laboratory, University of Cambridge†

[Received November 17, 1955]

Abstract

Experiments on single crystals of cadmium at temperatures between 1·2° and 4·2°K have shown that measurable transient creep occurs, and that the amount of such creep does not fall off rapidly with decreasing temperature. It is suggested that this creep is due to the quantum mechanical tunnel effect, which allows dislocations to penetrate barriers to their motion that cannot be overcome by the action of the applied stress alone.

§ 1. Introduction

It is now 25 years since Meissner, Polanyi and Schmid (1930) first reported results of tests on metal single crystals immersed in liquid helium. Their main concern at that time was to show that plastic deformation still occurred at stresses well below the 'theoretical' yield stress for a perfect crystal at temperatures very close to absolute zero, and that plasticity was therefore not a purely thermal effect. Since that time dislocation theory has provided an adequate explanation for the discrepancy between the observed and the 'theoretical' yield stress, but one of their results is of interest in a rather different connection. They noticed that, even at these temperatures, there seemed to be a small amount of transient creep; that is to say that, after application of the stress, the strain continued to increase for some time. In their paper they showed two creep curves for cadmium crystals, one at 4·2°K the other at 1·2°K and the creep in these two cases was not very different in magnitude.

Recent theories of transient creep all assume that the phenomenon is due to thermal fluctuations assisting the applied stress to force dislocations past some obstacle, and therefore on these theories creep should vanish as the temperature approaches absolute zero, unless zero point energy can supply the necessary fluctuations in the same way as thermal energy. As this point is of some interest in the theory of creep, and as no further experiments seem to have been reported to confirm the results of Meissner, Polanyi and Schmid (which they themselves admit might have been due to accidental fluctuations of the stressing system), an attempt has been

† Communicated by Professor N. F. Mott, F.R.S.

made to investigate this phenomenon, and to find out somewhat more about this low temperature creep. This paper presents a preliminary account of the results.

Fig. 1

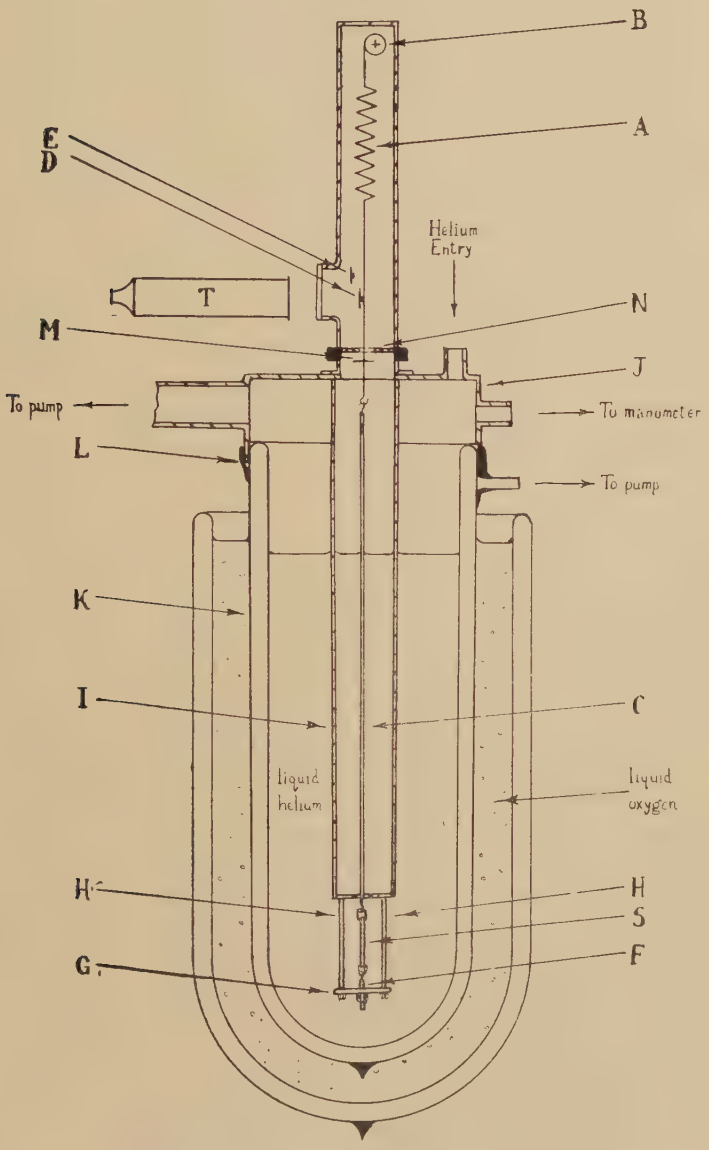

Schematic diagram of the testing machine used.

§ 2. Specimens and Apparatus

The crystals used were made of Johnson Matthey spec-pure cadmium (batch no. 4753X) by the Andrade technique. Lengths of wire about 10 cm long and 2 mm diameter were sealed in an argon atmosphere in glass tubes, of which the diameter was somewhat greater than the wire

diameter, and a travelling furnace was then passed over the tubes to melt the wire and allow it to resolidify from one end. The resulting crystals were long enough to allow two or more short specimens to be cut from each. The cutting was done with a flame, and the specimens were melted onto copper loops at each end. Back reflection Laue patterns were used to determine the orientation.

The apparatus used was a simple testing machine, specially designed for operation in liquid helium. A diagrammatic sketch of the assembly is shown in fig. 1. The load from the spring A, which could be extended using the winch B, was applied to the specimen S through the thin German silver tube C. The movement of the top of the tension system was measured directly by means of the telescope T, which was focused through a window onto an electron microscope graticule D fastened onto the wire which transferred the load from the spring A to the tube C. The telescope could be moved up and down with a micrometer, whose reading gave the movement of D to an accuracy of 0·002 mm. A second graticule, shown schematically at E, was also measured to allow for bodily movements of the machine relative to the telescope. The bottom of the specimen was hooked to the small threaded rod F, which carried a nut that could be screwed up to the bar G at the beginning of a test. G was connected by two rods HH to a second German silver tube I, which was connected at its top end to the main case J. This case was airtight, so that, when the specimen had been mounted and the vacuum flask K put in position with a rubber band L, the whole assembly could contain helium. A second vacuum flask containing liquid oxygen was placed round the helium flask. A stop M was provided on the tension wire, so that, if the specimen broke, it would come against the adjustable annulus N. The whole assembly, other than the telescope, was removed bodily to the helium liquifier for filling with liquid helium.

The design of the machine was intentionally kept as simple as possible, so that modifications could be made after the magnitude of the creep was known, and for this reason there are some disadvantages. The extension of the specimen shortens the spring, and therefore reduces the load, and this not only involves a calculation to deduce the load, but also means that a slight fall in load occurs during creep, although with the small amounts of creep expected this effect is not large. Also the long distance between the measuring point and the specimen means that the elastic deformations of the machine, determined from a blank test, must be taken into account when deducing the stress–strain curve from the data. However, as neither of these points stop the machine from demonstrating the existence of creep, it was decided to make a series of experiments without further modification.

§ 3. Results

Four specimens have so far been tested, some on more than one occasion. One of these was made of commercial purity cadmium, and the other three from the spec-pure material. In all cases there was no doubt that

creep occurred. When the winch was moved to its next stop, the graticule moved up a large distance, and also oscillated sideways with the rod, but if the cross-wires were set on it, it could be seen to continue rising, and after the oscillations had died down, it continued slowly to rise for the next half-hour. As it seems unlikely that stray oscillations picked up from the laboratory floor could have been of the magnitude of the initial oscillations, the continued stretching after the initial oscillations were over is strong evidence for the existence of true creep, not caused by the load attaining a new maximum in oscillations.

Figure 2 shows the load–extension curves obtained. The amount of creep observed at any one setting of the winch is marked by the roughly horizontal lines. Specimens 1 and 2 were cut from the same crystal ($\chi=38°$, $\lambda=39°$), specimen 3 from another, whose Laue pattern showed pronounced asterism, while specimen I was made from commercial purity cadmium.

A number of the creep curves are shown in fig. 3. It will be noted that the creep falls off very rapidly, and in fact appropriate plots showed that, while the strain is more nearly proportional to $\ln t$ than to $t^{1/3}$, it actually fell off faster than predicted by either of these laws. This could be attributed to the drop in load as the specimen extends, as this drop, though small (of order $\frac{1}{2}\%$), is greater than that needed to keep the stress constant, but similar creep curves at the temperature of liquid nitrogen seemed to be more nearly proportional to $\ln t$, and reasons will be advanced below for expecting such a rapid decrease theoretically. It is also interesting that decreasing the temperature during a test did not affect the amount of creep by anything like the ratio of the temperatures. Unfortunately, pumping off helium vapour to reduce the temperature caused severe oscillations, both from the pump itself, and also from the violent agitation of the helium until the λ point was reached. For this reason the stress was usually lowered somewhat before pumping was started, and only raised again when the specimen was down to the lower temperature and the helium was still. In all cases the load–extension curve appeared to be raised above its extrapolated course before cooling, so that some temperature-dependent effect remains even at these temperatures. A further difficulty arose in these tests below the λ point: the whole machine tended to move due to forces in the connection to the pump, and so the changes in the zero were more serious than in the tests at 4·2°K. This further reduced the accuracy in these creep curves, a fault that it is hoped to remedy in further experiments.

A few tests were also performed at liquid nitrogen or liquid oxygen temperature to find the magnitude of the creep at these temperatures. The spring used was rather harder than was really desirable for tests on single crystals, but the creep found was very nearly proportional to $\ln t$, which further shows that the failure of this law at helium temperatures is not due to the machine. As yet tests at intermediate temperatures have not been possible.

Fig. 2

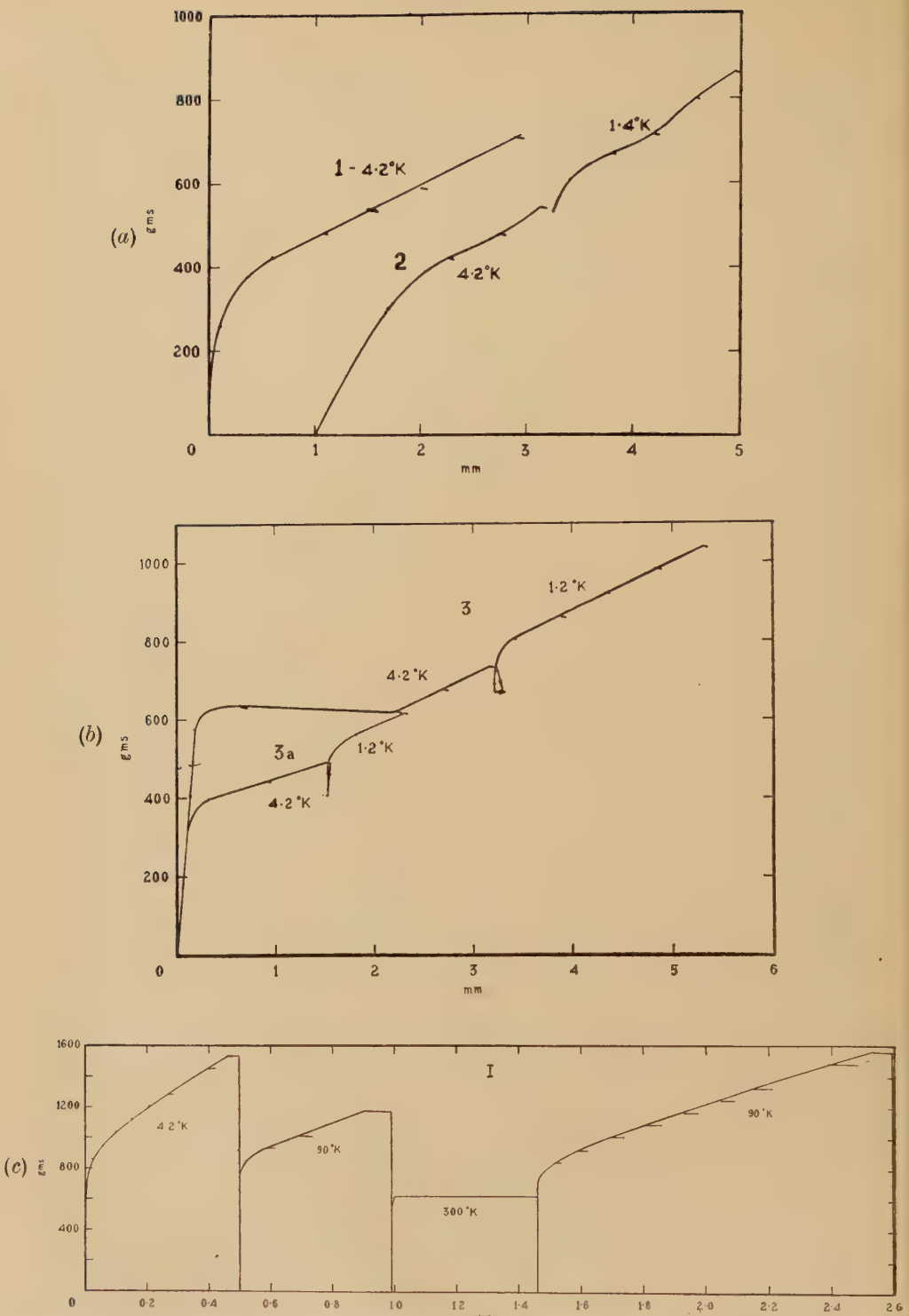

Load–extension curves: (*a*) shows the curves for tests 1 and 2, which were on specimens cut from the same crystal, of which the initial orientation was $\chi=38°$, $\lambda=39°$. (*b*) shows the results of test 3 in which a specimen cut from a crystal which showed pronounced asterism, was tested on two different occasions with a room temperature anneal between. (*c*) shows the curves for specimen I, made from commercial purity cadmium, and tested at various temperatures with room temperature anneals between each.

Fig. 3

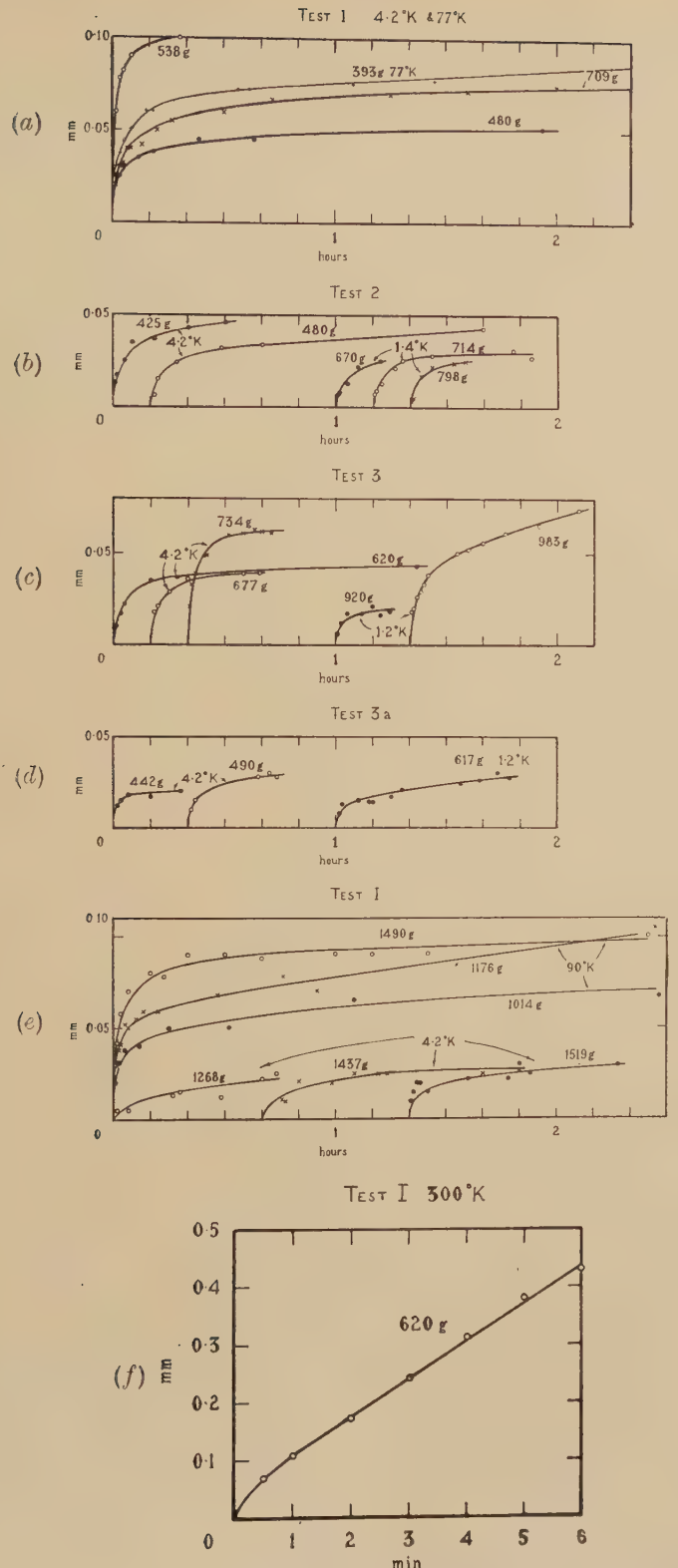

Some of the creep curves obtained. The curves from each test are shown on a separate diagram. (*a*) Test 1, (*b*) test 2, (*c*) test 3, (*d*) test 3*a*, the same specimen as test 3 re-tested after a room temperature anneal, (*e*) test I, (*f*) test I, creep curve obtained at room temperature. Note the different scales in this case.

§ 4. Discussion

The first question that must be answered is whether the creep observed might not be the normal, thermally activated creep. Wyatt (1953) has found experimentally that at low enough temperatures (usually about the liquid nitrogen range) most metals obey a creep law of the form

$$\epsilon = \alpha \ln (\gamma t + 1), \qquad \ldots\ldots (1)$$

where α is proportional to the absolute temperature, and it is difficult to see how, on any theory depending on thermal activation for the creep, the temperature variation could be slower than this. Furthermore, a theoretical estimate of the value of α can be obtained from the theory of Mott (1953). On this theory

$$\alpha_{\mathrm{TH}} = \frac{kT}{B} \Big/ \frac{1}{\sigma}\frac{d\sigma}{d\epsilon}, \qquad \ldots\ldots (2)$$

where B is the activation energy needed to overcome the elementary barrier to flow, and this can be expected to be about 1 ev, both on general grounds, and also in agreement with creep measurements at higher temperatures; $d\sigma\, d\epsilon$ is the gradient of the stress–strain curve.

In order to compare the present results with these predictions, it is convenient to deduce a value of α from the difference between the strains at two times t_1 and t_2 after the application of the load. Using eqn. (1) above

$$\epsilon_2 - \epsilon_1 = \alpha \ln \frac{\gamma t_2 + 1}{\gamma t_1 + 1}, \qquad \ldots\ldots (3)$$

and if $\gamma t_1 \gg 1$

$$\epsilon_2 - \epsilon_1 = \alpha \ln (t_2/t_1). \qquad \ldots\ldots (4)$$

Furthermore, if $\gamma t_1 \gg 1$ 'is not true', the value of α obtained from (4) will be smaller than the correct value obtained from (3).

The values of α obtained using (4) for various creep tests are shown in the table, together with the values expected on Mott's theory if B is taken as 1 ev. It will be noticed that only for temperatures above the helium range is the value of α of the same order of magnitude as the expected values α_{TH}. At the low temperatures the value of α is too large by about a factor 10, and is more nearly independent of temperature than proportional to it.

As the usual theories of creep fail to account for the creep at helium temperatures, it is necessary to consider what effects have been neglected in their formulation, and one of these is zero point energy. It is not, however, sufficient simply to add some term, such as $k\Theta$ to the term kT, as creep presumably depends on the cooperative movement of many atoms, and the spectrum of zero point energy is very different from that of the thermal oscillations. It is perhaps more enlightening to consider the effect, not as due to the zero point oscillations of the lattice, but as due to the tunnel effect through the energy barrier trapping the

Results of Creep Tests Analysed to show the Amount of Agreement with the Theory of Temperature Activated Creep

Test	Temp. (°K)	Load (g)	$\frac{1}{\sigma}\frac{d\sigma}{d\epsilon}$	t_1 (sec)	t_2 (sec)	α ($\times 10^5$)	α_{TH} ($\times 10^5$)
Spec-pure							
1	4·2	480	6·6	1	60	44	5·4
1	4·2	538	6·2	1	18	53	5·8
1	4·2	715	5·3	1	60	43	6·8
1	77·4	393	18·2	1	60	37	36·7
2	4·2	425	6·6	1	30	42	5·4
2	4·2	480	5·4	1	30	40	6·6
2	4·2	544	7·4	1	42	60	4·8
2	1·4	714	4·7	1	43	24	2·5
2	1·4	798	7·1	1	15	30	1·7
2	1·4	861	4·5	0·5	7·5	21	2·7
3	4·2	620	3·7	1	82	40	9·8
3	4·2	677	3·5	1	19	35	10·4
3	4·2	734	3·3	1	25	44	11·0
3	1·2	920	2·8	0·5	14	30	4·2
3	1·2	983	2·7	1	46	65	4·4
3*a*	4·2	442	4·1	1	18	12	8·8
3*a*	4·2	490	3·8	1	24	26	9·5
3*a*	1·2	617	4·3	1	34	20	2·4
Commercial purity							
I	4·2	1268	18·5	1	50	29	1·9
I	4·2	1437	15·6	6	74	36	2·3
I	4·2	1519	14·4	1	60	28	2·5
I	90	1014	13·1	0·5	56	40	59
I	90	1176	11·5	1	93	66	67
I	300	620	—	0·5	6	783	Steady state creep
I	90	845	30	1	3	49	25·8
I	90	927	18·2	0·5	4	41	43
I	90	1013	13·7	0·5	4	23	57
I	90	1092	12·1	0·5	9	36	64
I	90	1170	11·4	0·5	3	70	68
I	90	1251	10·7	0·5	4	70	72
I	90	1330	10·1	0·5	4	62	76
I	90	1490	7·8	0·5	60	64	100
I	90	1570	7·4	1	27	61	104

dislocation. The dislocations that are responsible for the first creep are those for which the applied stress is very nearly adequate to take them over their barriers, and therefore the barriers facing them are very low and very narrow. To make a proper calculation of the creep which can arise from this effect would involve, among other things, an exact knowledge of the shape of the potential barrier faced by dislocations

and of the effective mass of dislocations, but it is certain that some dislocations, unable to surmount their potential barriers with which they are faced with the aid of stress alone, will be able to penetrate them, given time, by the normal quantum mechanical tunnel effect. The oscillations of the lattice in modes other than that considered as the movement of the dislocation will probably assist the tunnel effect, as the barrier will itself fluctuate in height due to their action. The only question is whether this effect produces enough creep to be observable.

While the theoretical solution of this problem must be left for the present, the experiments described above seem to indicate that some effect such as the tunnel effect can give measurable creep. The creep produced in this way should be independent of temperature, and it should also fall off with time more rapidly than would be the case were the same dislocations overcoming the same barriers with the aid of thermal motions, since a higher barrier is also broader, and the tunnel effect falls off exponentially with both height and width. In both these respects the observed creep agrees qualitatively with the predictions.

Acknowledgments

I should like to thank Professor N. F. Mott and Mr. J. M. Ziman for helpful discussions, and Mr. F. Sadler for assistance in the design and construction of the machine. Finally I am most indebted to Dr. D. Shoenberg for permission to work in the Royal Society Mond Laboratory.

References

Meissner, W., Polanyi, M., and Schmid, E., 1930, *Z. Phys.*, **66,** 477.
Mott, N. F., 1953, *Phil. Mag.*, **44,** 742.
Wyatt, O. H., 1953, *Proc. Phys. Soc.* B, **66,** 459.

XL. *Thermal Expansion of Diamond*

By J. Thewlis and A. R. Davey
Atomic Energy Research Establishment, Harwell†

[Received December 7, 1955]

Abstract

X-ray measurements are reported of the thermal expansion of industrial and gem-quality diamond from −150°C to +950°C. It is found that the thermal expansion of industrial diamond shows an anomaly at low temperatures. No such anomaly is found for gem-quality diamond, for which Grüneisen's law holds in general throughout the range. The values of the unit-cell dimension at 20°C are: industrial diamond, $a_0=3{\cdot}5669_2$ Å, gem-quality diamond, $a_0=3{\cdot}56684$ Å.

§ 1. Introduction

The value of the thermal expansion coefficient of diamond and its variation with temperature are of considerable interest in the study of the graphite–diamond equilibrium diagram since the thermal expansion is directly related to the difference between the specific heats at constant pressure and constant volume. Berman and Simon (1955) and Liljeblad (1955) have recently put forward suggested diagrams; and Berman and Thewlis (1955) have shown that Berman and Simon's diagram is to be preferred in the light of recent measurements of thermal expansion up to 900°C. It is the purpose of the present note to describe these measurements.

§ 2. Method

X-ray powder photographs were used in making the measurements, the temperature range covered being from −150°C to +950°C, a greater range than has previously been achieved in one series of experiments. The low-temperature photographs were taken with a modified 19 cm Unicam camera (Thewlis and Davey 1955) in which the specimen is cooled by a stream of cold nitrogen, and the high-temperature photographs with a Unicam high-temperature camera of early design, of which the specimen holder had been modified.

Two batches of diamond were examined, industrial and gem-quality, the latter being ground to give crystallites less than 5 microns in diameter. The material to be examined was held in thin-walled silica capillaries of internal diameter 0·5 mm.

†Communicated by the Authors.

The approximate temperature was measured in the low-temperature camera by chromel–alumel thermocouples and in the high-temperature camera by platinum–platinum–rhodium thermocouples. The actual temperature was measured, however, by measuring the lattice parameter of silver, pure silver powder being mixed with the diamond powder so that both sets of reflections occurred on the same photograph. For temperatures below room temperature the lattice parameter values used were those given for silver by Owen and Williams (1954); above room temperature those of Hume-Rothery and Reynolds (1938) were used. Unfiltered Cu K radiation was employed throughout except for a few high-temperature photographs of industrial diamond, where Co K was substituted.

The accurate value of the unit-cell side for each photograph was determined by plotting the observed value against the Nelson–Riley function (Nelson and Riley 1945) for a number of reflections and extrapolating to $\theta=90°$. Independent extrapolations for the $K\alpha_1$, $K\alpha_2$ and $K\beta$ reflections were carried out to allow for systematic errors in reading the positions of the $K\alpha_1$ and $K\alpha_2$ reflections (Thewlis 1955), the mean value being taken as correct.

§ 3. Results

Figures 1 and 2 show the values of the unit-cell dimensions at different temperatures for industrial and gem-quality diamond repectively. It will be seen that the high-temperature values are very similar but that, for industrial diamond, there is an anomaly at about −30°c. This anomaly is brought out more clearly in fig. 3, where the linear coefficient of expansion, α (i.e. $(1/a)(da/dt)$ where a is the unit cell side and t the temperature), is plotted against temperature for industrial diamond. None is present in fig. 4, which shows a plot of α against temperature for gem-quality diamond.

It will be seen, as is to be expected from figs. 1 and 2, that the two types of diamond give very similar values of α at the high temperatures which are of interest in connection with the graphite–diamond equilibrium diagram, but there is a small region near 0°c where, for industrial diamond, the coefficient of expansion becomes negative†. The anomaly could presumably arise from some intra-crystalline impurity, and it is interesting to note that previous hints of anomalies in this temperature region are not unknown. For example Röntgen (1912) refers to a density maximum at −41·7°c, the observation of which is attributed to Fizeau.

§ 4. Discussion

Figure 2 shows, as well as the results of the present measurements, the values obtained by Krishnan (1946) and Straumanis (1951), the only other workers, as far as we know, who have measured the unit-cell dimensions of diamond at different temperatures. It will be seen that the agreement is satisfactory.

†The values of α in the anomalous range are not precise, and the slight negative value should not be regarded as established beyond doubt.

Fig. 1

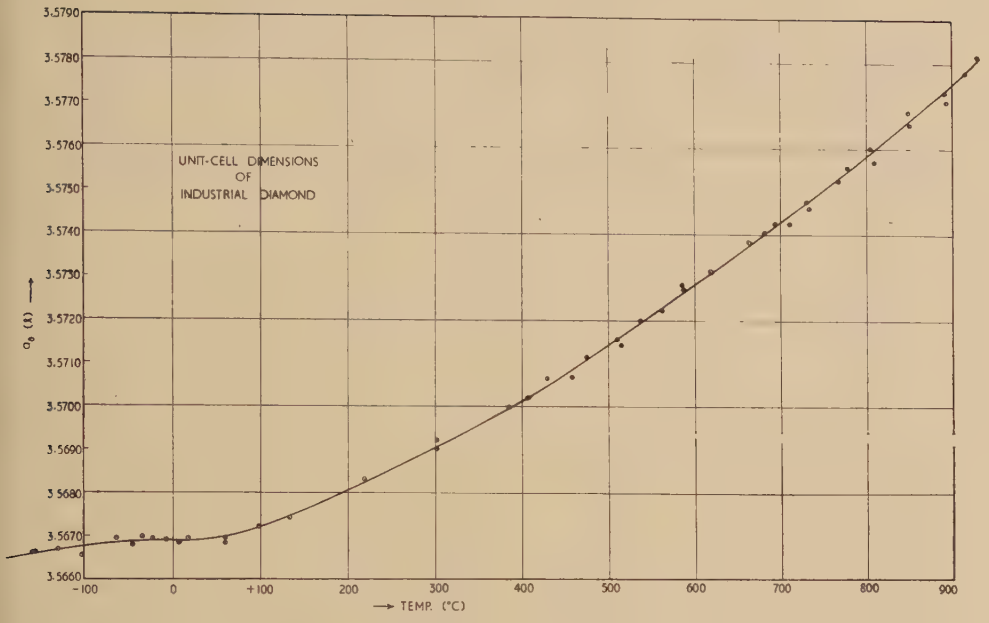

Unit-cell dimensions of industrial diamond.

Fig. 2

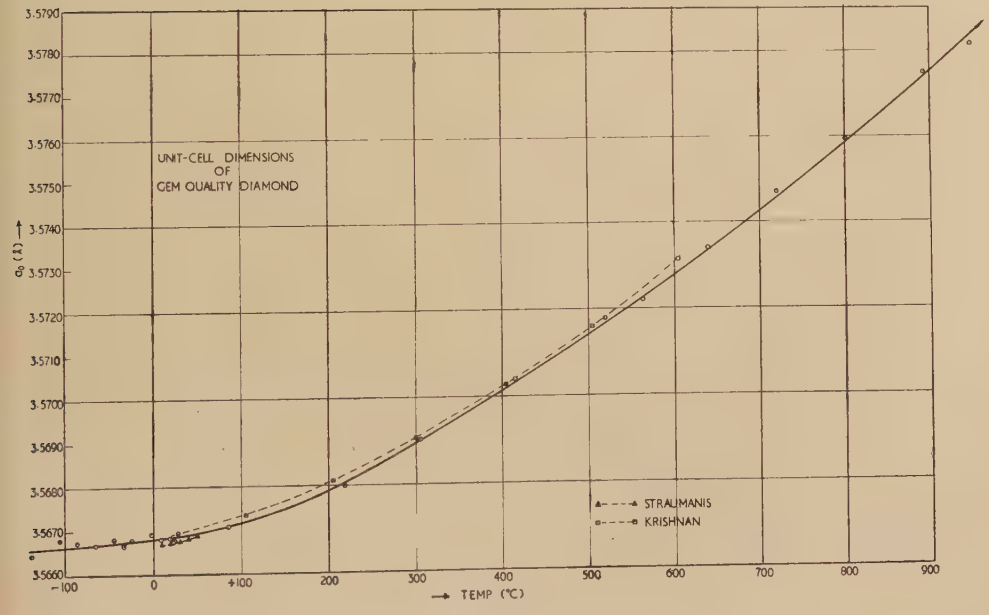

Unit-cell dimensions of gem-quality diamond.

In fig. 4 the results of these and other observations of the thermal expansion coefficient of diamond are shown. Joly's (1897) results differ widely above 400°c from ours but consideration of his method (the measurement of the optical projection of a small heated diamond) shows that this is hardly surprising. Krishnan's values, and those of Dembowska (quoted by Röntgen 1912), are in fair agreement with ours, although the shoulder at about 250°c is less pronounced in Krishnan's

Fig. 3

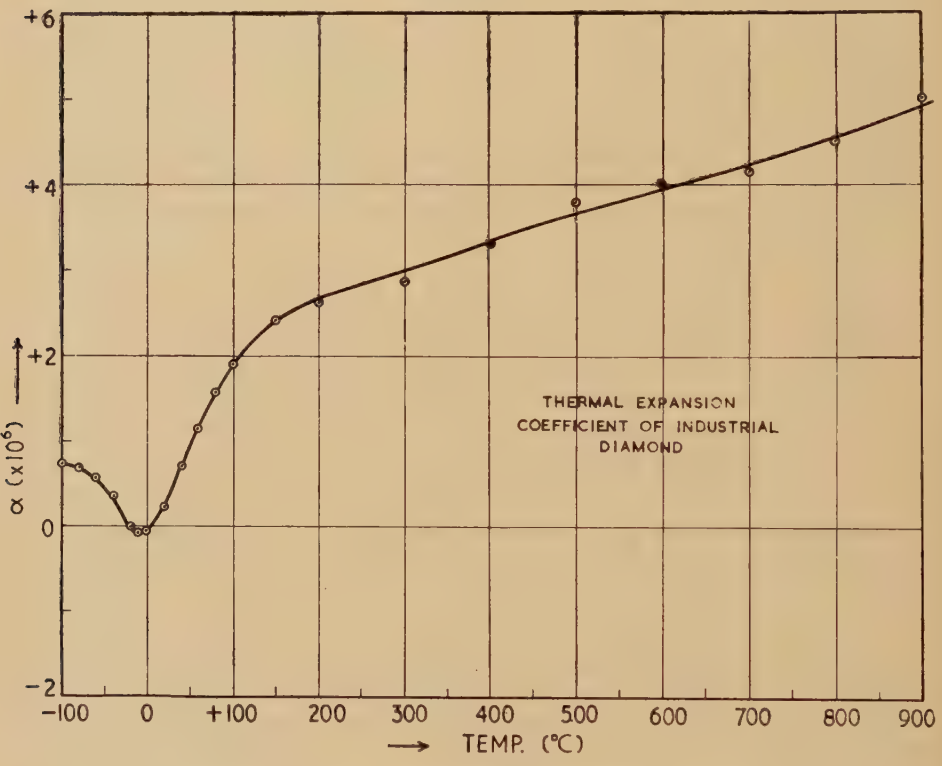

Thermal expansion coefficient of industrial diamond.

curve. The results of Fizeau (1869) and Straumanis correspond to such restricted temperature ranges and to such relatively few actual measurements that little comment is called for. It is our opinion that the true values for the linear expansion coefficient of diamond up to 600°c lie between the Krishnan–Dembowska curve and ours. Above that temperature the consistency of the observed values of the unit-cell dimensions, as shown in fig. 2, suggests that the errors in our curve are small. Berman and Thewlis (1955) point out that this curve agrees with what would be expected if Grüneisen's law held, and is the justification for extrapolating to higher temperatures according to that law.

§ 5. Note on the Accuracy of Measurement of the Unit-Cell Side

As will be seen from figs. 1 and 2 the random errors of individual measurements of the unit-cell side do not exceed 0·0001 Å, and are usually less. This is consistent with the degree of accuracy attained in our previous work (e.g. Thewlis 1955). Our value for the unit-cell side of gem-quality diamond at 20°C is $3{\cdot}5668_4$ Å, the literature values ranging

Fig. 4

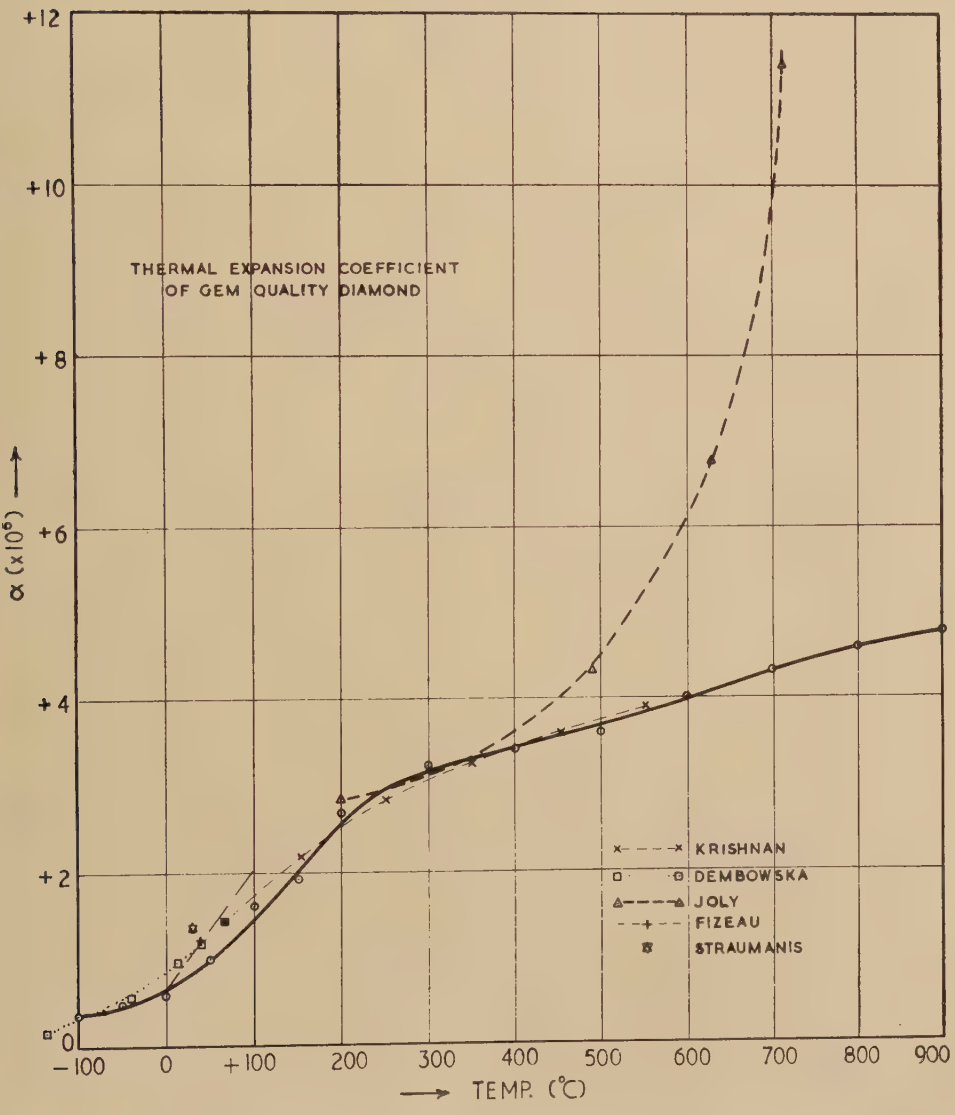

Thermal expansion coefficient of gem-quality diamond.

from $3{\cdot}5667_5$ Å (Straumanis) to $3{\cdot}5669_3$ Å (Lonsdale 1944). For the unit-cell side of industrial diamond at 20°C we obtain the value $3{\cdot}5669_2$ Å.

No allowance has been made for refraction, as the correction on this account is only 0·00001 Å. The wave-length of Cu $K\alpha_1$ radiation has been taken as 1·54050 Å.

Acknowledgments

The authors are grateful to Dr. P. Grodzinski, of the Industrial Diamond Information Bureau, for the supply of gem-quality diamonds; to Mr. S. F. Patching, of the Atomic Energy Research Establishment, for carrying out the grinding operations on them; and to Mr. S. A. Wilson, also of that Establishment, for taking the high-temperature x-ray photographs. The work was undertaken at the suggestion of Sir Francis Simon.

References

Berman, R., and Simon, F., 1955, *Z. Elektrochem.*, **59**, 333 (Volmer Widmungsheft).
Berman, R., and Thewlis, J., 1955, *Nature, Lond.*, **176**, 834.
Fizeau, A. H. L., 1869, *Comptes Rendus*, A, **68**, 1125.
Hume-Rothery, W., and Reynolds, P. W., 1938, *Proc. Roy. Soc.* A, **167**, 25.
Joly, J., 1897, *Sci. Trans. Roy. Dublin Soc.*, **6**, 283.
Krishnan, R. S., 1946, *Proc. Ind. Acad. Sci.* A, **24**, 33.
Liljeblad, R., 1955, *Arkiv för Kemi*, **8**, 423.
Lonsdale, K., 1944, *Nature, Lond.*, **153**, 22.
Nelson, J. B., and Riley, D. P., 1945, *Proc. Phys. Soc.*, **57**, 160.
Röntgen, W. C., 1912, *Münchener Ber.*, 381.
Owen, E. A., and Williams, G. I., 1954, *J. Sci. Instrum.*, **31**, 49.
Straumanis, M. E., 1951, *J. Amer. Chem. Soc.*, **73**, 5643.
Thewlis, J., 1955, *Acta Cryst.*, **8**, 36.
Thewlis, J., and Davey, A. R., 1955, *J. Sci. Instrum.*, **32**, 79.

XLI. *The Internal Friction of Cold Worked Copper at Low Temperatures*

By D. H. Niblett and J. Wilks
Clarendon Laboratory, Oxford†

[Received December 24, 1955]

Bordoni (1949 and 1954) has reported the existence at low temperatures of a large peak in the values of internal friction plotted against temperature for several cold worked metals, and we are making a more detailed survey of the position. Our work has so far been confined to experiments on 99·999% 'polycrystalline copper, and it has been shown (Niblett and Wilks 1955) that the different types of results obtained by Bordoni for different metals can all be induced in copper by subjecting it to varying amounts of cold work. Although measurements are still in progress it seems worth while to give a preliminary report, particularly of those results which appear to be inconsistent with an explanation of the peaks, published recently by Mason (1955).

All the measurements have been made on bars of copper which were first annealed in argon for one hour at 600°c and then plastically deformed in a tensometer. The ends of the bar, which had been gripped in the jaws of the tensometer, were cut off and the bar mounted in the cryostat on the edges of razor blades. Measurements of the internal friction were then made by driving the bar electrostatically into transverse vibration at its resonant frequency (about 1100 c/s) and observing the subsequent decay of the oscillations. The strain amplitudes, that is the strain due to the vibrations, have always been small ; of the order of 10^{-7}. All our results have been corrected for damping due to the thermo-elastic effect, but this is in any case small.

It turns out that the friction depends on the prior cold work in a rather complicated manner, but for deformations greater than about 2% a curve of the type shown in fig. 1 is obtained. This behaviour is similar to that reported by Bordoni for copper except that his measurements do not seem to have been sufficiently sensitive to show the subsidiary peak. For lesser amounts of cold work the two peaks are still observed, but are smaller and appear to be superposed on a background of friction arising from some obviously different mechanism (fig. 2). This background friction is also of interest for its own sake and further investigations are in progress particularly to determine more fully the complex amplitude dependence.

The peaks appear to be of the type associated with relaxation phenomena. Thus the friction is to a first approximation independent of

---

† Communicated by Sir Francis Simon, F.R.S.

Fig. 1

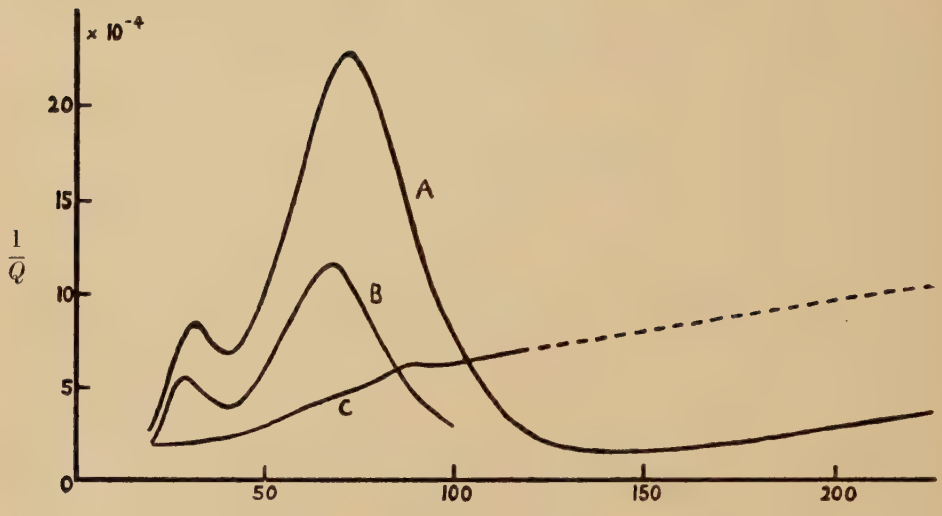

The internal friction of polycrystalline copper.

A. Strained 8·4%.
B. After a subsequent anneal for 1 hour at 250°C.
C. After a further anneal for 1 hour at 350°C.

Fig. 2

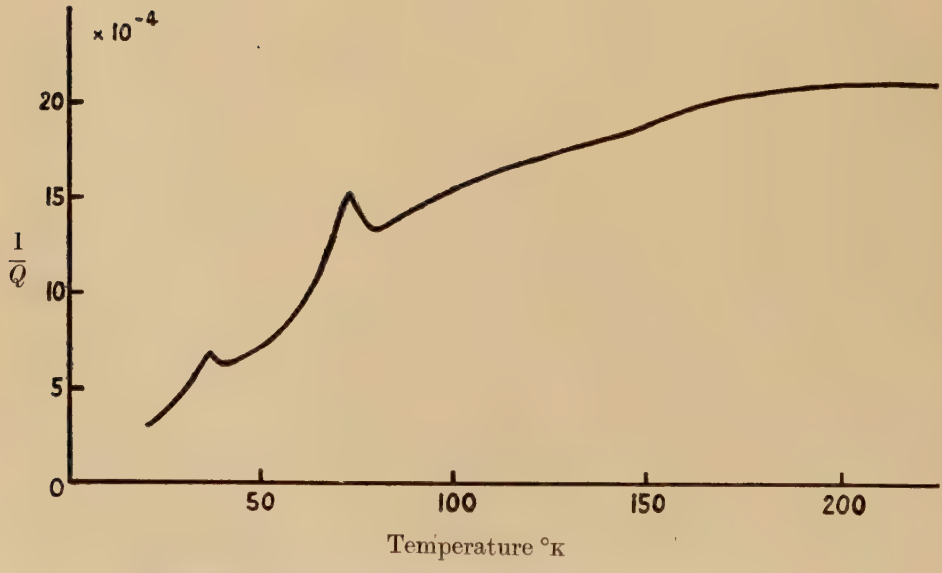

The internal friction of polycrystalline copper strained 0·1%.

strain amplitude, while the positions of the maxima depend on the frequency. A thinner bar vibrating at about 400 c/s had its main maximum some 7° lower than that shown in fig. 1 ; such a shift corresponds to an activation energy of 0·07 ev and this value is also consistent with the shape of the friction versus temperature curve. (However, if one should also use Bordoni's peak in copper at 30 kc/s to determine the energy one arrives at a somewhat higher value, say about 0·1 ev.) As the specimens were deformed at room temperature and left there for several days prior to an experiment, this activation energy cannot correspond to the motion of a free defect such as a vacancy or interstitial for in this case the defects would have diffused out. Thus the most likely source of the damping is the motion of a short segment of dislocation line, as is confirmed by the fact that the friction does not anneal out save by heating to 350°c (see fig. 1).

Fig. 3

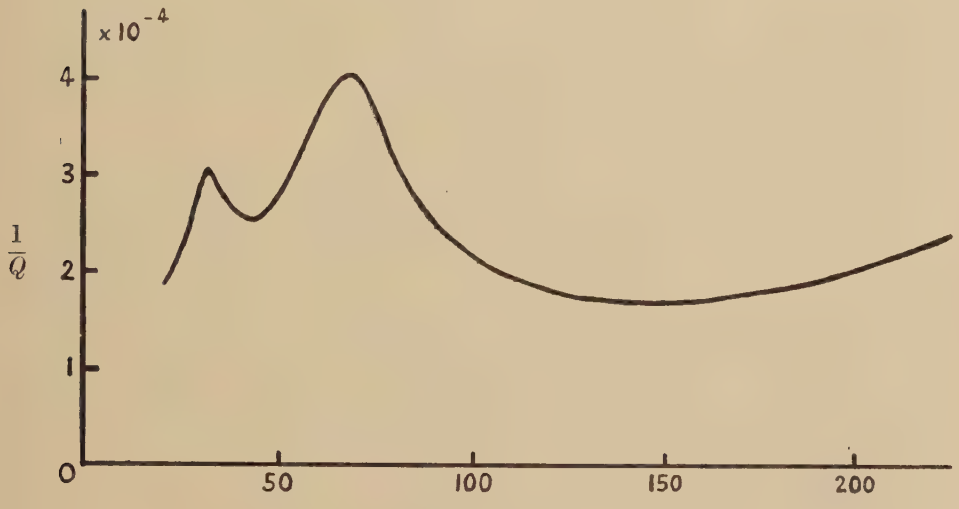

The internal friction of copper, containing 0·0026% Bismuth, and 0·032% Phosphorus, strained 5·5%.

A detailed mechanism has been proposed by Mason (1955) which, he claims, gives rise to an activation energy of the right order of magnitude. He envisages the dislocations as being anchored at pinning points, and that the lengths between these points suffer small displacements. Hence he arrives at an activation energy which is proportional to the distance l between the pinning points for the length of dislocation is question. As this length l can presumably take up a very wide range of values, it is not clear how such a mechanism can give rise to a fairly well defined activation energy, with a characteristic peak at a given temperature. Moreover, if the pinning is due to the interaction of dislocations then the distance l should decrease with increasing cold work, but as mentioned above the shape and

position of the peak in our experiments is virtually independent of the amount of prior deformation. Alternatively, if the pinning is due to impurities then the addition of further impurities should reduce the value of l and give rise to a lower activation energy. Our results for copper containing appreciable amounts of phosphorus and bismuth and strained 5·5% are shown in fig. 3. Although the amplitude of the peak is considerably reduced, the shape and position of the curve is substantially the same as that for pure copper, if allowance is made for the relatively larger contribution of the background damping. Thus the present results are not in agreement with Mason's treatment.

A much more promising explanation has been given by Seeger (1955) who considers the displacement of a dislocation line lying parallel to the lattice lines. He has shown that the initial motion will consist of the displacement of a short segment of line whose length is such that the resulting energy change is a minimum. Thus the vibrations of the bar set in motion sections of dislocations of a unique length and with a unique activation energy, and this energy may be shown to be of the right order of magnitude. Moreover, as in a f.c.c. lattice there are two principal directions in which the displacements can take place, we would expect there to be two peaks rather than one.

Finally we note that while the increase of the friction with increasing cold work is almost certainly due to the increasing density of dislocations, some other mechanism is needed to account for the fact that the maximum friction observed after about 8% deformation is rather less than that after 2%. Of course, a decrease of internal friction is often observed following largish amounts of cold work and is usually, if somewhat vaguely, accounted for by supposing that the dislocations become tangled up with one another. In the present case however it is clear that the interactions which reduce the friction must be such as not to affect the value of the activation energy. Further experiments to elucidate the nature of this mechanism are now in progress.

References

Bordoni, P. G., 1949, *Ricerca Scientifica*, **19**, 851 : 1954, *J.A.S.A.*, **26**, 495.

Mason, W. P., 1955, *Bell Tel .Tech. Journal*, **34**, 903.

Niblett, D. H., and Wilks, J., 1955, *Proceedings of International Conference on Low Temperature Physics, Paris*, p. 484.

Seeger, A., 1955, *Theorie der Gitterfehlsstellen, Handbuch der Physik*, Bd. 7/1 (Berlin–Gottingen–Heidelberg), p. 602 *seq.* See also paper by Seeger, in the press.

XLII. *Rock Magnetism in India*

By J. A. Clegg and E. R. Deutsch
Department of Physics, Imperial College of Science and Technology
and
D. H. Griffiths
Department of Geology, University of Birmingham †

[Received December 10, 1955]

Abstract

Measurements have been made of the magnetic polarization of 450 specimens of basaltic lavas of the Deccan Trap taken from two sites about 500 miles apart. With the exception of some nearly randomly magnetized specimens, the main direction of magnetization is N. 155° E. and the dip is 53° downwards. The most plausible interpretation of this result is (*a*) that India has drifted north from a position about 34° south of the equator when the rocks were formed some 70 million years ago and has rotated anti-clockwise through 25°, and (*b*) that either the earth's field was reversed when the rocks were formed or that the rocks became magnetized in the opposite direction to the field by some physico-chemical mechanism.

The pole position corresponding to these results does not agree with that found by other workers for British and American rocks of the same period. This suggests that a movement of India, relative to North America and Europe, has taken place at some time during the past 70 million years.

§ 1. Introduction

In October 1954 the Physics Department of Imperial College embarked on a three-year project of palaeomagnetic research in India. The scheme arose as a result of a previous survey made in Britain when it was found that certain sediments laid down over a wide area during the late Palaeozoic and early Mesozoic eras are consistently magnetized along a north–east south–west axis, and had a considerably lower inclination than the present earth's field (Clegg, Almond and Stubbs 1954). This result could only be explained with any degree of plausibility on the assumption that the land mass of England has drifted northward, and has rotated approximately 30° in a clockwise sense, relative to the earth's geographical axis, at some time since the end of the Triassic period. Further evidence of past movements of the British land mass has also been obtained from palaeomagnetic measurements made by Creer, Irving and Runcorn (1954), and the data now to hand are sufficiently

† Communicated by the Dr. J. A. Clegg.

conclusive to encourage the belief that by carrying out palaeomagnetic surveys on a global basis it may be possible to determine the positions occupied by the various land areas of the earth relative to the poles during different geological epochs. Recent work on American rocks by Du Bois (1955), Runcorn (1955) and Graham (1955) lends strong support to this expectation.

Among the areas of the world especially suitable for rock magnetic studies is the sub-continent of India. Of especial significance is the permo-carboniferous glaciation which suggests that the geographical latitude of India may not always have been what it is to-day.† Moreover, Indian geology has been studied in detail, and numerous exposures exist revealing a large part of the stratigraphical column. In particular, the Indian peninsular contains the important volcanic formation known as the Deccan Trap. This extensive series of basaltic lava flows covers an area of some 200 000 square miles, and was most likely extruded during the late Cretaceous and early Eocene, and so prior to the culmination of the Alpine orogeny when the great tectonic movements responsible for the raising of the Himalayas were in progress. Its advantages as a field for palaeomagnetic work were first pointed out by Irving (1954), who obtained a few samples of the Deccan Trap lavas from different localities, and found them to have a consistent axis of magnetization, directed roughly south in azimuth, but dipping towards the south. Despite the small number of specimens examined, the consistency of the results suggested that a more extensive magnetic survey of these rocks would be of interest, and we decided, in planning the present expedition, to concentrate initially on the Deccan Trap area.

The first phase of the work has now been completed. Two of us (E. R. D. and D. H. G.) spent two months in India during the winter of 1954–1955 and collected, in all, 208 rock samples. These were taken from a number of lava flows occurring in two different localities some 550 miles apart; the first in the neighbourhood of Linga near the District Capital of Chhindwara in the Central Provinces, and the second close to Khandala on the Bombay–Poona highway. The two areas will be considered separately.

The rock samples, which weighed in all about half a ton, were shipped to England for measurement. The standard method used for cutting cylindrical samples from the original blocks, and of determining the direction of magnetization using a simplified version of the astatic magnetometer described by Blackett (1952), has been described elsewhere (Clegg, Almond and Stubbs 1954).

2. Results from the Linga Area

Over an area of some 50 square miles around Linga there are a number of isolated exposures of basaltic lavas of the lower Deccan Trap series. The district has been mapped by Fermor and Fox (1916), who recognized

† For summary of some of the palaeo-climatological evidence see Holmes (1952) and Gutenberg (1951).

five separate flows which they designated by the numbers, 1, 2, 2*a*, 3 and 4 in ascending order. They estimated the age of these rocks to be late Cretaceous or possibly early Eocene and considered that the lowest flow (no. 1) might well be the oldest in the Deccan Trap series. A total of 69 samples was taken from nine sites including stream beds, quarries and road cuttings, spaced a few miles apart. At the first six sites to be visited it was possible to recognize each of the individual exposures as belonging to one of the flows 1, 2 or 2*a*. At the remaining three sites flows 3 and 4 were exposed, but it was not easy to differentiate between the two.

Laboratory measurements showed that all the samples with the exception of those from flow 2 have preferential directions of magnetization towards the south–east with rather steep downward dips. The combined results of the measurements of declination and dip for flows 1, 2*a*, 3 and 4 are shown as histograms in figs. 1 (*a*) and 1 (*b*), and on a Schmidt projection in fig. 3 (*a*).

The samples from flow 2 were found to have random directions of magnetization, and the results have therefore been omitted from the histogram, but are included as open circles in the projection.

§ 3. Results from the Khandala Area

Close to Khandala, on the steep face of the Bhor Ghat, a large vertical sequence of basaltic lava flows are exposed in a relatively small area. They are thought to belong to the upper part of the middle section of the Deccan Trap, and according to Fermor and Fox (1916) they were probably laid down during the early Eocene period, and are younger than the Linga rocks. 139 rock samples were collected from 20 separate sites on the hillside, at heights ranging from 475 to 2525 feet above sea level. Since the individual exposures were on the whole small and scattered, and the flows numerous and often no more than a few feet in thickness, it was impossible to identify the latter individually.

The complete results for the whole Khandala area are shown in figs. 2 (*a*), 2 (*b*) and 3 (*b*). It can be seen from the histograms and the projection that the majority of the specimens are again magnetized in a general south–easterly direction with rather steep downward dips. A significant feature of the distribution in fig. 3 (*b*) is the group of points in the north–east quadrant and which produce the small secondary maximum in fig. 2 (*a*). They were all cut from four blocks, two of which came from the lowest flows at the base of the Ghat, and the other two of which were collected from the top of the mountain at heights of 2275 and 2525 feet. It will be seen from fig. 3 (*b*) that these anomalous specimens are magnetized in a direction considerably closer to the direction of the present earth's field than are the great majority of the specimens. It is therefore possible that their polarizations have been pulled round towards the present field, owing to partial magnetic instability. There are also three specimens from this area which show upward dips. These again were taken from a single clock belonging to one of the uppermost flows.

Fig. 1

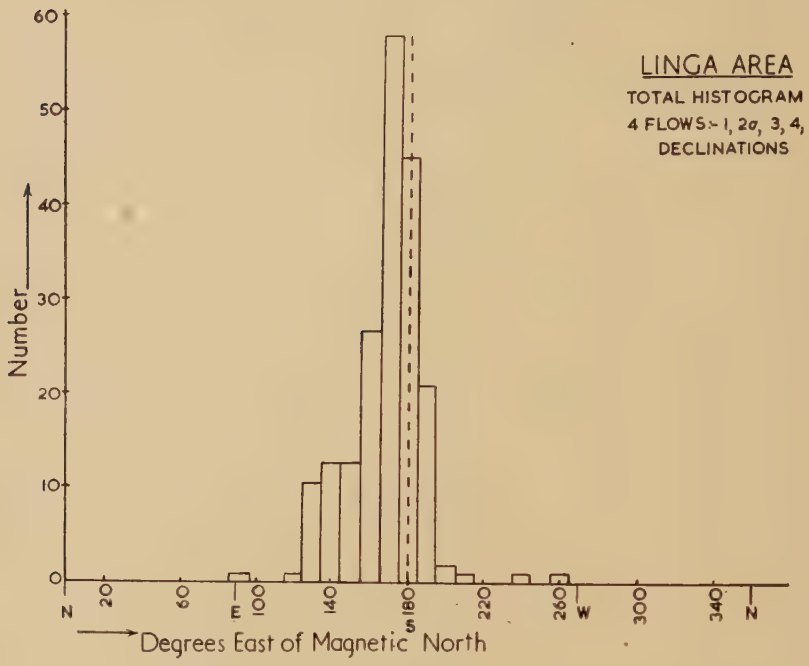
LINGA AREA
TOTAL HISTOGRAM
4 FLOWS:-1, 2σ, 3, 4,
DECLINATIONS
Number
60
50
40
30
20
10
0
N
20
60
E
100
140
180
S
220
260
W
300
340
N
Degrees East of Magnetic North

(*a*)

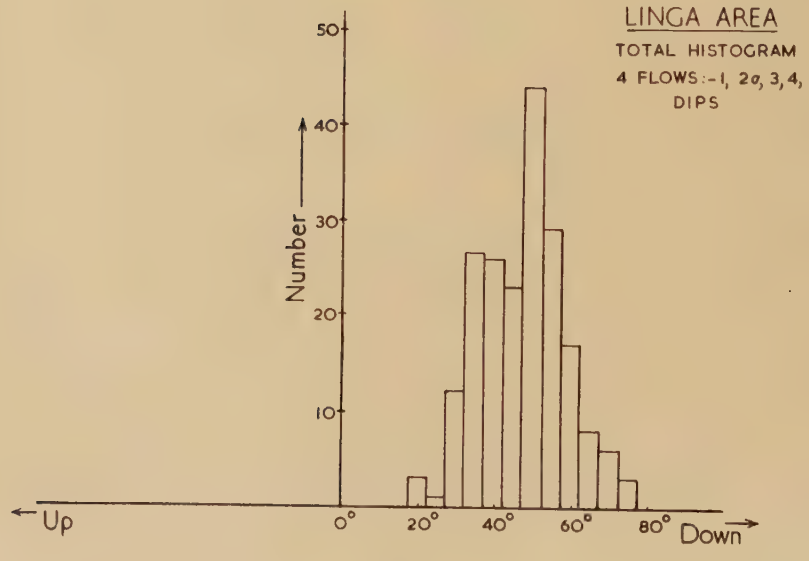
LINGA AREA
TOTAL HISTOGRAM
4 FLOWS:-1, 2σ, 3, 4,
DIPS
Number
50
40
30
20
10
Up
0°
20°
40°
60°
80°
Down

(*b*)

Fig. 2

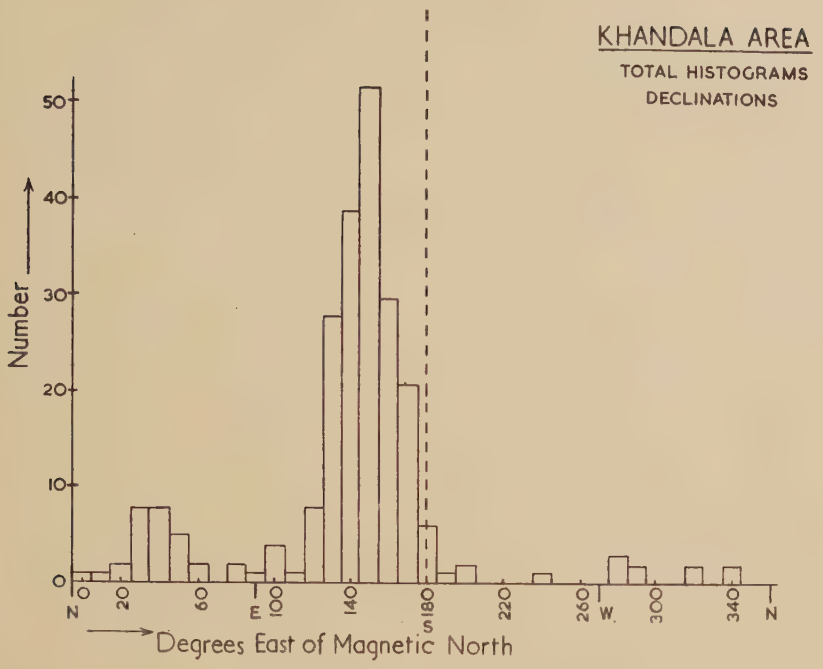
KHANDALA AREA
TOTAL HISTOGRAMS
DECLINATIONS
Number
50
40
30
20
10
0
N
20
60
E
100
140
S
180
220
260
W
300
340
N
Degrees East of Magnetic North

(*a*)

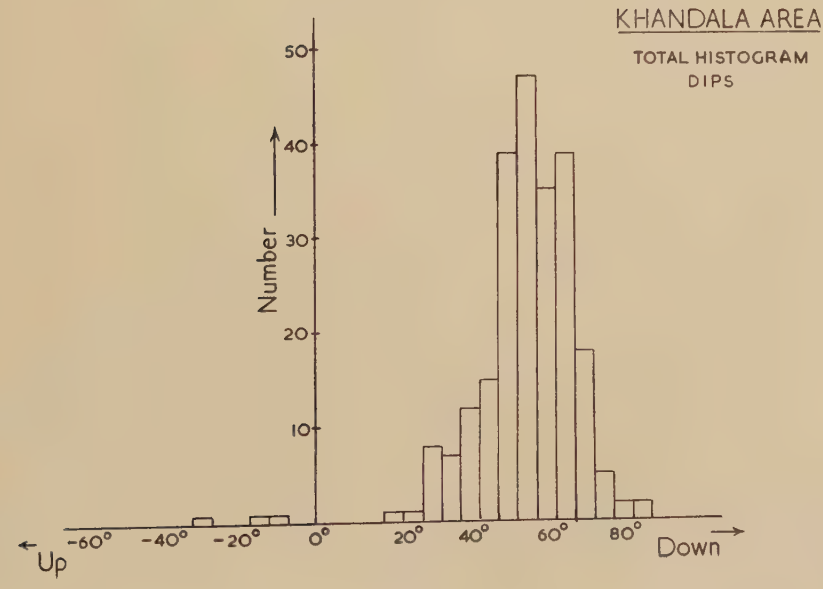
KHANDALA AREA
TOTAL HISTOGRAM
DIPS
Number
50
40
30
20
10
-60°
-40°
-20°
0°
20°
40°
60°
80°
Up
Down

(*b*)

1 Locality	2 Mean latitude	3 Mean longitude	4 Total no. of sites visited	5 Total no. of specimens measured *	6 Mean intensity of magnetization $\times 10^{-3}$ c.g.s.	7 Mean declination east of true south	8 Mean dip †	9 Radius of 50% circle of confidence ‡
Linga area	21° 58′ N.	78° 55′ E.	9	195§	$4{\cdot}72\times10^{-3}$	164°	+48° down	1·0°
Khandala area	18° 45′ N.	73° 22′ E.	20	233	$3{\cdot}12\times10^{-3}$	139° (147°)¶	+62° down (+58°)¶	1·4°

Mean for both sites N. 155° E. and +53° down.

* The term ' specimen ' applies to the individual cylinders cut from the original blocks. Two or more of these were often taken from a single block.

† The dips were measured relative to a horizontal plane.

‡ Computed by the method of Fisher (1953).

§ These specimens were taken from flows 1, 2*a*, 3 and 4. Flow 2 was randomly polarized and the results have not been included.

¶ The figures in brackets give the mean declination and dip for the two sites when the anomalous specimens from the Khandala area are omitted.

§ 4. Discussion of Results

Further details of the results for the two areas are given in the table. Although the declinations of the individual samples were measured with respect to magnetic north, the mean values shown in column 7 of the table

Fig. 3

(*a*)

Linga Area—Flows 1, 2*a*, 3 and 4 : ● ; Flow 2 : ○.

Schmidt Projection

Circles and dots, lower hemisphere : ● ○ ; Crosses, upper hemisphere : + ;
North Pole, present : ● N ; dipole : ● N′ ; South Pole, present : + S ;
dipole : + S′.

are expressed in degrees east of true north. In the particular region concerned the declination is very small, being 0·6° west. The lava flows sampled were all very nearly horizontal, and the magnetic dips (column 8) were therefore measured relative to a horizontal plane. This marked

horizontality over large areas is a characteristic feature of the Deccan Trap lavas, which are believed to have been laid down as level flows and to have remained free, for the most part, from subsequent folding or tilting (Fermor and Fox 1916).

Fig. 3

(*b*)

Khandala Area—All flows : ●.

Schmidt Projection

Circles and dots, lower hemisphere : ● ○ ; Crosses, upper hemisphere : + ; North Pole, present : ● N : dipole : ● N′ ; South Pole, present : + S : dipole : + S′.

The figures given in the table show that the general direction of magnetization is similar in both areas. However, the rocks from Khandala have, on the whole, a significantly bigger downward dip and a more easterly declination than those from Linga. This difference is partly

due to the anomalous and probable partially unstable specimens from the Khandala, which have already been discussed. If these 23 anomalous specimens are omitted, the mean values for declination and dip for Khandala obtained from the remaining 210 specimens become 147° and +58° (shown in brackets in the table), which are somewhat closer to Linga figures.

The origin of the random scatter of the specimens from flow 2 in the Linga area is unknown. Lightning, weathering or some other disturbance are possible causes.

Though the difference between the results from the two sites is still significant and is under further study, for the purposes of the present discussion we will use the mean value for the two locations. Thus we get for the direction of the magnetic intensity (north seeking pole) when the rocks were magnetized, the following figures :

Declination	N. 155° E.
Inclination	+53° down.

It will be seen from figs. 3 (*a*) and (*b*) that the direction of magnetization of most of the rocks is almost perpendicular to that of the present magnetic field in India. The majority of the rocks, with the possible exceptions which have already been mentioned, must therefore have had a considerable degree of magnetic stability over long periods of time, so that it is likely that their polarizations give a true indication of the earth's field at the time of cooling. The relatively narrow peaks in both declination and dip shown in figs. 1 (*b*) and 2 (*b*) strongly suggest a high degree of stability for most of the specimens. For when magnetic instability in rocks is found it generally affects different specimens differently, leading to a wide distribution in measured directions.

We conclude that throughout the whole period during which the lava flows of the Linga and Khandala were being laid down, the earth's magnetic field was directed either along a south–east axis dipping downwards, or, if the rocks were self-reversed, along a north–west direction dipping upwards. Since the period of time over which the Deccan Trap was extruded was probably much longer than the period of the secular variation, we can reasonably assume that the mean direction of magnetization of all the measured flows should be close to that corresponding to an axial dipole, which we assume to be co-axial with the geographical axis of the earth.

Our results therefore suggest that the Indian peninsular occupied a very different position relative to the geographical poles during the late Cretaceous and early Eocene periods from that at the present time. In particular, in order to account for the rather steep downward dip of 55° compared† with the present 25°, it is necessary to suppose that India

† It should be noted that the dip in India corresponding to an axial dipole is 36°.

was then situated considerably farther from the equator. For if the earth's field corresponded on the average to that of an axial dipole, the relationship between the mean magnetic dip, θ, and the geographical latitude, λ, would be given by

$$\tan \lambda = \tfrac{1}{2} \tan \theta.$$

Substituting the mean values of θ of 53° from column 8 of the table, we obtain the values of 34° for λ. After taking into account the direction and sign of the dips, we therefore have two possibilities, namely :

(*a*) This particular area of Central India may then have been about 34° south of the equator. In this case it is necessary to assume either that the direction of the field was opposite to that at the present time, or alternatively that the rocks took on a reverse magnetization on cooling. We must therefore suppose that the whole sub-continent has moved northward across the equator at some time during the intervening 70 million years between that time and the present day. The south–easterly declinations indicate that this transitional movement was accompanied by an anti-clockwise rotation of 25°.

(*b*) The observed directions of polarization are also compatible with the assumption that the rocks were formed in the northern hemisphere, at a position approximately 34° north of the equator. But if this were so, the directions of the declinations and dips show that India must have rotated through nearly 180° or alternatively have drifted across one of the poles to its present position.

Of these various possibilities the first, that of a northward drift and a small clockwise rotation, is evidently by far the most plausible both on physical and geological grounds.

We thus finally conclude that the results are best explained on the postulate that India lay about 34° south of the equator during the late Secondary and early Tertiary eras, and that at some subsequent time it moved into the northern hemisphere and rotated about 25° clockwise relative to the earth's geographical axis. A latitude shift from 34° south to the present 20° north, that is, of 54°, corresponds to a linear movement of 5000 km.

It is very hard to see how this conclusion can be avoided except by some very special and unlikely hypothesis. A conceivable way of reconciling the polarization of these rocks with the present geographical position of India would be to assume that the polarizations were all originally along the reversed direction of the present field (i.e. south and 25° upwards, point S in figs. 3 (*a*) and (*b*) and that they have been just sufficiently unstable to have been all pulled round through some 90° to the present position of the peak, that is, 25° east and south and 55° downwards. This is so unlikely that it will be provisionally rejected.

In considering the mechanism whereby such a large movement of India might have occurred, one is immediately tempted to consider tectonic causes, since current theory of mountain building suggests that

India evidently advanced towards the main Asiatic land mass during the building of the Himalayas.

Now the extent of this movement of India, relative to Siberia during the Alpine orogeny, is in great doubt and various authorities give figures varying from 100 km (Jeffreys 1906) to 3000 km (Van der Gracht 1928). Taking a few hundred kilometres as a reasonable mean estimate of the relative motion of India and Siberia, the rock magnetic measurements would indicate a much bigger northward movement of India relative to the geographical axis than relative to Siberia. Whether, in fact, Siberia shared in this greater northward movement or not, should be determinable by rock magnetic measurements in Siberia.

§ 5. Five Comparisons with Other Work

It has been shown by Runcorn (1955) and more recently by Graham (1955) that the directions of magnetization found in certain British, North American and Icelandic rocks are consistent with the assumption that the earth's mantle has moved as a whole—that is, according to the polar wandering hypothesis.

Of particular significance, by reason of the large number of specimens studied, is Graham's comparison of his results for Permo-Triassic sandstones in North America with the results of Clegg *et al.* for the Triassic sandstones of England. Taken together these results indicate a pole position 180 million years ago as 45° N. and 130° E.

Graham considers that no rotation or translation of Europe relative to North America as great as 20° would be consistent with the magnetic results. Gold (1955) has given theoretical arguments which indicate that polar wandering is much more likely to have occurred than relative motion of continents.

It is interesting to consider our results for the Deccan Trap in relation to these hypotheses. The position of the north pole in Eocene-Cretaceous times (70 million years ago) as deduced from our measurement is

28° N. 85° W.

This can be compared with the estimate by Runcorn of the pole position in Eocene-Cretaceous times, as deduced from measurements of British, North American and Icelandic rocks, which is

76° N. 130° E.

It is evident that this large difference between the pole position calculated from our results and that calculated by Runcorn indicates that India must have moved relatively to Northern Europe and North America.

Some slight evidence for a rotation of India relative to South Africa is obtained by comparing our results with those of Gough (1955) for the Pilansburg Dyke system, which is thought to be between 300 and 400

million years old. These measurements gave the following values for the direction of the polarization :

Declination N. 24° E.
Inclination +69° down.

The corresponding position of the pole—the north pole if the earth's field was reversed or the south pole if it was not—is given by Gough as 8° north and 43° east, which is situated in Abyssinia.

Using similar arguments to those which we have applied to our Indian results, one can conclude that the most likely explanation of Gough's result is that South Africa has drifted right across the south pole to reach its present position and has rotated 24° clockwise in so doing. Although the general northward movement of South Africa in the last 300 to 400 million years is in the same direction as that of India in the last 70 million years, the relative rotations are in the opposite sense : for South Africa 24° clockwise, for India 25° anti-clockwise ; this gives our relative angular rotation of nearly 50°. However, the wide differences in ages of the rocks makes this comparison of only suggestive importance.

Whatever the mechanism responsible for the postulated northward drift of the Indian peninsular, our present results clearly indicate many lines of future research in rock magnetic studies in India.

In the first place, the discrepancy between the measurements at Linga and Khandala require further investigation. It seems possible that some part of the difference may be due to the secular variation. To investigate this more fully, it is evidently necessary to carry out a more detailed survey of the two locations, and to extend the scope of the work to cover other parts of the Deccan Trap area. It will be noted that the Linga rocks have the smaller dip ; whereas if they are in fact older, they would have been expected to have larger dips, due to the postulated northward drift and so to their greater southern latitude when formed.

Secondly, it is well known that Southern India suffered heavy glaciation during Permo-Carboniferous times. If climatic conditions then prevailing over the earth were similar to those of the present day, this would suggest that some 250 million years ago India was in a high southern latitude, say, not less than 65° south. The latitude of 34° south found in the present investigations for Cretaceous-Eocene times is intermediate between this and the latitude today. It is therefore important to make further measurements on rocks of both pre-Cretaceous and post-Eocene ages in order to obtain more detailed information concerning the position of India during these periods. This investigation is now proceeding.

Acknowledgements

We wish to express our gratitude to Professor P. M. S. Blackett, at whose instigation this work was undertaken, for his continued advice and encouragement. We also wish to thank Mr. A. Chapman, Mr. G. W. Massé and Mr. C. W. F. Everitt, for the help which they gave in cutting and measuring many of the specimens and computing the results.

We are indebted to the Department of Scientific and Industrial Research for the award of a grant to finance the survey.

We have received valuable help and advice from members of the staffs of the Geological Survey of India and of the Tata Institute of Fundamental Research, Bombay, to whom we express our very sincere thanks.

References

Blackett, P. M. S., 1952, *Phil. Trans. Roy. Soc.* A, **897,** 309.

Clegg, J. A., Almond, M., and Stubbs, P. H. S., 1954, *Phil. Mag.*, **45,** 583.

Creer, K., Irving, E., and Runcorn, S. K., 1954, *Jour. Geomag. and Geodec.*, **6,** 163.

Du Bois, P. M., 1955, *Nature, Lond.*, **176,** 506.

Fermor, L. L., and Fox, C. S., 1916, *Records, Geol. Survey of India*, **47,** Part II, 81.

Gold, T., 1955, *Nature, Lond.*, **175,** 526.

Graham, J. W., 1955, *Journ. Geophys. Res.*, **60,** 329.

Gutenberg, B., 1951, *The Internal Constitution of the Earth* (Washington: National Research Council).

Holmes, A., 1951, *Principles of Physical Geology* (London: Thomas Nelson and Sons, Ltd.), Ch. 21.

Irving, E., 1954, *Ph.D. Thesis* (University of Cambridge).

Jeffreys, H., 1916, *Phil. Mag.*, **32,** 575.

Runcorn, S. K., 1955 a, *Nature, Lond.*, **176,** 505; 1955 b, *Advances in Physics*, **4,** 244.

Runcorn, S. K., and Day, A. A., 1955, *Nature, Lond.*, **176,** 422.

Van Waterschoot der Gracht, W. A. J. M., 1928, *Theory of Continental Drift: Introduction* (American Association of Petroleum Geologists).

XLIII. *Calculation of μ-Mesic Energy Levels in Heavy Atoms*

By Sheila Brenner†
Department of Mathematics, University College of Swansea‡

[Received October 5, 1955]

Abstract

In this paper μ-mesic energy levels are calculated for various nuclear charge distributions. Only the Coulomb attraction between the μ-meson and the nucleus is considered. It is found that the energy levels are almost independent of small changes in the charge distribution provided the 'radius of the distribution' (defined by the fourth moment of the distribution) is kept constant.

The calculations were done with the aid of a desk machine. The methods used are fairly simple and can easily be used with any reasonable charge distribution.

§ 1. Introduction

Recently there has been considerable interest in the nuclear charge distribution and various experimental data have been interpreted to give a value for the radius of this distribution (see, for example, Hill and Ford 1954 b). The most satisfactory of these, both because of the possibility of making accurate measurements and because of the comparative simplicity of doing calculations, are the differential cross section for high energy electron scattering and the energies of x-rays from μ-mesic atoms.

In this paper μ-mesic energy levels are calculated for various nuclear charge distributions. Only the Coulomb attraction between the nucleus and the μ-meson is considered. Other effects are probably small and are discussed by Hill and Ford (1954 a).

Low energy electron scattering (up to ~20 Mev) is determined completely by the 'radius of the charge distribution', R_s, defined by

$$4\pi \int_0^\infty \rho(r) r^4 \, dr = \tfrac{3}{5} Z e R_s^2, \quad \ldots\ldots\ldots \quad (1)$$

$$R_s = r_0 A^{1/3} 10^{-13} \text{ cm}. \quad \ldots\ldots \quad (2)$$

However, electron scattering experiments have been done more accurately at energies from 80 to 180 Mev (Hofstadter *et al.* 1953) than at low energies. From these experiments r_0 is found to be in the range $1{\cdot}16 < r_0 < 1{\cdot}26$.

† Communicated by Professor R. E. Peierls, F.R.S.
‡ Now at Royal Holloway College (University of London).

(This can be deduced from the work of Ravenhall and Yennie (1954); the same result was found by Brown and Elton (1955).) The small and medium angle scattering at even higher energies is relatively insensitive to the detailed features of the charge distribution. It is interesting to see whether further or different information about the nuclear charge istribution can be obtained from a study of x-rays from μ-mesic atoms.

The charge distributions used here are chosen from those used by Brenner, Brown and Elton (1954) and by Brown and Elton (1955) for high energy electron scattering. They are :

(i) The square distribution

$$\left.\begin{aligned}\rho(r)&=\rho_0 \qquad r<R,\\ \rho(r)&=0 \qquad r>R.\end{aligned}\right\} \quad . \quad . \quad . \quad . \quad . \quad . \quad . \quad . \quad (3)$$

(ii) Distributions of the form

$$\rho(r)=\rho_0 \frac{1}{1+\exp\{(r^2-R^2)/\beta^2\}}, \quad . \quad . \quad . \quad . \quad . \quad . \quad (4)$$

with (*a*) $\beta^2=R^2/4$ and (*b*) $\beta^2=R^2/2$. The quantities ρ_0 and R occurring in (3) and (4) are determined from (1) and the condition

$$4\pi \int_0^\infty \rho(r) r^2 \, dr = Ze. \quad . \quad . \quad . \quad . \quad . \quad . \quad . \quad (5)$$

It is particularly interesting to investigate whether the length β of the transition range affects the energy levels. In other words an attempt is made to answer the question : " Does the gross energy-level structure of the μ-mesic atom give information only about the extent of the charge distribution, or can it be used to distinguish between various distributions with the same radius R_s ? " Since the energy of the 1s level in lead is only about half what it would be for a point nucleus with the same charge, it is clear that the difference between the potential of a nucleus of finite extent and that of a point nucleus cannot be considered as a small perturbation. It might be thought, therefore, that the difference between the energy levels corresponding to these types of nuclei would depend on higher moments of the charge distribution than the fourth (which determines R_s, see (1)). However, it will be shown that the energy levels are almost independent of small changes in the charge distribution provided R_s is kept constant.

While this point was being investigated convenient methods for calculating μ-mesic energies were found. These methods are particularly useful for a hand computor. In general it is only necessary to evaluate power series expansions for the quantities involved, though for some distributions a small amount of numerical integration must be done.

§ 2. Formulation of the Problem

It is assumed that the μ-meson is a Dirac particle, i.e. that it has spin $\frac{1}{2}$ (Tiomno and Wheeler (1949), Fitch and Rainwater (1953) believe they

observed a 0·2 Mev splitting of the 2p levels for lead, which would confirm the assumption), and that its wave function satisfies the Dirac equation†

$$\{\boldsymbol{\alpha}\cdot\mathbf{p}+\beta\mu-V(r)\}\psi(\mathbf{r})=E\psi(\mathbf{r}) \quad . \quad . \quad . \quad . \quad . \quad . \quad (6)$$

where $\boldsymbol{\alpha}$, β are the usual Dirac matrices, $\mathbf{p}$, μ are the momentum and mass of the μ-meson. The potential $V(r)$ is determined from the equation

$$\nabla^2 V(r)=4\pi e\rho(r) \quad . \quad . \quad . \quad . \quad . \quad . \quad . \quad . \quad (7)$$

so that $$V(r)\sim -Z\alpha/r \qquad \text{as} \qquad r\to\infty$$

where Z is the atomic number of the atom and α is the fine structure constant. Since the charge is concentrated near the origin, $V(r)$ has the form $-Z\alpha/r$ for all r greater than a certain R which depends on the charge distribution but is of the order of the radius of the nucleus.

Although eqn. (6) can be solved directly, it is of interest to estimate relativistic effects. The wave function $\psi(\mathbf{r})$ occurring in eqn. (6) is a four-component function. It can be replaced by two two-component functions ϕ_a, ϕ_b satisfying

$$\left.\begin{aligned}(E-V+\mu)\phi_a+\boldsymbol{\sigma}\cdot\mathbf{p}\phi_b=0,\\ (E-V-\mu)\phi_b+\boldsymbol{\sigma}\cdot\mathbf{p}\phi_a=0,\end{aligned}\right\} \quad . \quad . \quad . \quad . \quad . \quad . \quad (8)$$

where the σ's are the Pauli spin matrices. The small component ϕ_a can be eliminated to give

$$\left(\frac{\mathbf{p}^2}{2\mu}+V+E'\right)\phi_b-\left\{\frac{E'+V}{2\mu}\frac{\mathbf{p}^2}{2\mu}+\frac{(E'+V)^2}{\mu}-\frac{(E'+V)^3}{4\mu^2}\right\}\phi_b$$
$$-\frac{1}{4\mu^2}\frac{dV}{dr}\frac{\partial\phi_b}{\partial r}+\frac{1}{2\mu^2}\frac{1}{r}\frac{dV}{dr}\mathbf{L}\cdot\mathbf{S}\phi_b=0 \quad . \quad . \quad . \quad . \quad (9)$$

where $E'=\mu-E$, and $\mathbf{L}$ and $\mathbf{S}$ are the orbital and spin angular momenta of the μ-meson. The approximation $E'+V=-\mathbf{p}^2/2\mu$ may be used in the first two terms in the second bracket since they are small. The third term in this bracket is much smaller and may be neglected. This gives

$$\left(\frac{\mathbf{p}^2}{2\mu}+V+E'\right)\phi_b-\frac{\mathbf{p}^4}{8\mu^3}\phi_b-\frac{1}{4\mu^2}\frac{dV}{dr}\frac{\partial\phi_b}{\partial r}+\frac{1}{2\mu^2}\frac{1}{r}\frac{\partial V}{\partial r}\mathbf{L}\cdot\mathbf{S}\phi_b=0. \quad . \quad (10)$$

The bracketed terms are those of the non-relativistic Schrödinger equation, and the last term is the spin–orbit coupling term.

The kinetic energy $\mathbf{p}^2/2\mu$ is roughly $\frac{1}{2}E'$. Even in the 1s level, where it is largest, E' is only about $\mu/10$ (see table 1). The term $\mathbf{p}^4/8\mu^2$ thus never exceeds about 1·5% of the total binding energy.

To estimate the remaining term it is necessary to evaluate

$$I\equiv\frac{1}{4\mu^2}\int_0^\infty \phi_b\frac{dV}{dr}\frac{\partial\phi_b}{\partial r}r^2\,dr.$$

Using Poisson's equation this may be written

$$I=-\frac{\pi e}{2\mu^2}\int_0^\infty \rho\phi_b{}^2r^2\,dr\sim-\frac{3Z\alpha}{8\mu^2R^3}\int_0^R\phi_b{}^2r^2\,dr.$$

† Units such that $\hbar=c=1$ are used throughout.

Now for the 1s state in lead $\int_0^R \phi_b^2 r^2\, dr \sim \frac{1}{2}$

(Cooper and Henley 1953), and for other states it is very much smaller. Thus this term contributes about

$$\frac{3Z\alpha}{16\mu^2 R^3} \sim 0{\cdot}2 \text{ Mev}$$

to the 1s energy and does not affect the other levels significantly. The actual difference between the relativistic and non-relativistic 1s level is much less than this (table 1) since this term is about the same size as the term $\mathbf{p}^4/8\mu^3$, but has the opposite sign.

Thus the relativistic corrections to the non-relativistic μ-mesic energy levels are small and, except for the 1s level, the largest contribution comes from the term $\mathbf{p}^4/8\mu^3$. This depends mainly on energy and, to the accuracy needed here, should not vary significantly for small changes in the charge distribution. When spin–orbit coupling can be neglected (s states) the energy levels of the μ-meson will be given to better than 1% by the Schrödinger equation

$$\left\{\frac{1}{2\mu}\nabla^2 - V(r)\right\}\psi(\mathbf{r}) = E\psi(\mathbf{r}). \qquad (11)$$

However in cases where it is necessary to include the spin–orbit term it is easier to solve the relativistic eqn. (6).

§ 3. Method of Calculating Non-Relativistic Energy Levels

It is useful to discuss the non-relativistic problem first as it is somewhat simpler in structure and illustrates the essentials of the method of finding energy levels.

The radial wave equation can be written in the form

$$\left\{\frac{d^2F}{dx^2} - \frac{l(l+1)}{x^2}F\right\} + \mathscr{V}F = C^2F \qquad (12)$$

where F/r is the radial wave function and for convenience the following change of scale has been made :

$$\left.\begin{aligned} 2\mu Z\alpha r &= x, \\ V(r) &= -2\mu Z^2\alpha^2 \mathscr{V}(x), \\ E &= 2\mu Z^2\alpha^2 C^2. \end{aligned}\right\} \qquad (13)$$

Now substituting

$$\frac{1}{F}\frac{dF}{dx} = \eta$$

in eqn. (12), η satisfies

$$\eta^2 + \frac{d\eta}{dx} - \frac{l(l+1)}{x^2} + \mathscr{V} = C^2. \qquad (14)$$

In general the function η which corresponds to the solution of (12) regular at the origin is different from that which corresponds to the solution regular at infinity, but for those values of C^2 which are eigenvalues of (12)

they will be the same. The calculation proceeds as follows: The value of the function η corresponding to the solution regular at the origin is calculated at some point $x=X$ for various values of C^2 and the results plotted against $E(=C^2/2\mu Z^2\alpha^2)$. Then the procedure is repeated for the solution regular at infinity, and the points of intersection of the two curves give the required μ-mesic energy levels.

In practice it is not necessary to calculate many points on either curve. Since the potential $V(r)$ is never greater in magnitude than $Z\alpha/r$, the binding energy of a μ-meson in any level is never greater than that of a μ-meson in the corresponding level in the field of a point nucleus. Except in the case of the 1s level, where the binding energy is about half what it would be for a point nucleus, the difference is not very great and it is less for higher levels than for lower ones. It is therefore possible to make a rough estimate of the energy levels before starting on a calculation. Suppose now that η_0 is the function corresponding to the solution of (12) regular at the origin for some value C_0^2 of C^2 and consider the change $\delta\eta$ in η corresponding to the change δC^2 in C^2. Then, to first order, $\delta\eta$ satisfies the equation

$$2\eta_0\delta\eta+\frac{d}{dx}\delta\eta=\delta C^2. \quad . \quad . \quad . \quad . \quad . \quad . \quad . \quad . \quad (15)$$

This equation can be integrated to give

$$\delta\eta(X)=\delta C^2\exp\left[-\int^X 2\eta_0\,dx\right]\int^X\exp\left[\int^x 2\eta_0(y)\,dy\right]dx. \quad (16)$$

Now

$$\eta_0=\frac{1}{F_0}\frac{dF_0}{dx}$$

where F_0 is the solution of (12) corresponding to the value C_0^2 of C^2. Therefore

$$\delta\eta(X)=\delta C^2\frac{1}{\{F_0(X)\}^2}\int_0^X F_0^2\,dx$$

and, provided X is not in the region where F_0 has become small, $\delta\eta(X)$ is of the same order of magnitude as δC^2 and is proportional to it. Thus the calculation of $\eta(X)$ for three values of C^2 (or E) in the neighbourhood of the required energy level provides a check against random errors in calculation since these values should lie on a straight line. This argument applies equally to the function corresponding to the solution of (12) regular at infinity. The required energy level is therefore given by the intersection of two straight lines.

If the point $x=X$ is chosen so that $V(x)$ has the form $1/x$ for $x>X$ (corresponding to $V(r)$ having the form $-Z\alpha/r$ for $r>R=X/2\mu Z\alpha$, as mentioned in § 2), the solutions of (12) regular at infinity are the Coulomb functions

$$F(x)=W_{1/2C,\,l+1/2}(2Cx)$$

where $W_{k,m}(z)$ is a Whittaker function. This gives

$$\eta(x)=-C+\frac{l+1}{x}-\left(\frac{2C}{x}\right)^{1/2}\left(l+1-\frac{1}{2C}\right)\frac{W_{1/2C-1/2,\,l+1}(2Cx)}{W_{1/2C,\,l+1/2}(2Cx)}$$

which can be evaluated using the asymptotic expansions for the Whittaker functions when the principal quantum number n is given by $n=l+1$, $n\neq 1$. In the case $n=1$, the 1s state, η can be found directly by solving eqn. (15) in a power series in $1/x$. When $n\neq l+1$ the calculation is more difficult since in general the asymptotic expansion of the Whittaker functions cannot be used and it is then often easier to find the relativistic solution.

The function η corresponding to the solution of eqn. (12) regular at the origin can be found by solving eqn. (14) directly. When $\mathscr{V}(x)$ has a power series expansion convergent at $x=X$, it is usually possible to find a power series solution of (14) which is also convergent at $x=X$.

§ 4. Method of Calculating Relativistic Energy Levels

The Dirac eqn. (6) can be separated to give

$$\left.\begin{aligned}\{2\mu-E'-V(r)\}F-\left\{\frac{d}{dr}+\frac{\kappa}{r}\right\}G=0,\\ \{-E'-V(r)\}G+\left\{\frac{d}{dr}-\frac{\kappa}{r}\right\}F=0,\end{aligned}\right\}, \quad . \; . \; . \quad (17)$$

where F/r, G/r are the radial components of the wave function and $E'=\mu-E$ is the binding energy and is determined by the condition that F and G should both vanish at the origin and at infinity.

The most convenient units to use differ from those of § 3 by a factor $Z\alpha$ and are defined by

$$\begin{aligned}2\mu r&=y,\\ E'&=2\mu\epsilon,\\ V(r)&=-2\mu\mathscr{V}(y).\end{aligned}$$

Then $\mathscr{V}(y)\to Z\alpha/y$ as $y\to\infty$ and the eqns. (17) become

$$\left.\begin{aligned}\{1-\epsilon+\mathscr{V}(y)\}F-\left\{\frac{d}{dy}+\frac{\kappa}{y}\right\}G=0,\\ \{-\epsilon+\mathscr{V}(y)\}G+\left\{\frac{d}{dy}-\frac{\kappa}{y}\right\}F=0.\end{aligned}\right\}. \quad . \; . \; . \quad (18)$$

The required values of ϵ, i.e. those for which both F and G are regular at the origin and at infinity, can now be found in essentially the same way as the eigenvalues of eqn. (12) were found in § 3. Here the ratio F/G plays the part of the logarithmic derivative in the non-relativistic case. The procedure is to find those values of ϵ for which this ratio for the solution regular at the origin and that for the solution regular at infinity fit together to form a continuous function.

Writing $F/G=\xi$, eqns. (18) give

$$\{1-\epsilon+\mathscr{V}(y)\}\xi^2+\frac{d\xi}{dy}-\frac{2\kappa}{y}\xi+\mathscr{V}(y)-\epsilon=0. \quad . \; . \; . \quad (19)$$

By an argument similar to that in § 3 it can be shown that for either of the required solutions the value of ξ at any point varies linearly with ϵ for small changes in ϵ, and a similar method can be used for finding the required eigenvalues.

It is particularly easy to find the 1s level from eqn. (19). The solution regular at infinity can be found by substituting a power series in $1/y$ for ξ, and that regular at the origin by using a power series in y. For the square distribution these both converge at the edge of the nucleus, $y=2\mu R_s$, and for the other distributions used the latter series may be continued to a point outside the nucleus from a point within its radius of convergence by doing a small amount of numerical integration.

The method used by Gordon (1928) to find relativistic hydrogen-like wave functions can be followed through to find the functions F and G regular at infinity. It is then found that the corresponding function ξ is

$$\xi(y)=\left(\frac{\epsilon}{1-\epsilon}\right)^{1/2}\frac{P(y)+Q(y)}{P(y)-Q(y)} \quad . \quad . \quad . \quad . \quad . \quad . \quad (20)$$

where
$$P(y)=\frac{(-2\gamma)\,!}{(-\gamma-A)\,!}P_{\gamma}(y)-\frac{(2\gamma)\,!}{(\gamma-A)\,!}P_{-\gamma}(y)$$

and similarly for $Q(y)$, and

$$P_{\sigma}(y)=(2\beta y)^{\sigma}F\{\sigma-A+1,\ 2\sigma+1\ ;\ 2\beta y\},$$

$$Q_{\sigma}(y)=-\frac{Z\alpha/2\beta-\kappa}{\sigma-A}(2\beta y)^{\sigma}F\{\sigma-A,\ 2\sigma+1\ ;\ 2\beta y\},$$

$$\gamma^2=\kappa^2-Z^2\alpha^2,$$

$$\beta^2=\epsilon(1-\epsilon),$$

$$A=Z\alpha(1-\epsilon)/2\beta.$$

The function $F\{a, b\ ;\ z\}$ is a confluent hypergeometric function. Since γ and A are both irrational, the formula (20) can always be evaluated and the difficulties of the non-relativistic case (where the corresponding formula contains factorials of negative integers) do not arise.

The expression (20) for ξ can be written in the more compact form

$$\xi=-\left(\frac{\epsilon}{1-\epsilon}\right)^{1/2}\frac{W_{A+1/2,\gamma}(2\beta y)-(\kappa+Z\alpha/2\beta)W_{A-1/2,\gamma}(2\beta y)}{W_{A+1/2,\gamma}(2\beta y)+(\kappa+Z\alpha/2\beta)W_{A-1/2,\gamma}(2\beta y)}. \quad . \quad (22)$$

This expression can be evaluated sufficiently accurately using the asymptotic expansion for the Whittaker functions $W_{k,m}(z)$ for the lowest energy level corresponding to each negative except $\kappa=-1$ (the 1s state), since then $\kappa+Z\alpha/2\beta=0$ for the point nucleus and hence $\kappa+Z\alpha/2\beta$ will be small for the values of ϵ used in the calculation.

§ 5. Results

The methods of the last two sections have been applied to the calculation of several μ-mesic energy levels in lead. The results are given in the tables below for a μ-meson of mass equal to 207 electron masses (Smith, Birnbaum and Barkas 1953). The potentials used are defined in § 1.

The rather strange values for r_0 used arise because the calculations were in fact performed for a μ-meson of mass equal to 210 electron masses and the results appropriately modified.

Table 1. Energy Levels of a μ-Meson in the Field of a Point Nucleus and of two Charge Distributions of Finite Extent (see § 1)

Energies are given in MEV

	Non-relativistic			Relativistic		
r_0 / β^2/R^2	0†	1·217 0‡	1·217 $\frac{1}{2}$	0†	1·217 0‡	1·217 $\frac{1}{2}$
1s	18·94	$10{\cdot}33_5$	10·46	21·03	10·39	10·53
$2p_{3/2}$	4·73	4·53		4·84	4·60	4·60
$2p_{3/2}$1s	14·21	5·81		16·19	5·79	5·93
2s	4·73			5·39	3·55	

Table 2. The Variation of the Non-Relativistic 1s Energy Level with Radius for a Square Distribution

r_0	0†	1·116	1·217	1·319
1s energy in MEV	18·94	10·79	$10{\cdot}33_5$	9·91

Table 3. The Variation of the Non-Relativistic 1s Level with the Length of the ' Transition Region ', β, for $r_0=1{\cdot}217$

β^2/R^2	0†	$\frac{1}{4}$	$\frac{1}{2}$
1s energy in MEV	$10{\cdot}33_5$	10·41	10·46

† Point nucleus. ‡ Square distribution.

Energy levels for other μ-meson masses can easily be calculated from the results given here. Examination of eqns. (12) and (17) shows that, since the potential can be written in the form $V(r)=f(r/R)/R$, with $R=r_0A^{1/3}10^{-13}$ cm, changing the μ-meson mass from μ_1 to μ_2 is equivalent to multiplying r_0 by μ_1/μ_2 and the binding energy by μ_2/μ_1.

§ 6. CONCLUSIONS

It has been shown how, given any charge distribution, μ-mesic energy levels can be calculated without much difficulty.

The results obtained show that the 2p–1s transition energy for a square distribution of radius $1{\cdot}217A^{1/3}10^{-13}$ cm is slightly smaller than the experimental value of 6·0 MEV (Fitch and Rainwater 1953). Since the 1s level is most sensitive to changes in the radius of the charge distribution

(it changes about ten times as much as the 2p level for the same change in radius), this difference could be corrected by taking a square distribution of smaller radius. The 1s binding energy has been calculated for various radii (see table 2) and this gives the approximate change of the 2p–1s transition energy. From this it may be deduced that a square distribution of radius given by an r_0 in the range 1·16 to 1·18 would give the 2p–1s transition energy correctly. The calculations of Hill and Ford (1954 a) show that it is in fact given by a distribution with $r_0=1{\cdot}17$.

The charge distributions (ii) (*a*) and (*b*) defined in eqn. (4) are essentially square distributions with a Gaussian ' tail '. It has been found that distributions with varying lengths of tail (the β of eqn. (4)), but with the same $\langle r^2\rangle_{\text{av}}$ give only slightly different values of the 1s energy level. It is therefore not possible to obtain much information about the nuclear charge distribution from energy levels in μ-mesic atoms which could not be obtained from electron scattering.

Acknowledgements

Most of the work in this paper was done in the Department of Mathematical Physics at the University of Birmingham. The author is very grateful to Professor R. E. Peierls and Dr. G. E. Brown for suggesting the problem and for frequent helpful discussions. She is also grateful to the Department of Scientific and Industrial Research for a grant.

References

Brenner, S., Brown, G. E., and Elton, L. R. B., 1954, *Phil. Mag.*, **45**, 524.
Brown, G. E., and Elton, L. R. B., 1955, *Phil. Mag.*, **46**, 164.
Cooper, L. N., and Henley, E. J., 1953, *Phys. Rev.*, **92**, 801.
Fitch, V. L., and Rainwater, J., 1953, *Phys. Rev.*, **92**, 789.
Gordon, W., 1928, *Z. Phys.*, **48**, 11.
Hill, D. L., and Ford, K. W., 1954 a, *Phys. Rev.*, **94**, 1617 ; 1954 b, *Ibid.*, 1630.
Hofstadter, R., Fechter, H. R., and McIntyre, J. A., 1953, *Phys. Rev.*, **92**, 978.
Ravenhall, D. G., and Yennie, D. R., 1954, *Phys. Rev.*, **96**, 239.
Smith, F. M., Birnbaum, W., and Barkas, W. H., 1953, *Phys. Rev.*, **91**, 765.
Tiomno, J., and Wheeler, J. A., 1949, *Rev. Mod. Phys.*, **21**, 144.

XLIV. *Cloud Chamber Observations of Negative Heavy Mesons*

By E. G. Michaelis
Birkbeck College, London

and B. W. Powell†
The University, Manchester‡

[Received November 23, 1955]

Abstract

Earlier work by the Manchester Jungfraujoch group on slow, negative, heavy cosmic-ray particles observed in a magnet cloud chamber has been repeated. An upper limit to the frequency of slow K^--mesons which do not decay in the cloud chamber is now found to be $\sim 1\%$ of the frequency of slow protons. From other published data the probable ratio of the two frequencies is estimated as about 1 : 2000. The identity of the observed particles is discussed. The previous results giving a high frequency and a long mean lifetime for K^--mesons are not confirmed.

One event showing the possible simultaneous production of two slow K^--mesons and one example of an upward-moving S^+-particle are described.

§ 1. Introduction

Recent work with cloud chambers and nuclear emulsions has led to the identification of several species of positive K-meson. The identity of the negative K-mesons, on the other hand, is still uncertain. This is not only due to the relative infrequency of the K^--particles but also to the methods of observation. In emulsions and multi-plate cloud chambers both the nature and the sign of a decaying particle can only be determined unambiguously if the charged secondary or secondaries are π-mesons which can be followed to the end of their range. So far, no decay events of this type have been established for negative particles, most of which interact with atomic nuclei at the end of their range (σK events). In such events, however, no information on the nature of the K-particle can be obtained.

The results from magnet cloud chambers are therefore of particular interest. In such work only the τ^--meson has hitherto been identified with certainty (van Lint and Trilling 1953). There is also evidence for the χ^--meson (Armenteros *et al.* 1955 a) and in addition the observations

† Now at Imperial College, London.
‡ Communicated by Professor G. D. Rochester.

of Buchanan *et al.* (1954) indicate the existence of negative particles decaying with a mean lifetime exceeding 10^{-9} sec. Most of the results of cloud chamber and emulsion work suggest a low frequency for K^--mesons. However, the experiment of Astbury *et al.* (1953) apparently showed the existence of a negative K-particle occurring with a high frequency and having a mean lifetime exceeding 4×10^{-9} sec. The frequency of slow K^--mesons relative to protons with approximately the same velocity found by Astbury *et al.* exceeds the frequency of *all* K-mesons found by Dahanayake *et al.* (1955) in a systematic study of 'grey' tracks from nuclear interactions of energy greater than $\sim$2 Gev.

Since the results of Astbury *et al.*, if confirmed, would also suggest that not all K^--particles give rise to σK-events when brought to rest, we decided to repeat the experiment in order to obtain a better estimate of the frequency and, if possible, of the lifetime of the particles observed by them.

Our method consisted of finding tracks due to heavily-ionizing particles whose origin could be located and whose direction of flight and sign could therefore be determined. Tracks indicating particles with negative charge were further examined. Those due to light mesons were eliminated by momentum measurements and visual estimates of ionization. By choosing tracks of sufficient length the probability of including negative hyperons was made small, and it was assumed that the remaining tracks were due to K^--mesons. By correcting for the inefficiency in scanning the photographs and for the expected number of spurious events due to upward-moving protons the frequency of slow K^--particles was estimated and compared with that of slow protons.

We attempted to estimate limits to the frequency of the K^--particles by considering statistical fluctuations in their rate of occurrence and by allowing for extreme values of the scanning efficiency and of the number of spurious events. We also considered the nature of the particles observed by us and the possibility of estimating their mean lifetime.

No attempt was made to assess the frequency of K^+-mesons since the uncertainty in visual estimates of ionization prevents the separation of a small number of K^+-mesons from the much larger number of protons.

§ 2. Experimental Details and Results

The magnet cloud chamber at the Jungfraujoch has been described by Astbury *et al.* (1952) and by Newth (1954). When the photographs considered in this paper were taken, the chamber contained a wedge-shaped lead block immediately above the illuminated volume and a 12 mm copper plate across its centre. Since the earlier investigation of Astbury *et al.* (1953) the depth of the chamber has been increased so as to double its illuminated volume. The photographs used by us were therefore better suited to the observation of particles coming from well-defined origins. The results presented here were taken from 13 000 photographs, all of which were scanned at least twice.

The following criteria were used in the selection of possible K^--events:

(1) The track must show evidence of a likely origin.

(2) Its curvature must be uniform and indicate a negative charge assuming that the particle travelled downwards from its supposed origin.

(3) The ionization density of the track must be at least twice that of the track of a fast particle (i.e. $I \geqslant 2 \times I_0$).

(4) The track must be more than 10 cm long.

(5) Neither the photograph containing the track nor any neighbouring photograph must show evidence of any gross convective distortion occurring in the cloud chamber.

In establishing a likely origin it was demanded that, on three-dimensional reconstruction, the track should pass within 0·5 cm of a nuclear interaction. The limit of 0·5 cm was based on experience with the stereoscopic reprojector. The stipulation of an origin allowed the rare, downward-moving, negative particles to be distinguished from the comparatively frequent, upward-moving protons.

The requirement of uniform curvature was made to exclude tracks whose curvature is falsified by distortion at the edges of the illuminated

Measurements of Tracks of Slow Negative Particles

Serial number of event	Particle momentum (MeV/c)	Estimated ionization (I_0)	Mass of particle (m_e)
SJ 672	400^{+170}_{-90}	3 to 6	1050 to 2700
SJ 890	170 ± 25	>10	>1100
SK 560	280^{+80}_{-60}	2 to 4	550 to 1600
SQ 1437 A	152^{+22}_{-14}	>7	>850
SQ 1437 B	150^{+36}_{-30}	>6	>700

Measurements made on five tracks apparently due to negative heavy particles. The second column gives the momenta of the particles, the third the ionization density in the track and the fourth gives the mass values obtained by combining the figures from the previous columns. Event SQ 1437 is reproduced in Pl. 19.

volume of the chamber. The uniformity of the curvature was established by microscope measurements of the track. Tracks at least 10 cm long were demanded to ensure an accurate measurement of their curvature and to reduce the likelihood of their being due to negative hyperons. The mean lifetime of charged hyperons is less than 10^{-10} sec (Davies *et al.* 1955) and the mean decay length for heavily-ionizing hyperons is therefore less than 1·5 cm.

An 'origin' was defined as a nuclear interaction satisfying the following criteria:

(1) It must be situated in the lead wedge or copper plate and must lie within 6 cm of the illuminated volume of the chamber.

(2) In addition to the negative particle it must give rise to either two or more fast particles other than electrons or at least one heavily-ionizing particle.

Four events were found which fitted the criteria listed. In no case did the slow negative particle decay in flight in the cloud chamber. Details of the events are given in the table. The momenta quoted have been obtained and corrected by the method described by Barker (1954). The ionization estimates are the combined results of visual estimates by six observers; they are corrected for the dip of the tracks where necessary.

§ 3. Discussion of Events

The selection criteria listed in § 2 do not take into account the possibility that an upward-going proton without a visible origin may accidentally pass so close to a nuclear interaction in the plate or wedge that it appears as a negative particle coming from it. To estimate the number of such spurious events expected in 13 000 pictures we determined the number of tracks of upward-moving slow protons which showed no origin but otherwise fitted our selection criteria. From this number and the number of nuclear interactions observed we conclude that the expected number of spurious events in the sample is $\sim$1 for the lead wedge and $\sim$0·1 for the copper plate.

It follows that the probability of both events from the plate (SJ 672 and SK 560) being spurious is $\sim$0·01 and we therefore consider that at least one of them is genuine. Event SJ 890 from the wedge may be spurious in view of the greater probability of a chance coincidence in the wedge and of the high estimate obtained for the mass of the particle.

Event SQ 1437 (Pl. 19) is of great interest. The two steeply dipping tracks marked appear to come from a common point in the wedge. Mass estimates show that they may be due to negative K-particles. The point of intersection of the tracks is defined to within $\pm$0·2 cm. Since it lies only 1·5 cm in front of the plane marking the rear surface of

the illuminated region of the chamber it is possible that associated particles, if any, would not have been observed. From the measured rate of upward-going protons entering the wedge we estimate the probability of a chance association of two such particles to be $\sim 5\times 10^{-3}$ for a sample of 13 000 photographs.

Two events tentatively identified as the production of K^+–K^- pairs have so far been reported (Davis *et al.* 1955 and Ceccarelli *et al.* 1955 b). As interpreted these events are consistent with the formalism proposed by Gell Mann (1955). The same formalism would require the production of at least two other unstable particles to explain our event in terms of two K^--mesons. However, the possibility that our event may be spurious cannot be ruled out.

§ 4. The Relative Frequency of K^--Mesons and Protons

(i) *Estimate of Frequency*

For comparison with the results of other workers we have estimated the ratio of the frequency of our K^--particles to that of protons which have approximately the same velocity and fit our selection criteria. For this purpose it is sufficient to assume that all slow, positive, heavy particles are protons. From the number of protons found in a sample of 1000 pictures the number in 13 000 pictures was calculated to be 1070 ± 130 from the copper plate and 1900 ± 180 from the lead wedge. In this sample the scanning efficiency for slow protons was high and we assume it to have been unity. We estimate the efficiency of detecting non-decaying K^--particles in the batch of 13 000 pictures to have been about 0·5.

Assuming both events from the plate to be genuine we obtain a value for the frequency of slow K^--particles relative to that of slow protons

$$N(K^-)/N(P)=(2/1070)\times(1/0{\cdot}5)\sim 1/250.$$

The velocity ranges of the K-particles and the protons considered by us are slightly different ($0{\cdot}3\leqslant\beta\leqslant 0{\cdot}6$ and $0{\cdot}1\leqslant\beta\leqslant 0{\cdot}6$ respectively).

To estimate the upper limit of the frequency, the lower limit to the scanning efficiency is taken as 0·3 and all events which fit our criteria are considered as genuine. The possibility that the number of events present represents a fluctuation from the true mean rate is taken into account at the 5% confidence level. Values for the upper limit may be obtained for events from both the wedge and the plate. They are

$$\text{from the lead wedge}\quad N(K^-)/N(P)\leqslant 1/100,$$

$$\text{from the copper plate}\quad N(K^-)/N(P)\leqslant 1/80.$$

No useful lower limit may be set since the probability of both events from the plate being false is $\sim 0{\cdot}01$.

(ii) *Discussion*

This method assumes that the angular distributions of protons and K^--mesons are similar. It is evident that the results obtained from experiments with nuclear emulsion are free from this possible source of bias.

The upper limit to the frequency of K^--mesons disagrees with the value obtained by Astbury *et al.* (1953)† but is in agreement with other work. Armenteros *et al.* (1952), using a magnet cloud chamber, found one non-decaying, slow K^--meson among 900 protons. Since the 900 protons came from production layers both within and above the cloud chamber their result is not incompatible with ours.

In photographic emulsion Dahanayake *et al.* (1955) found ten decaying K-mesons among 2320 protons by tracing all grey tracks from cosmic ray stars to the end of their range. The results of Hornbostel and Salant (1955) and Chupp *et al.* (1955) indicate that at least 90% of artificially produced K^--mesons interact when coming to rest. If the K^--mesons in the cosmic radiation behave similarly the ten decaying K-mesons found by Dahanayake *et al.* would all be positive. Ceccarelli *et al.* (1955) in a systematic search for slow K-mesons found a value of 10 ± 3 for the ratio of the number of positive and negative particles. It follows that

$$N(K^-)/N(P)=N(K^-)/N(K^+)\times N(K^+)/N(P)\sim 1/10\times 10/2320\sim 1/2000$$

where the numbers refer to slow particles observed in nuclear emulsion.

The observed $N(K)/N(P)$ ratio will not be representative of the ratio of frequencies in other energy ranges unless the energy spectra of the two types of particle are similar. There is good evidence that the θ^0 and proton spectra differ at energies below about 200 Mev (James 1955), but it is likely that the production mechanism of K^--mesons is different from that of the majority of θ^0's (Gell Mann 1955). We therefore cannot assume the K^--spectrum to resemble either the proton or the θ^0 spectrum.

To obtain an accurate measurement of the frequency of K^--particles by our method a very large number of photographs would have to be examined. Such a search would not be worth while unless the systematic errors due to uncertainty in the scanning efficiency, spurious events, etc. could be reduced.

† We have re-examined the 10 K^--tracks found by Astbury *et al.* and find that only two fit our stricter criteria. Moreover, it has been pointed out to us by the authors of this work that there is an error in the calculation of the number of spurious events due to upward-moving protons. This arose from using the *average* number of nuclear interactions observed on the photographs to calculate the probability of a chance coincidence in space between a proton track and a nuclear interaction. If the criteria of association are not very strict it is possible for a single photograph to show so many nuclear interactions and so many proton tracks that a chance association is almost certain to arise. To estimate accurately the number of these chance associations it is necessary to consider the frequency distribution of nuclear interactions and proton tracks on the photographs. We have made a careful check of this point in our work and have found that, with our strict criterion of association, it is adequate to use the average numbers quoted above.

§ 5. Identity of the K⁻-Particles

The following modes of decay have been proposed for positive charged K-mesons :

$$\begin{aligned} K_\beta &\to \beta + ?^0 + ?^0, \\ K_\mu &\to \mu + \nu, \\ \kappa &\to \mu + ?^0 + ?^0, \\ \tau &\to \pi + \pi + \pi, \\ \tau' &\to \pi + \pi^0 + \pi^0, \\ \chi &\to \pi + \pi^0. \end{aligned}$$

The number of K_β-decays observed is small compared with the numbers of other K-decays present in photographic emulsion and none has yet been reported in cloud chamber work. Armenteros *et al.* (1955 b) have shown that the negative K_μ-meson is either very rare or non-existent, but in view of the difficulty of identification we think it possible that the K^-_μ may yet be frequent in comparison to other K⁻-particles.

Observations of decays at rest in stripped emulsions suggest either that the κ-meson is rare or that it has a very short lifetime (see Alvial *et al.* 1955).

A single magnet cloud chamber is inefficient for observing decays of long mean lifetime such as that of the τ-meson. Hence the low frequency with which τ-decays in flight are observed (9 in 100 000 photographs by our group) does not mean that non-decaying τ-mesons are rare. The existence of the negative τ-meson is well established and some or all of our events could therefore be so identified.

The situation with regard to χ^--particles is somewhat less clear, but direct evidence for their existence has recently been obtained by Armenteros *et al.* (1955 a) and Arnold *et al.* (1955 a). There is, in addition, indirect evidence from V^--events, some of which can most easily be identified as χ^--particles (Trilling and Leighton 1955). On the other hand, Alvial *et al.* (1955) have shown that slow χ^+-particles are more abundant than slow τ^+-mesons and Bridge *et al.* (1955) have found the mean lifetime of χ^+-mesons to be greater than 10^{-9} sec. Therefore the identification of our events as χ^--mesons is also possible.

In view of the scarcity of evidence on the nature of K⁻-particles with the exception of the easily identified τ-mesons there is no strong reason to assume that the relative frequencies of the different modes of decay of K⁻-mesons are different from those of the K⁺-mesons. Hence it is difficult to draw any definite conclusions on the identity of our non-decaying negative particles.

§ 6. Discussion of Lifetime

In view of the uncertainty as to the nature of the particles observed by us we are not justified in estimating a lifetime by the method of Astbury *et al.* We also point out that even by applying this method we obtain for the lower limit to the lifetime a value that is no greater than

10^{-9} sec. Buchanan *et al.* (1954) found a similar limit by the direct study of negative charged V-events. An estimate of the mean lifetime of artificially produced negative K-mesons based on decays in flight is given by Goldhaber *et al.* (1955) as $(0{\cdot}65\pm0{\cdot}45)\times10^{-8}$ sec. but Arnold *et al.* (1955 b) find evidence for a short-lived component among V^--events not due to hyperons.

§ 7. A Probable S-Event

In the course of our work we found one event which does not fit all our selection criteria but which is apparently an upward-moving, positive K-meson which comes to rest and decays in the copper plate. The event is reproduced in Pl. 20 and the measurements are given in the caption to the plate. While we recognize that the event may be a small nuclear interaction in the plate in which a negative K-meson is produced, we do not regard this interpretation as likely and we note that the number of upward-moving protons stopping in the plate is $\sim$200. We should therefore expect to find about one stopping K^+-meson.

§ 8. Conclusions

An upper limit of $\sim1\%$ has been found for the ratio of the frequencies of K^--particles with velocities $0{\cdot}3\leqslant\beta\leqslant0{\cdot}6$ to protons with $0{\cdot}1\leqslant\beta\leqslant0{\cdot}6$. This limit is compatible with the results of other groups. A most probable ratio of $\sim1/2000$ has been deduced from the available evidence. No definite conclusion as to the identity of the particles has been drawn.

The previous results of Astbury *et al.* (1953) concerning the frequency and mean lifetime of these particles have not been confirmed.

One event has been found which can be interpreted as the simultaneous production of two K^--mesons, another is probably an S-event due to an upward-moving, positive K-meson.

Acknowledgments

We thank our colleagues, Mr. A. H. Chapman, Mr. W. A. Cooper, Mr. G. D. James, Miss P. Miles, Mr. J. A. Newth and Mr. R. A. Salmeron for their help in obtaining and analysing the results presented. Professor G. D. Rochester and Professor P. M. S. Blackett have encouraged our work and made financial provision for it.

We are indebted to Mr. H. Wiederkehr and to the Administration of the Hochalpine Forschungsstation, Jungfraujoch, for making our work in Switzerland possible. One of us (B. W. P.) has received a grant from the Department of Scientific and Industrial Research during our work.

References

Alvial, G., Bonetti, A., Di Corato, M., Dilworth, C., Levi Setti, R., Milone, A., Occhialini, G., Scarsi, L., and Tomasini, G., 1955, *Report of the Pisa Conference on Elementary Particles* (to be published in *Il Nuovo Cimento*).

ARMENTEROS, R., BARKER, K. H., BUTLER, C. C., CACHON, M., and YORK, C. M., 1952, *Phil. Mag.*, **43**, 597.

ARMENTEROS, R., ASTIER, A., D'ANDLAN, C., GREGORY, B., HENDEL, A., HENNESSY, J., LAGARRIGUE, A., LEPRINCE-RINGUET, L., MUELLER, F., PEYROU, C., and RAU, R. R., 1955 a, *Report of the Pisa Conference.*

ARMENTEROS, R., GREGORY, B., HENDEL, A., LAGARRIGUE, A., LEPRINCE-RINGUET, L., MUELLER, F., and PEYROU, C., 1955 b, *Nuovo Cim.*, **1**, 914.

ARNOLD, W. H., BALLAM, J., HODSON, A. L., LINDEBERG, G. K., RAU, R. R., REYNOLDS, G. T., and TREIMAN, S. B., 1955 a, *Report of the Pisa Conference.*

ARNOLD, W. H., BALLAM, J., REYNOLDS, G. T., ROBINSON, K. M., and TREIMAN, S. B., 1955 b, *Report of the Pisa Conference.*

ASTBURY, J. P., CHIPPINDALE, P., MILLAR, D. D., NEWTH, J. A., PAGE, D. I., RYTZ, A., and SAHIAR, A. B., 1952, *Phil. Mag.*, **43**, 1283.

ASTBURY, J. P., BUCHANAN, J. S., CHIPPINDALE, P., MILLAR, D. D., NEWTH, J. A., PAGE, D. I., RYTZ, A., and SAHIAR, A. B., 1953, *Phil. Mag.*, **44**, 241.

BARKER, K. H., 1954, *Nuovo Cim.*, **11**, Suppl. 2, 309.

BRIDGE, H. S., DE STAEBLER, H., ROSSI, B., and SREEKANTAN, B. V., 1955, *Nuovo Cim.*, **1**, 874.

BUCHANAN, J. S., COOPER, W. A., MILLAR, D. D., and NEWTH, J. A., 1954, *Phil. Mag.*, **45**, 1025.

CECCARELLI, M., GRILLI, M., MERLIN, M., SALANDIN, G., and SECHI, B., 1955 a, *Report of the Pisa Conference.*

CECCARELLI, M., GRILLI, M., MERLIN, M., SALANDIN, G., SECHI B., 1955 b, *Nuovo Cim.*, Ser. X, **2**, 828.

CHUPP, W. W., GOLDHABER, G., GOLDHABER, S., and WEBB, F. H., 1955, *Report of the Pisa Conference.*

DAHANAYAKE, C., FRANCOIS, P. E., FUJIMOTO, Y., IREDALE, P., WADDINGTON, C. J., and YASIN, M., 1955, *Nuovo Cim.*, **1**, 888.

DAVIES, J. H., EVANS, D., FOWLER, P. H., FRANCOIS, P. E., FRIEDLANDER, M. W., HILLIER, R., IREDALE, P., KEEFE, D., MENON, M. G. K., PERKINS, D. H., and POWELL, C. F., 1955, *Report of the Pisa Conference.*

GELL MANN, M., 1955, *Report of the Pisa Conference.*

GOLDHABER, G., GOLDHABER, S., ILOFF, E., LANNUTTI, J. E., WEBB, F., WIDGOFF, M., PEVSNER, A., and RITSON, D., 1955, *Report of the Pisa Conference.*

HORNBOSTEL, J., and SALANT, E. O., 1955, *Phys. Rev.*, **98**, 218.

JAMES, G. D., 1955, *Report of the Pisa Conference.*

NEWTH, J. A., 1954, *Nuovo Cim.*, **11**, Suppl. 2, 297.

TRILLING, G. H., and LEIGHTON, R. B., 1955, *Phys. Rev.* (in the press).

VAN LINT, V. A. J., and TRILLING, G. H., 1953, *Phys. Rev.*, **92**, 1089.

XLV. *On the Dislocation Theory of Evaporation of Crystals*

By N. Cabrera and M. M. Levine
Physics Department, University of Virginia, Charlottesville, Va., U.S.A.†

[Received October 24, 1955]

Abstract

A complete treatment is given of the steady state spiral both in growth and evaporation of crystals, taking account of the strain energy around the dislocation. It is shown that when the crystal is evaporating there is a limiting value of the undersaturation beyond which there is no steady state solution of the problem. The core of the dislocation is then unable to remain closed and a macroscopic pit appears at the termination of the screw dislocation.

§ 1. Introduction

Although a theory of the spiral on growing crystals was developed a number of years ago by Frank (1949), and Burton, Cabrera and Frank (1951), there has been no attempt to extend the treatment to evaporating crystals. (The word evaporation is here understood in its general sense, that is to say, including dissolution, chemical etching, oxidation, etc.) Such an extension is particularly important in view of its possible application to the understanding of the formation of etch pits at dislocations. This paper develops such a theory and gives as well a more complete treatment of the steady state spiral in growing crystals. To distinguish between growth and evaporation it is necessary to take account of the supplementary energy localized around the dislocation itself. As a first approximation we consider only the strain energy, although other factors such as the effect of impurities must be taken in account if we want to understand completely the formation of etch pits. We limit ourselves of course, to dislocations finishing at the surface with a screw component, and giving rise to steps on the surface: the extension to pure edge dislocations has to be made from a different point of view and will be considered in a separate paper.

In § 2 a fundamental expression for the velocity of advance of a step on the crystal surface will be introduced and a discussion will be given of the conditions under which it is expected to be correct. In § 3, the theory of the steady state spiral will be developed both for growing and evaporating crystals. Finally a discussion of the physical implications of the results obtained will be given in § 4.

† Communicated by the Authors.

§ 2. The Movement of Steps

The basis of the treatment of the spiral given in § 3 is the following expression for the normal velocity of advance v of an element of step on the crystal face, located at a distance r from the point of emergency of the dislocation and having a local radius of curvature ρ :

$$v=v_\infty[1-(\rho_c/\rho)-(r_0\rho_c/r^2)]. \quad . \quad . \quad . \quad . \quad . \quad . \quad (1)$$

The quantities v_∞, ρ_c and r_0 have the following meaning :

(i) v_∞ is the velocity of a straight step far from the origin.

(ii) ρ_c is the radius of the critical nucleus for two-dimensional nucleation on the crystal surface, given by

$$\rho_c=\gamma\Omega/\Delta\mu_0, \quad . \quad . \quad . \quad . \quad . \quad . \quad . \quad . \quad (2)$$

where γ is the surface energy per unit surface of the edge of the step, Ω the volume per molecule in the crystal and $\Delta\mu_0$ the difference in chemical potential of a molecule in the surrounding medium and in the crystal (supposed perfect). According to whether $\Delta\mu_0 \gtrless 0$ the crystal is growing or evaporating.

(iii) Finally r_0 is given by

$$r_0=\mu\mathbf{b}^2/8\pi^2\gamma, \quad . \quad . \quad . \quad . \quad . \quad . \quad . \quad . \quad (3)$$

where μ is the shear modulus and $\mathbf{b}$ the Burgers vector of the dislocation. r_0 represents a measure of the strain energy around the dislocation ; it is assumed that the dislocation is normal to the crystal surface.

A justification for the right-hand member of (1), can be given in the following manner : If the advance of the step is controlled by some diffusion field, the velocity of advance should be proportional to the difference in chemical potential in the surrounding medium far and near the step. Assuming equilibrium to be maintained near the step this difference is $\Delta\mu_0$ if the step is straight and far from the origin ; if this is not the case, there are two main contributions which will change this difference by altering the chemical potential near the step : (i) the curvature $1/\rho$ of the step increases the latter by $\gamma\Omega/\rho=(\rho_c/\rho)\Delta\mu_0$, (ii) the presence of a dislocation normal to the surface of the crystal introduces a density of strain energy roughly equal to $\mu\mathbf{b}^2/8\pi^2r^2$ and consequently an increase of the chemical potential $\mu\mathbf{b}^2\Omega/8\pi^2r^2=(r_0\rho_c/r^2)\Delta\mu_0$. These two effects decrease $\Delta\mu_0$ by the factor appearing at the right-hand side of (1).

It will be noticed that (1) is valid for both growth ($\Delta\mu_0>0$) and evaporation ($\Delta\mu_0<0$). In the latter case the radii of curvature ρ_c and ρ become negative, this does not change the sign of the second term in (1) but changes the sign of the third term because the strain energy due to the presence of the dislocation opposes growth and favours evaporation. We must also mention that, in taking account of the strain energy during a steady state process, we must consider the strain at the interior of the crystal, as the strain near the surface will continuously reproduce itself. Finally the length, r_0, has no physical meaning for small $\mathbf{b}$ and large γ

being then smaller than the atomic dimensions ; however, if **b** is large and γ small, Frank (1951) showed that the dislocation should have a hollow core of radius given by (3) where now γ is the surface energy of the surface of the hollow, which is not necessarily equal to our γ. In what follows the two γ's will be assumed equal, which is a good simplifying assumption for close packed surfaces.

Finally, let us emphasize that eqn. (1) is valid only under the following conditions : (i) the step is far away from any other step so that the diffusion fields are independent of each other ; (ii) the curvature of the step is everywhere small, so that it cannot advance by surface nucleation ; (iii) the influence of the crystallographic orientation of the step is completely neglected.

Conditions (i) and (ii) are satisfied only for low $|\Delta\mu_0|$ (large $|\rho_c|$). Condition (iii) should be satisfied provided equilibrium around the step is maintained ; this is likely to be true for atomic steps advancing under any kind of diffusion field. There are also cases, where the condition seems to be satisfied for a multi-atomic step centred on a dislocation of large Burgers vector (for instance the spirals in SiC crystals) ; our treatment will include these cases. The reasons for these multiatomic steps to remain together instead of separating into many atomic steps will not be discussed here.

§ 3. Theory of the Spiral

Going back now to our problem, it is well known that a step should wind itself in a spiral around the point of emergence of the dislocation, and that the steady state of this spiral should be represented by a rotating one with the equation

$$\theta = f(r) - \omega t, \quad . \quad . \quad . \quad . \quad . \quad . \quad . \quad . \quad . \quad . \quad (4)$$

in polar coordinates, where ω is the angular velocity of (let us say) clockwise rotation of the spiral. In terms of ω the rate of growth (or evaporation) R of the crystal and the distance d between successive turns of the spiral far from the centre are given by

$$R = \omega b'/2\pi, \quad d = 2\pi v_\infty/\omega, \quad . \quad . \quad . \quad . \quad . \quad . \quad . \quad (5)$$

where b' is the height of the step as well as the component of the Burgers vector of the dislocation normal to the surface.

Our problem is then to find the function $f(r)$ and the value of ω, by using the expression (1). In polar coordinates, the normal velocity v of advance of the step and its radius of curvature ρ are given by

$$v = -r\dot{\theta}/[1+(r\theta')^2]^{1/2}, \quad \rho = [1+(r\theta')^2]^{3/2}/[2\theta' + r\theta'' + r^2\theta'^3],$$

where

$$\dot{\theta} = \partial\theta/\partial t = -\omega, \quad \theta' = \partial\theta/\partial r.$$

Replacing v and ρ in (1) we obtain the equation

$$r\omega[1+(r\theta')^2] = v_\infty[1-(r_0\rho_c/r^2)][1+(r\theta')^2]^{3/2} - v_\infty\rho_c[2\theta' + r\theta'' + r^2\theta'^3].$$

By introducing the new non-dimensional variables s, ϕ given by

$$r=s\rho_c, \quad r(\partial\theta/\partial r)=s(\partial\theta/\partial s)=\tan\phi, \quad \ldots\ldots \quad (6)$$

where ϕ is clearly the angle between the radius vector and the tangent to the step, the differential equation reduces to

$$\phi'=[1-(s_0/s^2)]\sec\phi-(1/s)\tan\phi-\omega_1 s, \quad \ldots\ldots \quad (7)$$

where the notations

$$r_0=s_0\rho_c, \quad \omega=\omega_1 v_\infty/\rho_c, \quad \ldots\ldots \quad (8)$$

have been used. The non-linear eqn. (7) has to be solved for $\phi(s)$ and ω_1 given the boundary conditions at both large and small s. In terms of ω_1, R and d are given by

$$R=\omega_1 b' v_\infty/2\pi\rho_c, \quad d=(2\pi/\omega_1)\rho_c. \quad \ldots\ldots \quad (9)$$

In all the cases we are going to consider, it will be assumed that the crystal is so large that the step becomes circular at large s; developed in inverse powers of s the solution is easily shown to be

$$\phi(s)=\tfrac{1}{2}\pi-1/(\omega_1 s)+1/(\omega_1 s^2)-\ldots, \quad s\gg 1. \quad \ldots \quad (10)$$

At small s we must consider several cases according to whether s_0 is negligible or not, and in the later case, whether growth or evaporation is occurring.

3.1. $s_0=0$: *Growth and Evaporation*

For small Burgers vector **b** and large γ, the length r_0 is of the order of atomic dimensions, therefore s_0 is negligible particularly for the large values of ρ_c (10^{-4} cm or more), in which we are specially interested. We begin then by assuming $s_0=0$ altogether, which implies that there is no difference between growth and evaporation.

Under those conditions, the step should reach the centre $s=0$. The solution for s small is then easily found to be

$$\phi(s)=\tfrac{1}{2}s-\tfrac{1}{3}\omega_1 s^2+\ldots, \quad s\ll 1, \quad \ldots\ldots \quad (11)$$

giving the right curvature $1/\rho_c$ at the centre. The corresponding value $\omega_1=0{\cdot}33$ is then obtained by matching the two solutions (10) and (11). The complete solution $\phi(s)$ is represented in fig. 1 ($s_0=0$) and the corresponding spiral is shown in fig. 2. It should be noticed that the distance between successive turns reaches very rapidly the limiting value $d=19\rho_c$. The radius of curvature of the step becomes very rapidly large with respect to ρ_c so that for purposes of calculating, for instance, diffusion fields the spiral can be replaced by concentric circles distant d from each other.

This solution assumes however, that the point of emergence of the dislocation remains anchored as the spiral turns around. On the other hand, the step finishing at the dislocation has an energy per unit length (tension $t=\gamma b'$) which is not small with respect to the tension T of the dislocation itself (see Nabarro 1952); consequently it should tend to make the dislocation move. When growth occurs near the melting

Fig. 1

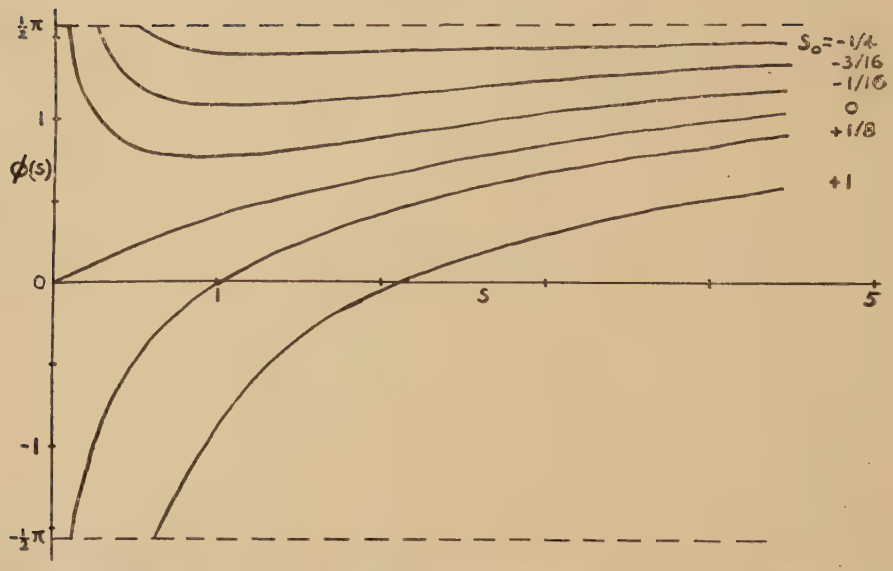

Representing the angle $\phi(s)$ between the radius vector s and the tangent to the spiral, for the different spirals corresponding to different values of the parameter s_0 (see text). $s_0<0$ corresponds to evaporation, $s_0>0$ to growth.

Fig. 2

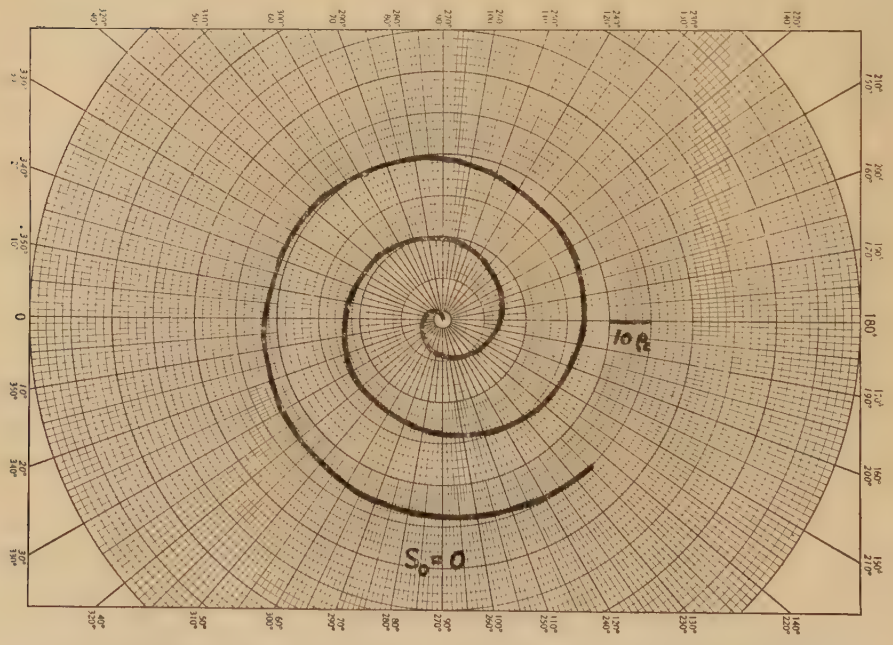

Theoretical spiral, when the strain energy at the dislocation is neglected ($s_0=0$).

point it might be assumed that the dislocation can climb as well as glide ; then, assuming that the dislocation is anchored at a distance h beneath the surface (say $h \sim 10^{-4}$ cm) the point where the dislocation meets the surface should turn in a circle of radius r' of the same order as h, or more precisely $r'=ht/2T[1-(t/2T)^2]^{1/2}$ if image forces are taken in account. The end of the step should remain tangential to the radius vector. Therefore if we define $r'=s'\rho_c$ the solution near s' should be

$$\phi(s)=\tfrac{1}{2}(s-s')-\tfrac{1}{3}\omega_1(s-s')^2+\ldots,$$

and the value of ω_1 would change with s'. For a value $s'=1$ we find $\omega_1=0{\cdot}28$, which does not differ very much from the value for $s'=0$. If growth occurs at lower temperatures, at which only glide can occur, the dislocation should move in its gliding plan and the point of emergency should oscillate around $s=0$.

3.2. $s_0>0$: *Growth*

For large Burgers vector **b** and/or small γ, s_0 is not negligible. Taking the characteristic values $\gamma \sim 5\times 10^2$ erg/cm^2, $\mu \sim 5\times 10^{11}$ erg/cm^3, and a small rate of growth corresponding to $\Delta\mu_0 \sim 10^{-15}$ erg, s_0 is larger than $0{\cdot}1$ if b is larger than 10^{-7} cm which is known to occur in polytypes. On the other hand, the dislocation should have at equilibrium a hollow core of radius $r_0>10^{-5}$ cm, which would make it immobile.

For a given value of $s_0>0$, we want a solution of (7) representing a step which becomes circular as it approaches a limiting radius c (as yet undetermined and not equal to s_0) representing the radius of the hollow core of the dislocation during growth. The boundary condition for $s\to c$ must be then $\phi \to -\frac{1}{2}\pi$, the minus sign because the step is now turning in the reverse sense to what it does at large s. For every value of ω_1, there is a solution of (7) which cuts $\phi=-\frac{1}{2}\pi$ at a certain value c of s. All those solutions however, are of the form $\phi=-\frac{1}{2}\pi+a(s-c)^{1/2}$ unless c is the positive root of

$$c^2+c-s_0=0. \qquad (12)$$

In this case the solution is of the form

$$\phi=-\tfrac{1}{2}\pi+a(s-c), \quad s\to c, \qquad (13)$$

with a given by $\quad c^2a^2+\omega_1c^3a+1+2c=0.$

This latter solution is the one we are interested in, as it is the only one to satisfy the further condition $\theta \to -\infty$ as $s\to c$, necessary for a hole to exist. The radius of this hole $r_0'=c\rho_c$ has the following value :

$$r_0'=\tfrac{1}{2}\rho_c\{[1+4(r_0/\rho_c)]^{1/2}-1\}\,; \qquad (14)$$

it tends to r_0 for very large ρ_c and decreases slowly as ρ_c decreases.

The complete solution $\phi(s)$ for any value of s_0, and the corresponding value $\omega_1(s_0)$, can then be found by numerical integration. Figure 1 includes the solutions for $s_0=\frac{1}{8}$ and for the rather extreme value $s_0=1$. Figure 3 gives the curve $\omega_1(s_0)$ $(s_0>0)$ which is seen to decrease very slowly as s_0 increases.

Fig. 3

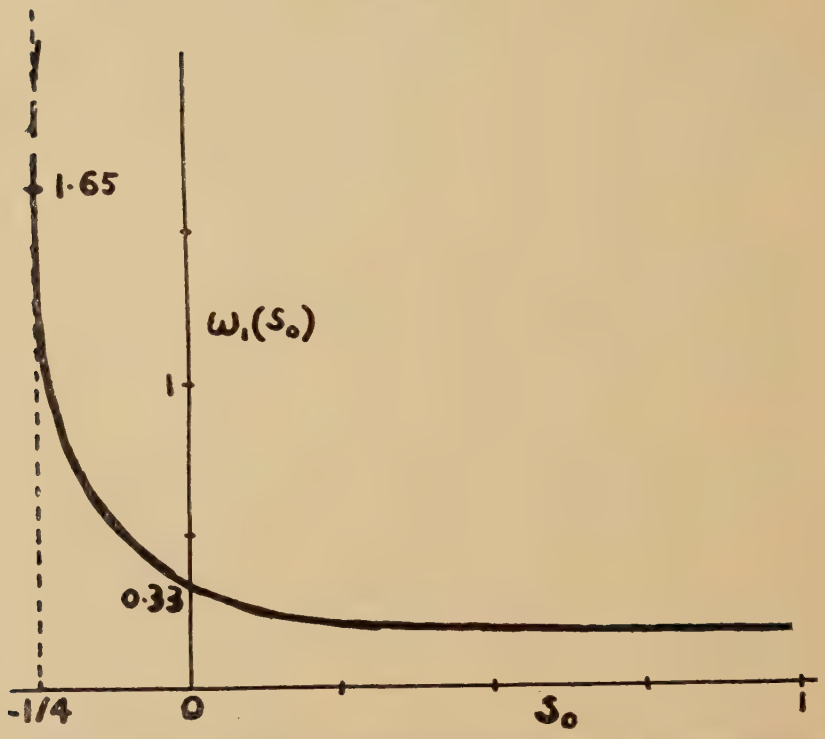

Angular frequency ω_1 of rotation of the spiral in units $v_\infty \rho_c$, for different values of the parameter s_0 (see text). $s_0<0$ corresponds to evaporation, $s_0>0$ to growth.

3.3. $s_0<0$: *Evaporation*

It is then useful to redefine s and s_0 as positive quantities, that is to say $r=|\rho_c|s$. Equation (7) becomes

$$\phi'=[1+(s_0/s^2)]\sec\phi-(1/s)\tan\phi-\omega_1 s.$$

The boundary condition for $s\to c$ (c is again still undetermined) is now $\phi\to\frac{1}{2}\pi$ as the step does not change its sense of rotation with respect to s large. The solution for $s\to c$ is then given by

$$\phi=\tfrac{1}{2}\pi-a(s-c), \quad s\to c, \qquad \ldots\ldots\ldots \quad (15)$$

provided the value of c is determined from the equation

$$c^2-c+s_0=0. \qquad \ldots\ldots\ldots \quad (16)$$

and a is calculated from

$$c^2a^2-\omega_1 c^3 a+2c-1=0.$$

The two roots of (16) are now positive (provided $s_0<\frac{1}{4}$, see below); however, it will be shown in § 4 that only the smallest root corresponds

to a minimum for the free energy of the evaporating crystal. The radius $r_0'=c|\rho_c|$ of the hollow core of the dislocation becomes then

$$r_0'=\tfrac{1}{2}|\rho_c|\{1-[1-4(r_0/|\rho_c|)]^{1/2}\}, \quad . \quad . \quad . \quad . \quad . \quad (17)$$

which is, of course, the same as (14) if $\rho_c=-|\rho_c|$. The important point in this expression is that for $|\rho_c|<4r_0$ there is no real solution of (16), and therefore no steady state spiral. The physical implications of this result will be discussed in § 4.

In fig. 1, several solutions ($s_0<0$) are given, including the limiting one for $s_0=\frac{1}{4}$. The curve $\omega_1(s_0)$ is represented in fig. 3 ($s_0<0$), it is seen that ω_1 increases very rapidly as $s_0\to\frac{1}{4}$. At $s_0=\frac{1}{4}$, $\omega_1(\frac{1}{4})=1{\cdot}65$ and joins, with a vertical tangent, the curve $\omega_1'(s_0)$ for the solutions corresponding to the second root of eqn. (16).

§ 4. Discussion

The physical reason for the formulae (14) or (17) giving the radius of the hollow core of the dislocation does not appear clearly in the argument of § 3. The following, more general derivation (Cabrera *et al.* 1954) might clarify this point. Let a crystal with a hollow dislocation of radius r be growing from or evaporating into a medium, the difference in chemical potential of a molecule in the medium and in the crystal being $\Delta\mu_0$. An increase of r to $r+dr$ will produce a change dG in the free energy of the crystal per unit length of dislocation given by

$$\begin{aligned} dG&=(2\pi r/\Omega)\Delta\mu_0\,dr+2\pi\gamma\,dr-2\pi r(\mu\mathbf{b}^2/8\pi r^2)\,dr \\ &=(2\pi\gamma\rho_c/r)(c^2+c-s_0)\,dr, \end{aligned}$$

where the notations used in § 3, $r=c\rho_c$, $r_0=s_0\rho_c$ have been introduced, and the explicit assumption that γ remains constant has been made. The roots of (12) or (16) make, therefore, G stationary. It is also seen that the positive root of (12) and the smallest root of (16) make G a minimum. It is therefore concluded that the radius r_0' of the hollow core of the dislocation remains at the value (14) or (17) while the crystal grows or evaporates.

The more interesting result in this paper is the existence of a critical value $|\Delta\mu_{0c}|$ for $|\Delta\mu_0|$ beyond which a dislocation in an evaporating crystal cannot remain closed; otherwise, it must 'open-up'. Then the crystal evaporates from the free surface as well as sidewise from the core of the dislocation outwards, forming a macroscopic pit. At the critical value itself ($|\rho_c|=4r_0$) the radius of the core $r_0'=2r_0$ remains submicroscopic. The critical value $|\Delta\mu_{0c}|$ is given by

$$|\Delta\mu_{0c}|=2\pi^2\gamma^2\Omega/\mu\mathbf{b}^2, \quad . \quad . \quad . \quad . \quad . \quad . \quad . \quad (18)$$

where (2) and (3) have been used. In the simplest cases of evaporation into a vapour or dissolution into a diluted solution we can write

$|\Delta\mu_0| = kT \ln(p_0/p)$ where p_0 is the saturation pressure (concentration) and p the actual one occurring above the crystal; then we obtain

$$p_c/p_0 = \exp[-2\pi^2\gamma^2\Omega/kT\mu\mathbf{b}^2],$$

where p_c is the critical pressure below which the dislocation should open-up. To illustrate the numerical values that we should expect let us assume $\gamma \sim 5\times10^2$ erg/cm^2, $\mu \sim 5\times10^{11}$ erg/cm^3, $\Omega \sim 10^{-22}$ cm^3, $kT \sim 10^{-13}$ erg. Then we obtain $(p_0-p_c)/p_0 \sim 10^{-2}$ if $b \sim 10^{-6}$ cm and $(p_c-p_0) \sim 10^{-4}$ if $b \sim 10^{-8}$ cm. This indicates that a very low undersaturation will be sufficient to open-up a dislocation of large Burgers vector; on the contrary very large undersaturations might be necessary to open up dislocations with an elementary Burgers vector. The actual values of p_c p_0 will of course be very sensitive to the assumed value for γ.

Another result worth further discussion is the value obtained for the semi-vertical angle β of the conical surface of the crystal. As long as $|\Delta\mu_0|$ is small, it is well known that the surface remains practically flat so that β is practically equal to $\frac{1}{2}\pi$. This is also true for the obtainable values of $\Delta\mu_0$ above a growing crystal. In the case of an evaporating crystal it is interesting to consider the value of β when the critical value $|\Delta\mu_{0c}|$ is attained. Then

$$\tan\beta = d/b = 0{\cdot}19\times\mu b/\gamma.$$

Assuming the same characteristic values for μ and γ we get $\tan\beta \sim 2\times10^8\, b$ (b being measured in cm) which indicates that β remains very nearly $\frac{1}{2}\pi$ for a large Burgers vector but diminishes to values of the order of $\pi/3$ when $b \sim 10^{-8}$ cm.

The application of the results of this paper to dislocations of small Burgers vector, when the critical value $|\Delta\mu_{0c}|$ is approached, should be considered doubtful. Then the value of ρ_c is so small that the basic expression (1) should not be valid anymore, particularly because the internal part of the spiral should then be able to advance by surface nucleation. The importance of surface nucleation in the formation of etch pits is also implied in the fact that etch pits *do* form also at pure edge dislocations. This point of view will be developed in a forthcoming paper.

Acknowledgments

We are pleased to acknowledge the continuous help of Dr. J. S. Plaskett of this Department, during the development of this paper. We are also glad to acknowledge the support of the U.S. Office of Naval Research.

References

Burton, W. K., Cabrera, N., and Frank, F. C., 1951, *Phil. Trans. Roy. Soc.*, **243**, 299.

Cabrera, N., Levine, M. M., and Plaskett, J. S., 1954, *Phys. Rev.*, **96**, 1153.

Frank, F. C., 1949, *Disc. Faraday Soc.* No. **5**, 5; 1951, *Acta Cryst.*, **4**, 497.

Nabarro, F. R. N., 1952 *Advances in Physics* **1**, 269.

XLVI. *Cyclotron Resonance under Anomalous Skin Effect Conditions*

By R. G. Chambers
The Royal Society Mond Laboratory, Cambridge†

[Received December 8, 1955]

Summary

The purpose of this note is to discuss the results to be expected from attempts to observe cyclotron resonance in metals. A brief summary is first given of the simple theory for a free-electron model, assuming the classical skin-effect equations to hold. Theoretical results are then given for a free-electron model under anomalous skin effect conditions, and a qualitative discussion is given of the results to be expected for a real metal under these conditions.

The theory of cyclotron resonance is most simply formulated if the r.f. fields within the conductor are assumed to be circularly polarized, so that e.g., $E=E_x+iE_y=E_0\,e^{i\omega t}$ (where E_0 may be complex), and the steady field H is applied in the z direction. Then for a degenerate gas of quasi-free electrons of mass m^* and relaxation time τ, it is easily shown that the conductivity σ_C is given by

$$\sigma_C=\sigma_0/(1+i\omega'\tau) \quad . \quad . \quad . \quad . \quad . \quad . \quad . \quad . \quad (1)$$

where σ_0 is the d.c. conductivity $Ne^2\tau/m^*$ and $\omega'=\omega-\omega_C=\omega-eH/m^*c$. This expression holds under 'classical' conditions, when the mean free path of the electron is small compared with the skin depth. If, instead of being circularly polarized, the applied electric field is linearly polarized, so that $E=E_x=R(E_0e^{i\omega t})$ the resultant currents are given by $J_x=R(\sigma_L E_0 e^{i\omega t})$, $J_y=R(\sigma_T E_0 e^{i\omega t})$, where

$$\sigma_L=\tfrac{1}{2}[\sigma_C(\omega_C)+\sigma_C(-\omega_C)],\ \sigma_T=-\tfrac{1}{2}i[\sigma_C(\omega_C)-\sigma_C(-\omega_C)], \quad . \quad . \quad . \quad (2)$$

and the values thus found for σ_L and σ_T agree with those given by Dresselhaus, Kip and Kittel (1955 a, b). If on the other hand the current is linearly polarized, $J=J_x=R(J_0e^{i\omega t})$, then $E_x=R(\rho_L J_0 e^{i\omega t})$, etc., and

$$\rho_L=\tfrac{1}{2}[\rho_C(\omega_C)+\rho_C(-\omega_C)],\ \rho_T=-\tfrac{1}{2}i[\rho_C(\omega_C)-\rho_C(-\omega_C)]\ ;\ (\rho_C=1/\sigma_C), \quad (3)$$

and using (1) and (3) we have

$$\rho_L=\rho_0(1+i\omega\tau),\ \rho_T=-\rho_0\omega_C\tau. \quad . \quad . \quad . \quad . \quad . \quad . \quad (4)$$

If now a specimen obeying these 'classical' equations is of thickness large compared with the skin depth the quantity observable experimentally is the surface impedance $Z=E(0)/I_t$, where $E(0)$ is the electric

---

† Communicated by the Author.

field at the surface and I_t is the total current flowing in the skin. We consider three simple cases :

(*a*) If the specimen is placed with its surface in the x–y plane and subjected to the r.f. field $E_x+iE_y=E_0e^{i\omega t}$ and the steady field H_z, the currents induced by the r.f. field will flow parallel to the surface, and the surface impedance Z_c will be given by the expression

$$Z_c^2=4\pi i\omega/\sigma_C c^2 \quad . \quad . \quad . \quad . \quad . \quad . \quad . \quad . \quad . \quad . \quad (5)$$

(Gaussian units) so that

$$Z_c=(4\pi\omega/\sigma_0 c^2)^{1/2}(i-\omega'\tau)^{1/2}. \quad . \quad . \quad . \quad . \quad . \quad (6)$$

(*b*) If the applied r.f. field, instead of being circularly polarized, is arranged so that either $E(0)$ or I_t is linearly polarized, the associated surface impedances Z_L and Z_T can be obtained from Z_c using equations similar to (2) and (3) respectively, with σ, ρ replaced by $1/Z$, Z ; the resulting expressions agree with those given by Dresselhaus, Kip and Kittel (1955 b) and Donovan and Sondheimer (1953). (See also Donovan 1954, 1955.)

(*c*) If the specimen is arranged with its surface in the x–z plane, we can no longer assume the r.f. fields and currents to be circularly polarized in the x–y plane, since we must now have $J_y=0$ (apart from the negligible currents needed to set up the space charges producing the Hall field E_y) ; we must consider a linearly polarized current J_x and apply eqns. (4). We then have $Z^2=4\pi i\omega\rho_L/c^2$, so that, from (4), Z is independent of ω_C and H_z entirely. These results have already been obtained and discussed briefly by Anderson (1955).

Now in attempting to observe cyclotron resonance experimentally conditions are normally chosen so that both ω and τ are as large as possible, since only if $\omega\tau$ is large compared with unity can the resonance point $\omega_C=\omega$ be located accurately. But in any reasonably good metallic conductor the electronic mean free path will then be much greater than the skin depth, so that conditions are ' anomalous ' rather than classical, and eqns. (1)–(6) are no longer applicable. The problem must now be reformulated taking the finite free path into account. This is readily done for a quasi-free electron model using the ' kinetic ' approach (Chambers 1952) and it turns out that for the geometry of case (*c*) above the problem is quite insoluble analytically, but that cases (*a*) and (*b*) are more tractable ; for case (*a*) in particular the integral equation to be solved is formally identical with that occurring in the ordinary theory of the anomalous skin effect (Reuter and Sondheimer 1948, eqn. (18)), except that the quantity $a=\omega\tau$ occurring in that equation has to be replaced by $\omega'\tau$.† The variation of Z_c with $\omega'\tau$ is thus identical with the variation of Z with $\omega\tau$ in ordinary anomalous skin effect theory, for which

† After completing this paper, it was found that Azbel' and Kaganov (1954) had arrived at the same formulation ; these authors however discuss only the behaviour in the classical and extreme anomalous limits.

series expansions and tables have been given by Dingle (1953). His tables cover only positive values of $\omega\tau$, because only these are relevant for $H=0$, but in cyclotron resonance negative values of $\omega'\tau$ must also be considered. His series expansions (6.3) and (6.4) have therefore been used to calculate values of Z_c for $\omega'\tau<0$.

The resultant curves are shown in the figure, where R_c/R_0 and X_c/X_0 are plotted against $-\omega'\tau=(e\tau/m^*c)H_z-\omega\tau$. Here $Z_c=R_c+iX_c$, and R_0, X_0 are the values of R_c, X_c for $\omega'\tau=0$. Curves are shown for several different values of the parameter α introduced by Reuter and Sondheimer : if $\delta=(c^2/2\pi\omega\sigma_0)^{1/2}$ is the classically calculated skin depth, neglecting relaxation, and l is the electronic mean free path, $\alpha=3l^2/2\delta^2$. Thus the classical limit corresponds to $\alpha\ll 1$ and the extreme anomalous limit to $\alpha\gg 1$. Now for most pure metals at 4°K and at microwave frequencies, $\alpha\sim 10^4$–10^8 ; it will be seen from the figure that under these conditions the variation of R_c/R_0 with $-\omega'\tau$ is very much less marked than in the classical

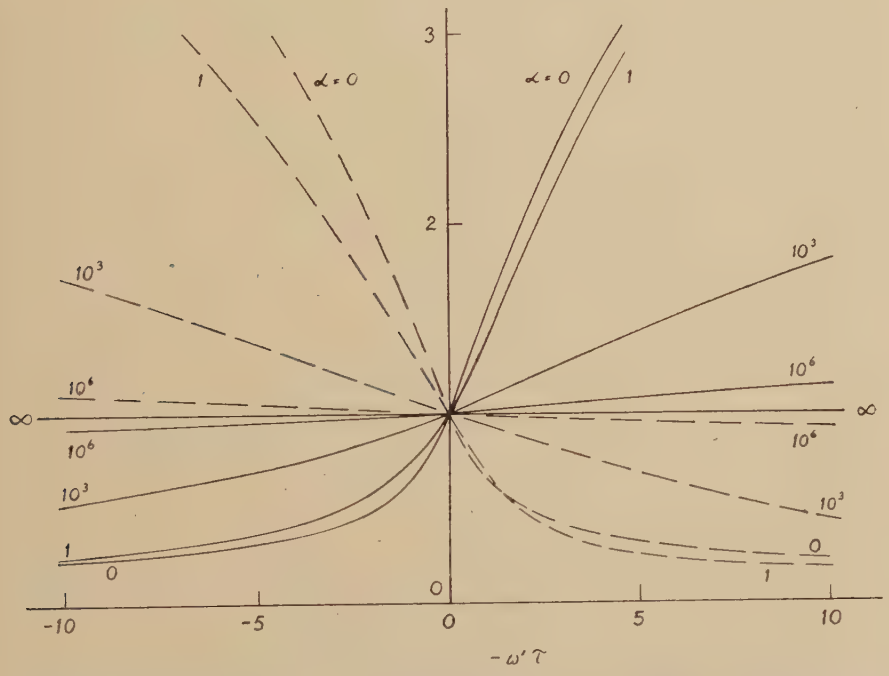

The variation with $-\omega'\tau$ of R_c/R_0 and X_c/X_0, for different values of the parameter α.

limit $\alpha=0$, and extremely accurate measurements would be needed to locate the ' resonance ' point $\omega_C=\omega$ at all closely. If the applied r.f. field is linearly rather than circularly polarized, corresponding to case (*b*) above, the values of Z_L and Z_T can again be obtained from Z_c by using equations similar to (2) or (3) ; they vary even more slowly with $\omega'\tau$. These results

thus confirm Kittel's (1954) suggestion that failure to observe cyclotron resonance in metals might be due to the large values of l/δ encountered.

If we write α in the alternative form

$$\alpha=\left[\frac{3\pi}{c^2}\,\frac{\sigma}{l}\,v^2\right]\frac{(\omega\tau)^3}{\omega^2},$$

where v is the velocity of electrons at the Fermi surface, and put $\sigma/l\sim10^{23}$ Gaussian units, $v\sim10^8$ cm/sec, representative of the values occurring in metals, we find $\alpha\sim10^{27}(\omega\tau)^3/\omega^2$. Now from the figure, we need $\omega\tau\gtrsim2$ and $\alpha\lesssim100$ say if experimental results are to lead to any useful estimate of m^*: we thus require $\omega\gtrsim10^{13}\,\mathrm{sec}^{-1}$, or a wavelength $\lambda\lesssim200\,\mu$. And at $\omega=10^{13}\,\mathrm{sec}^{-1}$, if $m^*\sim m$, the resonance condition $\omega_C=\omega$ requires a steady magnetic field $H_z\sim5\times10^5$ gauss. On this basis, therefore, there seems to be little hope of cyclotron resonance becoming a useful tool in the study of metals.

We now have to consider how far these results are likely to apply to real metals. For this purpose it is helpful to introduce resistive and reactive skin depths δ_r and δ_i, such that in the classical region, where $E(z)=E(0)\,\mathrm{e}^{-kz}$, $1/\delta_r+i/\delta_i=k$. In the anomalous region, $E(z)$ is no longer exponential, but we can define δ_r and δ_i by

$$1/\delta_r+i/\delta_i=-(dE/dz)_0/E(0)=4\pi i\omega_c c^2Z_c,$$

so that δ_r and δ_i can be derived from the measured surface impedance. Now for the free-electron model in the 'almost classical' region, the departure of R_c from its classical value is proportional to $l\,\delta_r$, and that of X_c to $l/\delta_i\sqrt{(1+\omega'^2\tau^2)}$. It is plausible to assume that similar results will hold for more complex models or for real metals, and that R_c or X_c will begin to depart from classical behaviour when a suitably averaged value of l or $l/\sqrt{(1+\omega'^2\tau^2)}$ becomes appreciable compared with δ_r or δ_i. In the anomalous region, where these ratios are large, we may expect that, as for the free-electron model, R_c and X_c will vary with H_z much more slowly than predicted classically. Thus, for example, minority carriers of small m^* will probably produce a much less clear-cut perturbation of R_c than the classical theory (Anderson 1955) predicts.

More complex models and real metals will differ from the free-electron model in three main respects. First, because of the spread of values of m^* and the presence of holes as well as electrons, different parts of the Fermi surface will 'resonate' at different values of H_z, resulting in an even greater blurring-out of the curves. Secondly, in any but the simplest models v_z for a given electron will vary periodically with time, so that the angle between the direction of motion and the surface of the metal will vary periodically. This makes the anomalous skin effect problem insoluble analytically, even for a simple spheroidal Fermi surface, but the 'ineffectiveness concept' approach (Pippard 1947, 1954) suggests that it may tend to increase both R_c and X_c somewhat when $|\omega_C\tau|$ becomes comparable with unity. Thirdly, any more realistic model will give a

non-zero d.c. magneto-resistance effect, and similarly the classically calculated values of Z_c, and of δ_r and δ_i, will tend to increase with $|H_z|$ more rapidly than for the free-electron model. For most metals, however, we shall still have $\delta_r \ll l$ up to the highest values of $|H_z|$ likely to be used, so that the metal will still be well in the anomalous region; the tendency to approach the classical region as $|H_z|$ increases will merely confuse the experimental results still further. For bismuth, however, the d.c. magneto-resistance is extremely large, and the results of Galt *et al.* (1955) suggest that a field $|H_z| \sim 1$ kg may increase δ_r sufficiently to restore approximately classical conditions. Working at 4°K and 24 000 Mc/s, they found that R_c rose rapidly from its zero-field value as $|H_z|$ was increased up to about 1 kg, and thereafter varied much less rapidly and followed a course resembling that for a classical free-electron model. Now at 4°K and 24 000 Mc/s, the zero-field value of l/δ_r for Bi is probably $\sim$100–1000, corresponding to $\alpha \sim 10^4$–10^6 (cf. Pippard and Chambers 1952, Chambers 1953); clearly we must suppose the effective value in fields >1 kg to be much smaller, to account for the observed results. Thus it is thought that the 'trough' in R_c around zero field is a magneto-resistance effect; only for $|H_z| \gtrsim 1$ kg can the results be interpreted, tentatively, on a classical model, and then only if calculation shows that in this region l/δ_r is not too large. Anderson (1955) has suggested an alternative interpretation of the trough, assuming the classical eqn. (5) to hold, in terms of a small contribution to σ_C from minority carriers of very small m^*. It is thought that this interpretation must be rejected, however, not only because in zero-field conditions (5) is certainly not valid, but also because, even if (5) were valid, a peak or a 'dispersion curve' would be obtained rather than a trough, unless m^* for the minority carriers exceeds m^* for the majority carriers, which is quite incompatible with Anderson's interpretation.

It has been suggested (Dyson, private communication) that a more pronounced resonance might be obtained in metals under anomalous conditions if measurements could be made on a film of thickness t small compared with the skin depth (and so, *a fortiori*, small compared with l), instead of on bulk metal. Even if such extremely thin films could be reliably produced, however, it is doubtful whether they would in fact show a very pronounced resonance: for the limiting case $t \ll \delta \ll l$, where we may assume E constant across the film, it is easily found that for a free-electron model Z_c is given by

$$\frac{1}{Z_c} = \frac{3\sigma_0 t^2}{4l}\left[\ln\left(\frac{1}{\kappa}\right) + 0{\cdot}4228 + \tfrac{2}{3}\kappa \ldots\right] \quad . \quad . \quad . \quad . \quad . \quad (7)$$

where $\kappa = t(1+i\omega'\tau)/l$ (cf. Fuchs 1938, Sondheimer 1950, eqns. (12), (25)), so that, for example, if $t/l = 10^{-2}$, R_c increases by only 4% as $|\omega'\tau|$ increases from 0 to 1, and the minimum in R_c at resonance is extremely

broad. We may note also that in the opposite limiting case of a classical thin film, with $l \ll t \ll \delta$, we have simply

$$Z_c = (1+i\omega'\tau)/\sigma_0 t \quad . \quad . \quad . \quad . \quad . \quad . \quad . \quad . \quad (8)$$

so that R_c shows no resonance effects at all.

Finally, it may be worth emphasizing the extent to which the effects observed in cyclotron resonance experiments will depend on the experimental arrangement. Any conductor placed in a static electric field normal to its surface will tend to screen out the field so that none appears in the interior. But if the conduction electron concentration is low enough, as in a semiconductor, the screening is imperfect, and if an r.f. field of sufficiently high frequency is used instead of a static field, it breaks down completely, so that the electric induction inside the conductor is equal to that outside. Thus if a small piece of the material is placed in a resonant cavity in a region of high electric field, the rate of power dissipation W will be proportional to $E^2R(\sigma)$, and since the stored energy in the cavity is proportional to E^2, the Q of the cavity (after correcting for other losses, including coupling losses) will be inversely proportional to $R(\sigma)$. If the concentration of carriers is higher, their effect in screening out the applied field can no longer be neglected ; it has been discussed in terms of the ' plasma frequency ' by Dresselhaus, Kip and Kittel (1955 b). For a metal, of course, the screening-out of a normally applied field E is practically perfect, even at the highest microwave frequencies, and if the only way of inducing a current to flow in a metal was by putting a small isolated specimen in a region of high electric field, it would indeed be impossible to observe cyclotron resonance in metals, even under classical skin effect conditions (Kittel 1954). But in fact currents can be perfectly easily induced by making the specimen part of the wall of the cavity, in a region of high r.f. magnetic field : the current flow is then everywhere tangential to the surface and ' plasma ' effects do not arise (cf. also Anderson 1955). We then have $W \propto I_t^2R(Z)$, or $W \propto H_t^2R(Z)$, where H_t is the magnetic field at the surface of the metal ; since the stored energy in the cavity is proportional to H_t^2, we now have the corrected Q of the cavity varying inversely with $R(Z)$.

The fact that a well-defined resonance peak is predicted theoretically for semiconductors but not for metals, even on classical skin effect theory, is due simply to the difference in experimental arrangements : semiconductors are measured under essentially constant-voltage conditions, so that $W \propto R(\sigma)$, and metals under constant-current conditions, so that $W \propto R(Z)$. If it were possible to measure a semiconductor under constant current conditions, with $W \propto R(\rho)$, no resonance would be observed (cf. (1) ; cf. also (8)) ; conversely, if a metal obeying (6) could be measured under constant voltage conditions, with $W \propto R(1/Z)$, a well-defined though asymmetrical peak would be obtained at $\omega'\tau = -1/\sqrt{3}$. However, under anomalous conditions the peak broadens out and the position of the maximum shifts (e.g. to $\omega'\tau \sim -9$ at $\alpha = 1000$), so that

even if such measuring conditions could be realized experimentally, cyclotron resonance experiments on metals would remain of doubtful value.

Acknowledgments

I am indebted to the workers at Berkeley and at the Bell Telephone Laboratories for showing me their results before publication, and to Professor F. J. Dyson, Dr. A. B. Pippard and Dr. D. Shoenberg for discussions.

References

Anderson, P. W., 1955, *Phys. Rev.*, **100,** 749.
Azbel', M. I., and Kaganov, M. I., 1954, *Doklady Akad. Nauk.*, **95,** 41.
Chambers, R. G., 1952, *Proc. Phys. Soc.* A, **65,** 458 ; 1953, *Physica*, **19,** 365.
Dingle, R. B., 1953, *Physica*, **19,** 311.
Donovan, B., 1954, *Proc. Phys. Soc.* A, **67,** 305 ; 1955, *Ibid.*, **68,** 1026.
Donovan, B., and Sondheimer, E. H., 1953, *Proc. Phys. Soc.* A, **66,** 849.
Dresselhaus, G., Kip, A. F., and Kittel, C., 1955 a, *Phys. Rev.*, **98,** 368 ; 1955 b, *Ibid.*, **100,** 618.
Fuchs, K., 1938, *Proc. Camb. Phil. Soc.*, **34,** 100.
Galt, J. K., Yager, W. A., Merritt, F. R., Cetlin, B. B., and Dail, H. W., Jr., 1955, *Phys. Rev.*, **100,** 748.
Kittel, C., 1954, *Proceedings of the 10th Solvay Congress.*
Pippard, A. B., 1947, *Proc. Roy. Soc.* A, **191,** 385 ; 1954, *Ibid.*, **224,** 273.
Pippard, A. B., and Chambers, R. G., 1952, *Proc. Phys. Soc.* A, **65,** 955.
Reuter, G. E. H., and Sondheimer, E. H., 1948, *Proc. Roy. Soc.* A, **195,** 336.
Sondheimer, E. H., 1950, *Phys. Rev.*, **80,** 401.

XLVII. *The Photoproduction of Charged Mesons from Calcium*

By W. R. Hogg and D. Sinclair
Department of Natural Philosophy, University of Glasgow†

[Received December 28, 1955]

Summary

The yields of π^- and π^+ mesons from calcium have been measured at 90° to a photon beam with a maximum energy of 330 ± 10 Mev. The mesons were detected in nuclear emulsions. The ratio of the numbers of π^- to π^+ mesons was determined to be $0{\cdot}86\pm0{\cdot}18$ at a pion energy of 80 Mev. Above 95 Mev the ratio fell rapidly to $0{\cdot}39\pm0{\cdot}12$ at 112 Mev. Approximate values for the cross sections for the production of π^+ and π^- mesons, as a function of pion energy, were also determined.

The experimental results may be given a semiquantitative explanation by the theory of Butler (1952). Preliminary calculations by Moorhouse and Laing (private communication) are in fairly good agreement with the measured data.

§ 1. Introduction

Littauer and Walker (1952) have measured the yields of π^- and π^+ mesons from a wide range of nuclei. Their results were obtained by observing pions with kinetic energies in the interval 50–80 Mev at an angle of 135° to a photon beam with a maximum energy of 310 ± 10 Mev. The yield of negative to positive mesons (π^-/π^+ ratio) from calcium was $0{\cdot}58\pm0{\cdot}06$. This ratio showed the greatest deviation from unity for the symmetric nuclei investigated. Motz *et al.* (1955), using a linear accelerator to produce a bremsstrahlung beam with a maximum energy of 300 Mev, obtained a value of $0{\cdot}70\pm0{\cdot}03$ for the π^-/π^+ ratio for calcium. In this experiment, mesons in the energy interval 43 to 63 Mev were detected at an angle of 75° to the direction of the photons. Both results are lower than the value calculated by Butler (1952) from a computation of the relative densities of neutrons and protons at the surface of the calcium nucleus.

The present paper describes measurements made on the yields of π^- and π^+ mesons from calcium as a function of their kinetic energy. Mesons emitted at 90° to the photon beam, with energies in the interval 60 to 120 Mev, were detected in nuclear emulsions. The irradiating flux was a bremsstrahlung spectrum from the Glasgow electron synchrotron with photons of a maximum energy of 330 ± 10 Mev.

† Communicated by Professor P. I. Dee, F.R.S.

§ 2. Exposure of the Plates

The plates used in the experiment were Ilford G5 and C2 nuclear emulsions of 100 microns thickness and total area 4 in. × 2 in. The geometry employed is shown in fig. 1 ; the top edge of each plate was 6·4 cm from the centre of the calcium target and the copper absorber was 2·20 cm thick. To provide a homogeneous medium for stopping the mesons, eight plates were spaced at regular intervals in a slab of glass about 2 in. thick, and of the same composition as that used as a backing for the emulsions. Thus the emulsions were used to sample the number of mesons stopping in the glass as a function of distance from the target.

Fig. 1

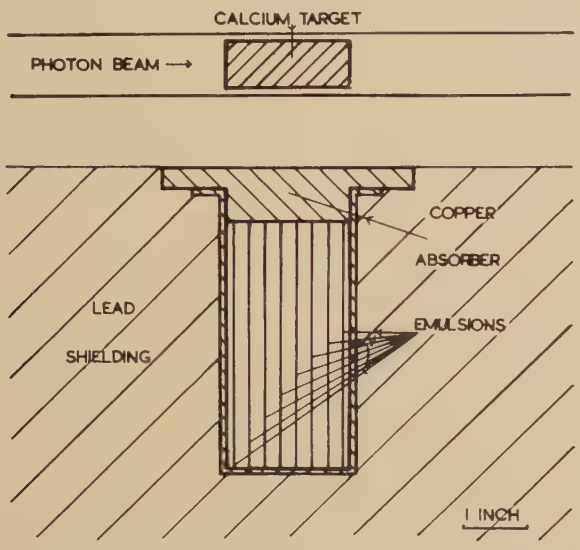

Experimental arrangement used to measure the yield of charged mesons from calcium at 90° to the direction of the photon beam.

With this geometry, the top edges of the plates received mesons with a maximum angular spread of $\pm 37°$ and a probable angular spread of $\pm 11°$ about a direction at right angles to the photon beam. while for the bottom edges of the plates the maximum and the probable angular spreads were $\pm 15°$ and $\pm 5°$ respectively. The kinetic energies of the mesons were obtained from range–energy relationships for the materials traversed (i.e. calcium, copper and glass). Mesons in the energy interval 60 to 120 Mev could be detected with the apparatus.

§ 3. Collection of Data

The combined results of Menon *et al.* (1950) and Adelman (1952) indicate that $(48{\cdot}7 \pm 0{\cdot}9)\%$ of all the π^- mesons ending in Ilford C2 emulsions have two or more secondary tracks, and $(23{\cdot}3 \pm 0{\cdot}7)\%$ have

only one secondary track. Since all π^+ mesons ending in an emulsion produce single-pronged events (viz. π–μ decays), the ratio of π^- to π^+ mesons in a given number of events is simply

$$\frac{\sigma_n}{0{\cdot}487\left\{\sigma_1 - \frac{0{\cdot}233}{0{\cdot}487}\sigma_n\right\}}$$

where σ_n is the number of mesons which end with two or more secondary tracks and σ_1 is the number which end with only one secondary track. This method of separation overcomes the uncertainties involved in distinguishing (*a*) μ mesons from π^- mesons with no secondary track, and (*b*) π–μ decays from π^- mesons with only one secondary track.

The plates were scanned for meson endings with one or more secondary tracks, and the position and nature of each event was noted, using the same convention for a star prong as that used by the authors referred to above. Several areas of each plate were scanned twice to determine the efficiency of scanning. The efficiency values obtained are indicated by comparing the figures given in columns 3 and 5 of the table with those in columns 4 and 6.

(1)	(2)	(3)	(4)	(5)	(6)	(7)	(8)
62– 83	80·2	146±12	218±26	63±7·9	70·5± 9·3	0·78±0·16	0·86±0·18
82– 89	87·6	183±14	246±22	67±8·2	76·6±10·1	0·75±0·14	0·84±0·16
88– 98	94·2	175±13	237±28	57±7·6	68·8±11·1	0·69±0·16	0·78±0·18
97–106	103·0	104±10	123±15	27±5·2	31·8± 6·5	0·60±0·16	0·69±0·19
106–119	111·9	91±10	109±14	14±3·7	16·4± 4·6	0·33±0·11	0·39±0·12

(1) Energy interval (Mev); (2) mean energy (Mev); (3) observed number of one-prongs; (4) corrected number of one-prongs (σ_1); (5) observed number of stars; (6) corrected number of stars (σ_n); (7) uncorrected π^-/π^+ ratio; (8) π^-/π^+ ratio corrected for absorption.

The total yield of charged mesons at 90° (laboratory coordinates) was found as a function of meson energy, and is given in fig. 2. Due to uncertainties in the beam calibration, the absolute scale of the differential cross section has an estimated error of ±30%.

The data for the analysis of the π^-/π^+ ratio are contained in the table, and the ratio as a function of pion energy is shown in fig. 3. At each point the errors given are statistical standard deviations, and include statistical errors arising from the efficiency determinations. The solid curves show the results when corrected for meson absorption. These corrections, although small (~10%), are somewhat uncertain. The method used is therefore given in an appendix.

§ 4. Discussion

The energy distribution of mesons obtained in the present work is consistent with a description in which the production arises from an interaction of the photon with a single nucleon in the nucleus. Butler

(1952) has shown that this production process, compared to that from a free nucleon, is modified as follows :

(*a*) As a result of the spread in the momentum of nucleons in the target nucleus, there exists no unique photon energy corresponding to a given energy and angle of emission of the meson. Instead, for each energy and angle of emission of the meson there corresponds a band of photons available for meson production.

Fig. 2

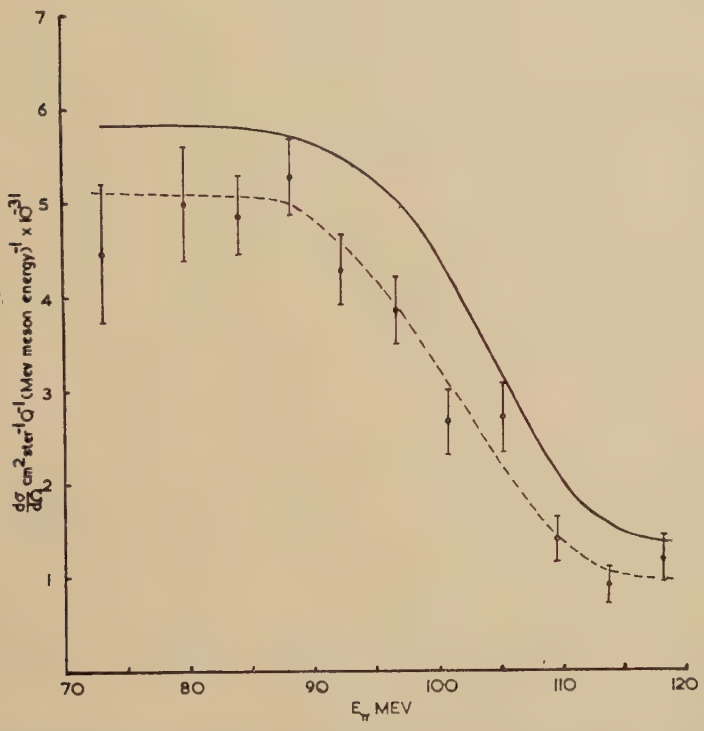

Energy distribution of charged mesons produced from calcium at 90° by a bremsstrahlung beam with a maximum energy of 330 ± 10 Mev. The solid curve shows the yield when corrected for absorption.

(*b*) In general, for a given energy and angle of emission of the meson, the average energy of the photons available for production from a nucleus is different from the photon energy required for production from a free nucleon. The difference depends upon the binding energies of the target nucleons, and the interactions of the recoiling nucleons and mesons with the product nucleus. These interactions include the Coulomb interaction.

The rapid change in the π^-/π^+ ratio above 95 Mev can be explained in terms of the differing positions on the bremsstrahlung spectrum of the bands of photons available for the production of the π^- and π^+ mesons respectively, and the existence of a cut off in the spectrum at 330 Mev.

As an illustration, we shall consider the factors influencing the production of π^- and π^+ mesons emitted at 90° to the photon direction, with energies of 90 and 110 MeV. In the case of meson production from the surface of the nucleus, Butler (1952) has estimated that the bands of photons are about 50 MeV wide, and that they are centred (approximately) about the photon energy required for production from a free nucleon. We shall further

Fig. 3

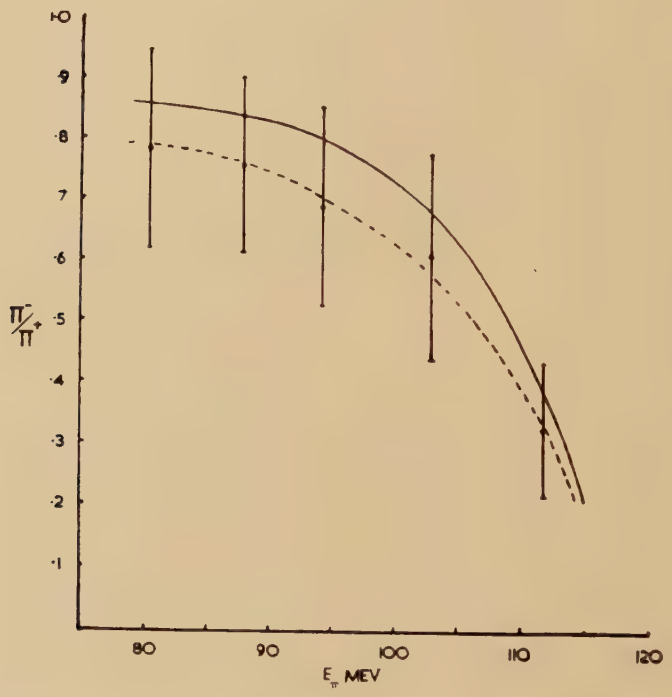

π^-/π^+ ratio as a function of pion energy for mesons produced from calcium at 90° by a bremsstrahlung beam with a maximum energy of 330 ± 10 MeV. The solid curve shows the ratio corrected for absorption.

assume that, on the average, the photon energy required for the production of the π^- meson is 10 MeV greater than that for the production of the π^+. A difference in energy of this magnitude would appear reasonable when considering the differences in the binding energies of the last neutron and proton in the ^{40}Ca nucleus. Thus a π^- meson emitted at 90° to the photon direction with a kinetic energy of 90 MeV has available for its production a range of photon energies in the bremsstrahlung spectrum from about 290 MeV to the cut-off at 330 MeV, while for a π^+ meson of the same kinetic energy and angle of emission the photon energies available are 280 to 330 MeV. At a higher kinetic energy of the pion, say 110 MeV, the photon

energies available for the production of the π^- and π^+ meson are respectively 320 to 330 Mev and 310 to 330 Mev. Thus a variation of the π^-/π^+ ratio with pion energy of the type observed will result in this way.

The value of the ratio at lower meson energies is in agreement with the value of 0·8 obtained by Butler (1952) by considering only the relative neutron and proton surface densities for calcium. The ratio obtained by Littauer and Walker (1952), as pointed out by Butler, is in a region where the effects of the cut-off in the photon spectrum cannot be neglected.

Preliminary calculations by Moorhouse and Laing (private communication), using an independent particle model with an oscillator potential, are in fairly good agreement with the experimental data for pion energies below about 100 Mev. The calculated results of these workers for the π^-/π^+ ratio are 0·79, 0·73 and 0·56 at pion energies of 80, 100 and 120 Mev respectively. Above about 100 Mev, the π^-/π^+ ratio becomes very sensitive to the shape of the bremsstrahlung spectrum and its maximum energy.

It is hoped that an examination of the production at different angles to the photon direction will throw more light on the production process. If this process can be regarded as a modified free nucleon production, then the meson energy at which the total yield becomes small, and at which the π^-/π^+ ratio rapidly varies, will be sensitive to the angle of production.

Acknowledgments

The authors wish to thank Dr. E. H. Bellamy and Dr. H. Muirhead for many stimulating discussions, and for their help in all possible ways. We are grateful to Dr. W. McFarlane and his associates of the Synchrotron Group for their co-operation in exposing the plates. We wish to thank Professor P. I. Dee for his interest and encouragement throughout the course of the work.

We are both indebted to the Department of Scientific and Industrial Research for the award of a grant which enabled us to carry out the research.

APPENDIX

The number of pions dN absorbed in a thickness dx of absorber is given by the relation

$$\frac{dN}{N} = -n\,\sigma\,dx \quad . \quad . \quad . \quad . \quad . \quad . \quad . \quad . \quad (1)$$

where n is the number of nuclei in unit volume of the absorber and σ is the absorption cross section. The difference in the absorption of positive and negative pions is given by

$$\frac{dN^-}{N^-} - \frac{dN^+}{N^+} = -n(\sigma^- - \sigma^+)dx \quad . \quad . \quad . \quad . \quad . \quad . \quad (2)$$

where the superscripts refer to the sign of the meson. Bernardini *et al.* (1951), Bernardini and Levy (1951), and Ferretti and Manaresi (1955) have measured the mean free paths of π^- and π^+ mesons in nuclear emulsions. The combined results of these workers indicate that the quantity $(\sigma^- - \sigma^+)$ is independent of the kinetic energy of the meson in the range 10 to 90 Mev. Using this result, eqn. (2) may be integrated to obtain the relation

$$\frac{N_0^-}{N_0^+} = \frac{N^-}{N^+} \exp\{n(\sigma^- - \sigma^+)x\}$$

where N_0 is the flux of mesons at the source.

This relation was used to correct the observed π^-/π^+ ratio (i.e. the ratio N^-/N^+ in the above notation) to the ratio at the source. An average of the results of the authors given above yielded a value of 0·26 barns for $(\sigma^- - \sigma^+)$, where σ is the cross section for star production together with inelastic scattering by the nuclei of an emulsion, excluding hydrogen. Since the average geometrical cross section of the elements in the glass was 0·67 of that for the complex nuclei in a nuclear emulsion, the quantity $(\sigma^- - \sigma^+)$ for glass was taken to be $0{\cdot}67 \times 0{\cdot}26$, to give 0·17 barns. For copper $(\sigma^- - \sigma^+) = 0{\cdot}46$ barns, a value found experimentally by Cassels (reported by Burcham 1955). Both these values have large experimental errors ($\sim 30\%$). A change of 30%, however, in the value of $(\sigma^- - \sigma^+)$ alters the value of the π^-/π^+ ratio by only 5%.

References

Adelman, F. L., 1952, *Phys. Rev.*, **85**, 249.
Bernardini, G., Booth, E. T., and Lederman, L., 1951, *Phys. Rev.*, **83**, 1075.
Bernardini, G., and Levy, F., 1951, *Phys. Rev.*, **84**, 610.
Burcham, W. E., 1955, *Nature, Lond.*, **176**, 371.
Butler, S. T., 1952, *Phys. Rev.*, **87**, 1117.
Ferretti, L., and Manaresi, E., 1955, *Nuovo Cimento*, **1**, 512.
Littauer, R. M., and Walker, D., 1952, *Phys. Rev.*, **86**, 838.
Menon, M. G. K., Muirhead, H., and Rochat, O., 1950, *Phil. Mag.*, **41**, 583.
Motz, H., Crowe, K. M., and Friedman, R. M., 1955, *Phys. Rev.*, **98**, 268.

XLVIII. *Thermodynamic Relations Applicable near a Lambda-transition*

By A. B. Pippard†
Institute for the Study of Metals, University of Chicago‡

[Received January 2, 1956]

It is well known that there are not many examples of higher-order transitions which can be justifiably compared with Ehrenfest's theory of such transitions. The specific heat C_p at a λ-transition does not usually exhibit a well-defined discontinuity (the superconducting transition is exceptional in this respect), but rather rises on the low-temperature side to a very high maximum whose ultimate height appears to be limited only by the shortcomings of experimental technique. This behaviour, while diminishing the practical value of Ehrenfest's method of approach, makes it possible to derive simple relations between various thermodynamic quantities which should be applicable in the vicinity of the λ-transition.

The entropy, considered as a function of temperature and pressure, rises steeply to a vertical or nearly vertical tangent along the λ-line, and the analytical form of the entropy surface is dominated by this circumstance. In the neighbourhood of the λ-line the surface may be regarded as cylindrical in the sense that the only principal curvature of significance is that in plane sections normal to the λ-line. If then we assume that over short distances the λ-line is straight and the entropy on the λ-line is a linear function of temperature, we may write for $S\,(p, T)$ the equation of a cylinder of arbitrary section whose generators are parallel to the λ-line,

$$\text{i.e. } S\,(p, T)=S_0+aT+f\,(\alpha T-p), \quad . \quad . \quad . \quad . \quad . \quad (1)$$

in which S_0 and a are constants, f is a function describing the nature of the approach of the entropy to the λ-point, and α is the pressure coefficient of the λ-point, $(dp/dT)_\lambda$. From (1) it follows that

$$\frac{\partial^2 S}{\partial T^2}=\alpha^2 f'', \quad \frac{\partial^2 S}{\partial T\,\partial p}=-\alpha f'' \quad \text{and} \quad \frac{\partial^2 S}{\partial p^2}=f'' ;$$

hence, by use of Maxwell's relations, over a short temperature interval

$$\left(\frac{\partial C_p}{\partial T}\right)_p=\alpha V T_\lambda\left(\frac{\partial \beta}{\partial T}\right)_p \quad \text{and} \quad \left(\frac{\partial C_p}{\partial p}\right)_T=\alpha V T_\lambda\left(\frac{\partial \beta}{\partial p}\right)_T, \quad . \quad (2)$$

in which β is written for

$$\frac{1}{V}\left(\frac{\partial V}{\partial T}\right)_p,$$

the volume coefficient of expansion. From (2) we see that over such regions as the cylindrical approximation is justified (and it becomes

† On leave from the Royal Society Mond Laboratory, Cambridge, England.
‡ Communicated by the Author.

increasingly more exact as the λ-line is approached) C_p and β are linearly related,

$$C_p = \alpha V T_\lambda \beta + \text{const.} \quad . \quad . \quad . \quad . \quad . \quad . \quad . \quad . \quad (3)$$

A similar argument applies to the volume, whose behaviour may be seen from (3) to follow that of the entropy closely, and yields

$$\beta = \alpha K + \text{const.} \quad . \quad . \quad . \quad . \quad . \quad . \quad . \quad . \quad (4)$$

in which K is the isothermal compressibility.

Fig. 1

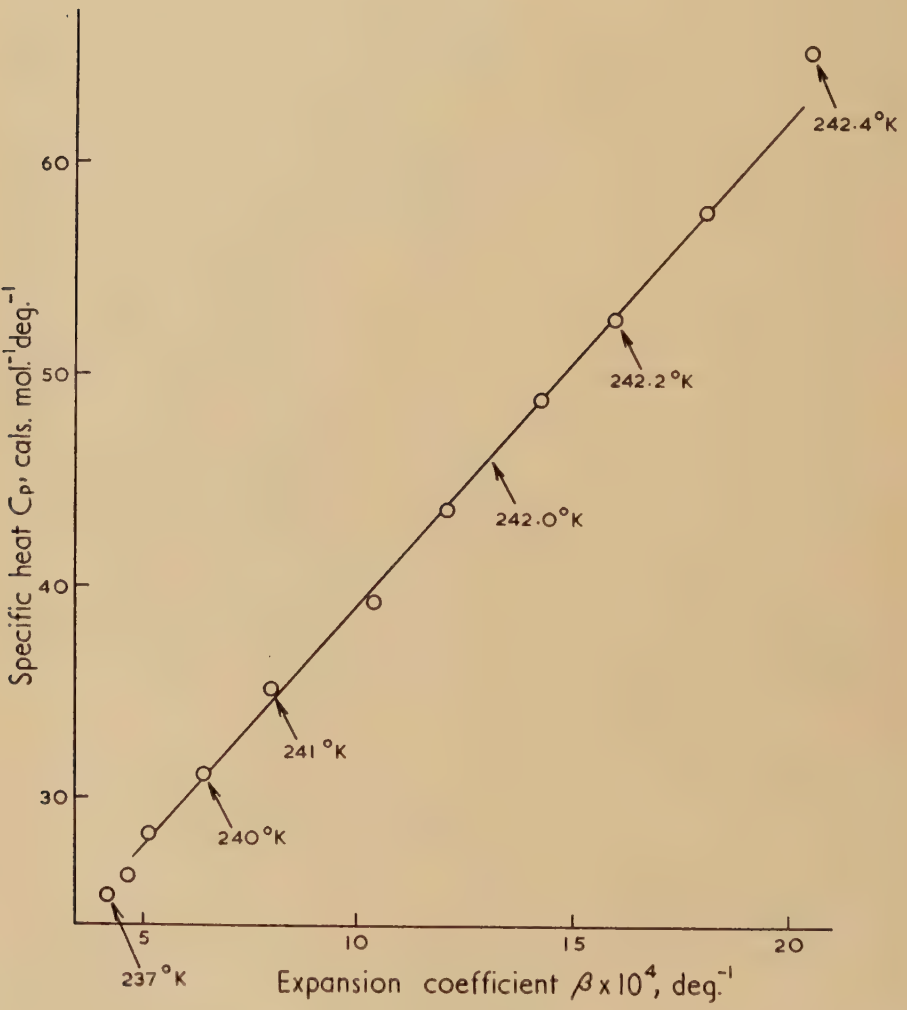

C_p v. β for NH_4Cl.

It is easy to see that at a true second-order transition, where the slope of the entropy surface changes abruptly, (3) and (4) yield Ehrenfest's relations for the discontinuities in C_p, β and K. It should be mentioned

that Kuper's (1955) analysis of the λ-transition implies (3) and (4); in fact there is no particular novelty attached to these equations, except that they do not appear to be derived explicitly anywhere in the literature.

The work of Simon, von Simson and Ruhemann (1927) and of Lawson (1940) on ammonium chloride provide suitable data for checking (3). In fig. 1 C_p is plotted against β, values of the temperature being shown along the line (the transition temperature is 242·8°K). A remarkably good straight line is obtained, from which it may be inferred that the cylindrical approximation holds over at least four degrees below the transition temperature, that is, the shape of the specific heat curve is not highly pressure-dependent. From the slope of this line the temperature coefficient

Fig. 2

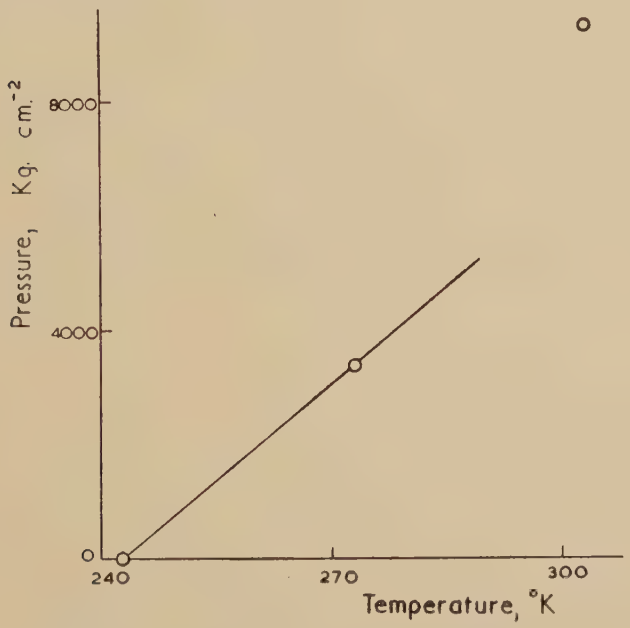

T_λ v. p for NH_4Cl. The line is drawn at the slope deduced from fig. 1.

is deduced as 113 kg cm^{-2} deg^{-1}. Figure 2 shows the transition temperature at zero pressure and two transition temperatures at high pressures, according to Bridgman (1931), together with the calculated slope of the λ-line at zero pressure. In view of the poverty of points the agreement may be regarded as satisfactory. Agreement with the data immediately above the transition temperature is not so good, the discrepancy being such as to suggest that the measured values of C_p are too high. This concords with an observation by Ziegler, quoted by Lawson (1940). The data for ammonium chloride have also been examined by Davies and Jones (1953) in connection with their thermodynamic theory of glasses, and been found not to be in accord with equations which they have derived on the basis of a model of the ordering process, and which bear a superficial

similarity to (3) and (4). In view of the good agreement found here with a purely phenomenological theory it seems likely that their discrepancy does not arise from the experiments so much as from the model or their interpretation of the parameters appearing therein.

An attempt to check the equations by means of the λ-point in liquid helium was not so successful. The values of C_p quoted in the literature are not accurate enough to be useful in this connection, so that only the validity of (4) can be examined. The data given by Atkins and Edwards (1955) on β and K appear good in themselves, but the value of α deduced from them differs by a factor of 2 from that measured directly. This discrepancy may be eliminated by assuming that the temperature scales for the two sets of data are shifted relative to one another by 0·001°K. An error of this magnitude is only too probable in practice. One may conclude from this comparison that if the validity of (3) and (4) be accepted, the equations may provide a sensitive test of experimental data in the neighbourhood of a λ-point.

References

Atkins, K. R., and Edwards, M. H., 1955, *Phys. Rev.*, **97,** 1429.
Bridgman, P. W., 1931, *Phys. Rev.*, **38,** 182.
Davies, R. O., and Jones, G. O., 1953, *Adv. in Physics*, **2,** 370.
Kuper, C. G., 1955, *Proc. Camb. Phil. Soc.*, **51,** 243.
Lawson, A. W., 1940, *Phys. Rev.*, **57,** 417.
Simon, F. E., von Simson, C., and Ruhemann, M., 1927, *Zeit. Physik, Chemie* A, **129,** 339.

XLIX. *Saturation Moments and d-Band Configurations in Iron and its Alloys*

By B. R. Coles† and W. R. Bitler
Carnegie Institute of Technology, Pittsburgh, Pa., U.S.A.‡

[Received February 23, 1956, and in revised form April 14, 1956]

Abstract

The saturation magnetic moments of certain iron alloys are difficult to interpret in terms of models found satisfactory for nickel alloys. It has been suggested that in pure iron the total number of empty d-band states is appreciably greater than the number of unpaired spins calculated from the saturation moment. The saturation moments of some iron–cobalt–aluminium alloys have therefore been measured and the effect of aluminium on the moments of iron–cobalt alloys is compared with its effect on the moment of pure iron. It is concluded that in iron the number of empty d-states exceeds the number of unpaired spins; the latter quantity is 2·22 per atom, while the value suggested for the former is greater than 3 per atom. The details of the effects found in the ternary alloys are discussed in terms of the d-band shape.

§ 1. Introduction

It is well known that when alloying elements such as copper, zinc, or aluminium are added to nickel the saturation magnetic moment at absolute zero falls as if atoms of the solute element contributed to the band structure of nickel a number of electrons equal to their conventional valency. Quantitative agreement with experiment results if it is assumed that the number of electrons per atom in the 4s-band (n_s) is unaltered and that the electrons entering the empty states in the 3d-band all have spins opposed to those which give rise to the resultant moment in nickel. The latter assumption amounts to identifying the number of unpaired spins per atom (q) with the total number of d-band holes, that is, to assuming a condition of maximum multiplicity to obtain in the d-band (fig. 1(a)).

When aluminium is added to iron, however, the effect on the saturation moment seems at first sight to be one merely of dilution, the moment *per iron atom* being unaffected. It has been suggested (Stoner 1947) that in iron the exchange interaction energy might be such that the separation of the half-bands containing spins parallel to and antiparallel to the resultant moment is insufficient to maintain maximum multiplicity (fig. 1 (b)).

† On leave of absence from Imperial College, London, S.W.7.
‡ Communicated by the Authors.

Empty states would then exist in both half-bands, an alloying element such as aluminium could contribute electrons to both (with little resultant change in the moment per iron atom), and the number of unpaired spins per atom (q) given by the saturation moment at absolute zero would be less than the total number (n_d) of d-band holes.

Fig. 1

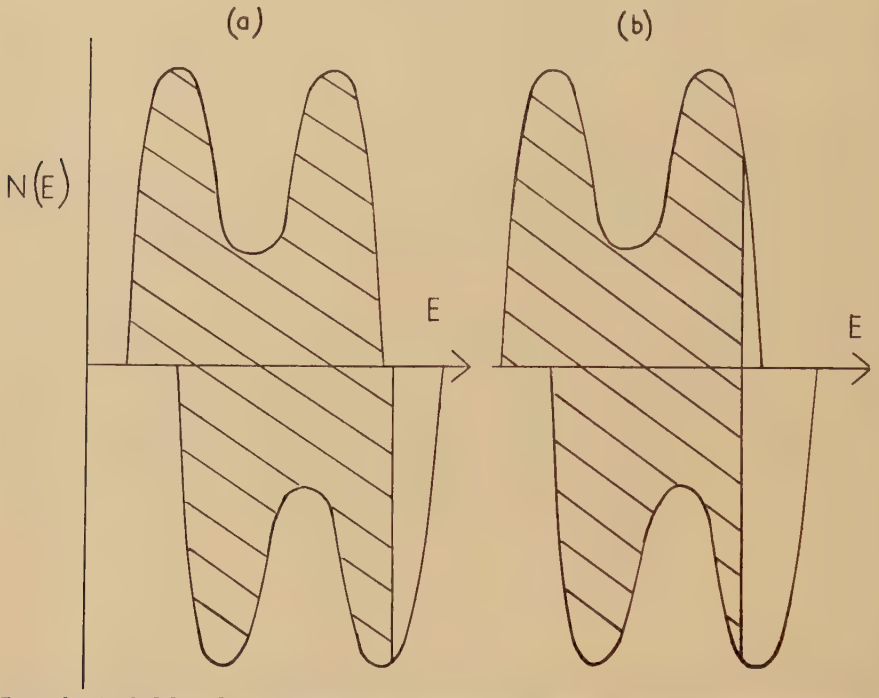

Hypothetical d-band configurations (density of states plotted against energy) for ferromagnetic transition metals ; shading indicates occupied states.
(*a*) Saturation moment q (in Bohr magnetons/atom)=total number of empty states per atom, n_d.
(*b*) $q<n_d$.

The possibility of the ratio (ζ_0) of q to n_d being less than 1·0 has been discussed by Wohlfarth (1949 a) in connection with the nickel–copper alloys which have small interaction energies. This situation may also arise when the interaction energy is large if n_d is large. Additions of cobalt to nickel increase n_d but an examination of magnetic data for this system (Wohlfarth 1949 b) suggests that ζ_0 is unity over the whole composition range. Saturation moment data for face-centred cubic cobalt-copper alloys (Crangle 1955) also indicate that ζ_0 is unity in this modification of cobalt. Additions of iron to cobalt still further increase the value of n_d but an analysis of the type used for the nickel-cobalt alloys is rendered impossible by the change from body-centred cubic to face-centred cubic structures with increase of temperature. It has been suggested, however

(Hume–Rothery and Coles 1954) that the decrease of q with iron content in the iron-rich iron–cobalt alloys indicates a fall of ζ_0 from unity. It was therefore of interest to examine the effect of aluminium on the saturation moments of iron–cobalt alloys, and the results of such an investigation are presented below.

§ 2. Materials, Methods and Results

Five iron–cobalt alloys were chosen as suitable materials to which aluminium additions might be made; these had cobalt contents of approximately 20, 35, 45, 50 and 60 atomic percent cobalt. Pairs of iron–cobalt–aluminium alloys were then prepared, each pair having an iron/cobalt ratio corresponding to one of the above compositions; one of each pair contained about 5 atomic percent of aluminium and the other about 9%. The three pure metals used for the preparation of the alloys were of a purity greater than 99·9%, and weighed quantities of them were melted together under argon in a high-frequency induction furnace. Homogenizing heat treatments of the ingots were carried out at about 1350°C. The alloys were all too brittle for hot-forging to be possible, one of the ingots shattering in preliminary attempts. Small cylindrical specimens (about 8 mm long and 4 mm in diameter) were therefore machined from the ingots, and these were subjected to further homogenization followed by a short annealing treatment in the body-centred cubic phase field above the ordering temperature of the binary iron–cobalt alloys. Microscopical examination of the specimens showed them to be single-phase after the above treatment. (The phase constitution of the ternary Fe–Co–Al system has been examined by Köster (1933) and

Nominal Atomic Ratio Co/(Fe+Co)	Analytical Results				Saturation Moments	
	Wt % Fe	Wt % Al	Atomic Ratio Co/(Fe+Co)	Atomic Fraction x of Al	Bohr Magnetons per Atom q	Bohr Magnetons per transition metal atom $q/(1-x)$
0·198	77·0	3·05	0·198	0	2·41	2·41†
	75·9	4·70	0·197	0·0616	2·24	2·39
				0·0936	2·12	2·34
0·346	62·0	3·15	0·346	0	2·44	2·44†
				0·0638	2·23	2·38
0·441	53·0	2·85	0·442	0	2·43	2·43†
	52·1	4·80	0·441	0·0585	2·22	2·36
				0·0961	2·09	2·31
0·520	44·9	2·70	0·525	0	2·39	2·39†
	45·2	4·25	0·515	0·0551	2·23	2·36
				0·0864	2·08	2·28
0·610	36·8	2·35	0·610	0	2·30	2·30†
	36·0	4·10	0·611	0·0483	2·14	2·25
				0·0837	2·00	2·18

† From the data of Weiss and Forrer (1929)

Edwards (1941).) Compositions obtained by chemical analysis of the actual specimens are shown in the Table, together with the atomic fraction x of aluminium and the cobalt content expressed as the atomic fraction of the combined iron and cobalt contents; this figure is the atomic fraction of cobalt in the binary iron–cobalt alloy to which the aluminium additions have effectively been made.

Fig. 2

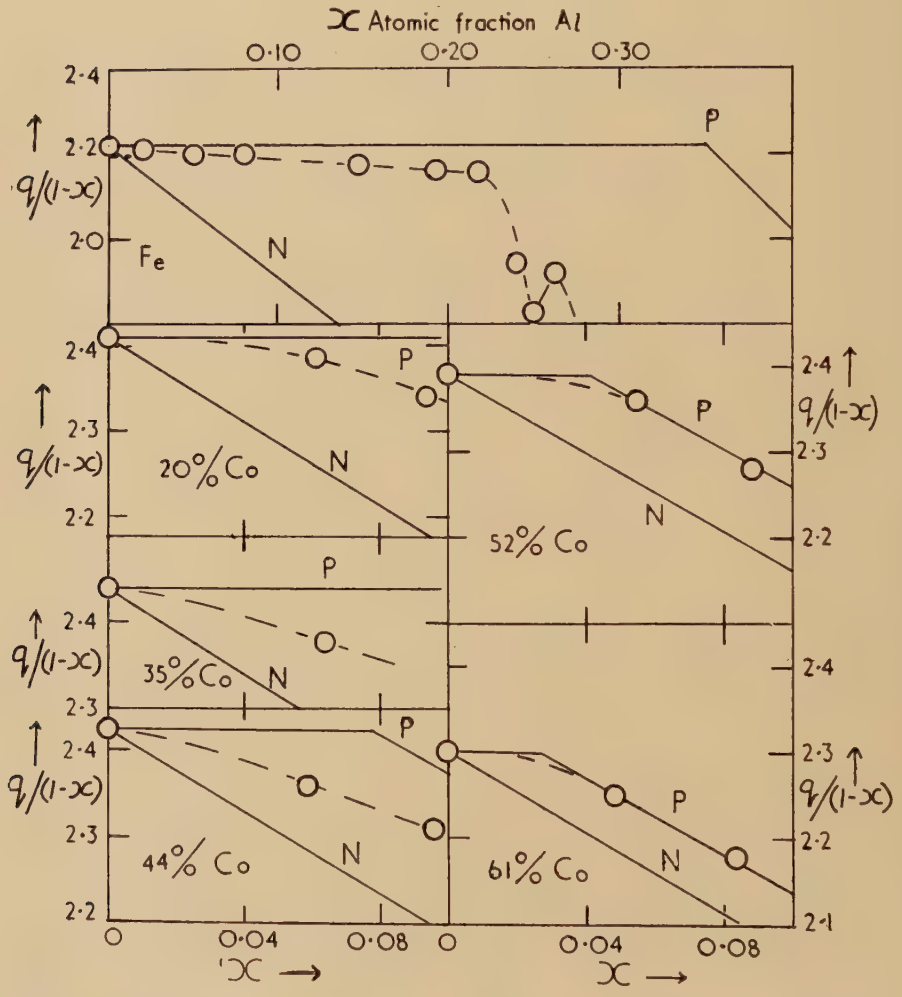

The effect of aluminium additions on the saturation moments of iron and binary iron–cobalt alloys; x is the atomic fraction of aluminium, and $q/(1-x)$ the saturation moment in Bohr magnetons per transition metal atom. The atomic percentage of cobalt in the binary alloy is indicated for each series of ternary alloys. The data for the iron–aluminium series are those of Fallot (1936) and Sucksmith (1933).

The saturation moment measurements were made at room temperature by a simple force method, the sample being suspended in that region of the pole-gap of an A. D. Little magnet where the field gradient is large and uniform over a vertical distance of about 0·5 cm. All measurements were made relative to a specimen of highly pure Armco iron for which the saturation moment was accurately known.† Specimens could be exchanged without any displacement of the balance and suspension, so that there was negligible uncertainty in the reproducibility of the specimen position. Fields of up to 15 000 oersteds were employed and no variation of magnetization with field was detected for fields of more than 7000 oersteds. All the alloys have Curie temperatures slightly higher than pure iron (Köster 1933) and only a very small error was introduced by assuming that the saturation intensities at room temperature bear the same ratio to those at absolute zero as does that of pure iron. If the same reduced magnetization against temperature curve applies to both iron and the alloys the ratio of the room temperature moment to that at absolute zero is 0·981 for pure iron and 0·987 for the alloys. From the measured saturation moments per gram and the known compositions values were derived for the saturation moment in Bohr magnetons per atom q and for the moment expressed as Bohr magnetons per transition metal atom $q/(1-x)$; these values are given in the table and values of $q/(1-x)$ are plotted against the aluminium content in fig. 2.

§ 3. Discussion

In the earlier stages of the following discussion it is assumed that the general form of the 3d-band of the body-centred cubic iron–cobalt alloys is little affected by variations of the iron/cobalt ratio or by small additions of aluminium, the main effect of compositional changes being to vary the number of occupied states in this band. The slight changes to be expected in the total d-band width and in the relative positions of the d-and 3-bands do not affect the arguments of §§ 3.1 and 3.2 and are shown in § 3.3 to be compatible with the model proposed. Discussion of the effects of variation of the exchange energy is also postponed to § 3.3.

3.1. *Saturation Moments and Total Numbers of d-Band Holes*

When copper is added to nickel one may regard the band system of the resulting alloy (overlapping 3d- and 4s-bands) as a property of the alloy as a whole, the effect of the extra electron possessed by each copper atom being to increase the number of occupied states. Since the density of states in the d-band is very much greater than that in the s-band nearly all the added electrons will occupy states in the former. When aluminium is added to nickel the behaviour of the saturation moment suggests that each aluminium atom contributes 3 electrons to the band structure, but it does not here seem justified to associate the d-states with the solute

† Its value was within 0·2% of that given for iron by Weiss and Forrer (1929) in their study of the iron–cobalt alloys.

atoms. The most appropriate method of indicating the d-band configuration in such an alloy of a transition metal with a non-transition metal would therefore seem to be in terms of the number of unoccupied d-states *per transition metal atom*, and this quantity will be given (if one ignores changes in n_s, the number of s-band electrons per atom) by the expression

$$[n_d(1-x)-x(v-n_s)]/(1-x),$$

where n_d is the number of empty states per atom in the d-band of the pure transition metal, x the atomic fraction of the non-transition metal, and v its conventional valency. This expression will also be appropriate when additions of a non-transition metal are made to a binary alloy of two transition metals, n_d and n_s then referring to the binary alloy.

As mentioned in §1, the above expression describes the behaviour of the saturation moments of many nickel alloys very well if it is assumed that q, the saturation moment in Bohr magnetons per atom is equal to the total number of d-band holes. This assumption (that there are no paired holes) does not give a satisfactory description of the behaviour of iron alloys, as is clearly shown by fig. 2 where the curves marked N show the values given by it for $q/(1-x)$, the saturation moment in Bohr magnetons per transition metal atom. Additions of aluminium to pure iron produce only a very small change in $q/(1-x)$, and if the tentative interpretation of §1 (that involving a band configuration of the type shown in fig. 1(*b*)) is correct, electrons contributed by the aluminium atoms would seem to be entering the two half-bands in almost equal numbers. At larger aluminium contents, however, marked changes should be observed when all holes in one half of the d-band have been filled.

In fig. 2 the curves marked P show the behaviour to be expected of $q/(1-x)$ if the values of n_d for the iron–cobalt alloys were those shown in fig. 3, and if electrons contributed by the aluminium entered the two halves of the d-band in equal numbers. (The latter assumption would require the densities of states in the two half-bands to be the same.) The experimental results do not show an initial constancy of $q/(1-x)$ for all cobalt contents, and the densities of states in the two halves of the d-band evidently differ in the alloys. This might have been expected, for on the collective electron treatment a rectangular band is inconsistent with $0<q/n_d<1{\cdot}0$ (Wohlfarth 1951). The final rate of fall of $q/(1-x)$ with increasing x is, however, independent of the band shape, since it is characteristic of aluminium contents sufficient to fill all holes in one half-band, and for the alloys where this region is reached good agreement between theory and experiment can evidently be obtained by using the n_d values given in fig. 3. The corresponding values of n_s and the observed values of q are also shown in this figure. The n_d values were chosen to give agreement with experiment for the effects of aluminium on the 52% and 61% cobalt alloys and to pass through the value of q obtained for pure cobalt by extrapolation from the body-centred cubic alloys. This value (1·80) is only slightly greater than that (1·75) for face-centred cubic

cobalt (Myers and Sucksmith 1951, Crangle 1955), and evidence that q is equal to n_d for that modification of cobalt has been referred to in § 1. The iron-rich portion of the n_d curve is quite uncertain, but a lower limit of 2·9 can be set for the n_d value of pure iron from the aluminium content of iron–aluminium alloys at which $q/(1-x)$ begins to fall sharply (Fallot 1936, Sucksmith 1939). This is, however, only a lower limit, for this fall takes place in the composition range where ordering effects become apparent.

Fig. 3

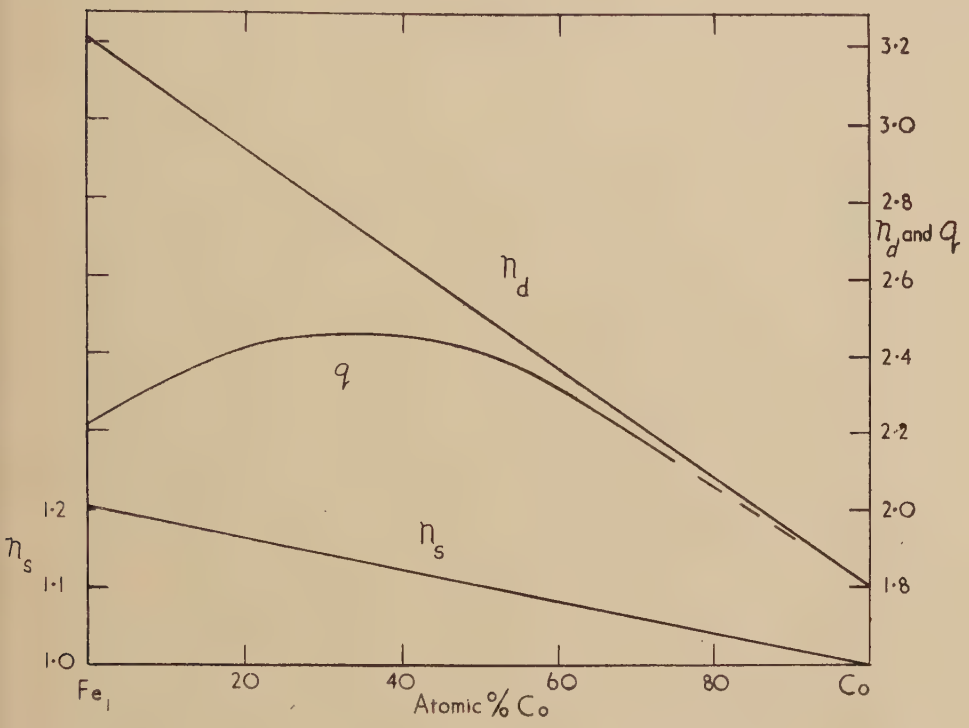

Saturation moments in Bohr magnetons/atom q and postulated numbers per atom n_d and n_s of d-holes and s-electrons in the body-centred iron–cobalt alloys.

3.2. *Band Shapes and Alloying Effects*

Some indication of the relative magnitudes of the densities of states $N(E)$ in the half-bands (p and a) containing electrons with spins parallel and antiparallel to the resultant moment can be obtained from the experimental results for the alloys with 20%, 35%, and 44% cobalt, for these relative magnitudes will govern the $q/(1-x)$ values of alloys with aluminium contents insufficient to bring about filling of the p half-band. For $q/(1-x)$ to be constant in such alloys $Np(E)$ must equal $N_a(E)$; if it is smaller $q/(1-x)$ will fall with increasing x, and if it is larger $q/(1-x)$ will increase. The results for the 20%, 35%, and 44% cobalt alloys

indicate that $N_p(e)$ is less than $N_a(E)$; and this is not surprising, for the p half-band is more nearly full. For the 52% and 61% cobalt alloys the experimental results seem to correspond to aluminium contents sufficient to bring about filling of the p half-band. The simplest band shape which would account for this behaviour is that shown in fig. 4(a), where the Fermi level in the half-bands of pure iron is indicated by F_1, and that in the iron-rich iron–cobalt alloy by F_2. For convenience a single diagram is used here and in fig. 4(b) to represent the configurations at two different

Fig. 4

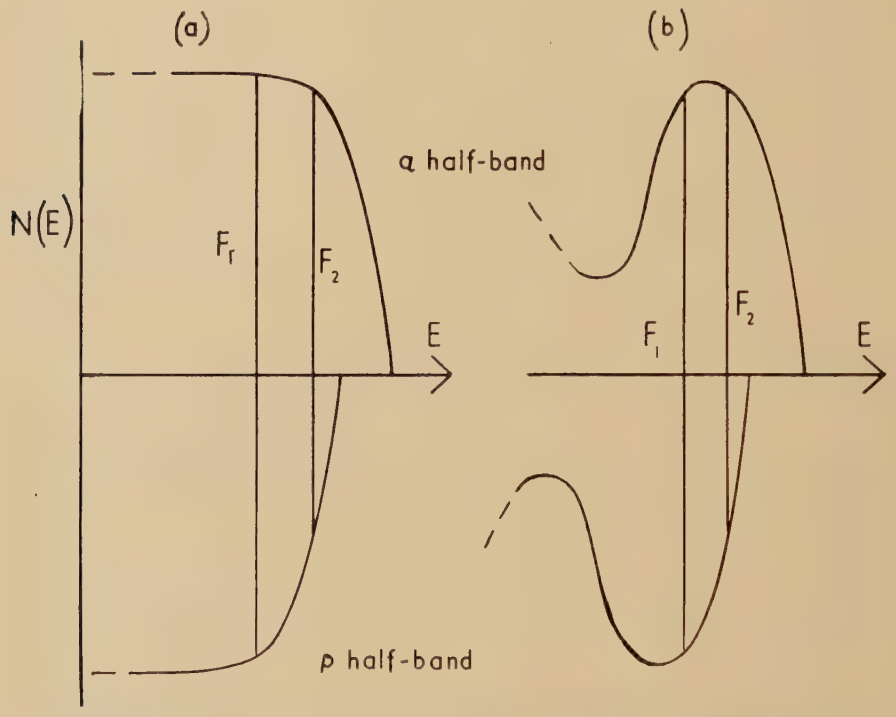

Hypothetical forms for the d-band density of states curve in ferromagnetic alloys. F_1 is the Fermi level in an alloy where $N_a(E)=N_p(E)$ and F_2 that in an alloy where $N_a(E)>N_p(E)$.

compositions. It is not intended to imply that the exchange energy is composition-independent. In view of the indications of a double-peaked d-band structure given by theoretical calculations (Fletcher and Wohlfarth 1951, Slater and Koster 1954, Koster 1955) consideration could also be given to configurations of the type shown in fig. 4 (b). An interesting consequence of the latter configuration is that additions to iron of manganese, which would increase n_d and lower the Fermi level, might produce alloys in which $q/(1-x)$ would rise for initial additions of aluminium.

3.3. *Interaction Energy and Band Widths*

As pointed out by Wohlfarth (1949) in his discussion of the nickel–copper alloys the ratio (ζ_0) of q to n_d can fall below unity when the exchange interaction energy becomes small. The parameter which governs ζ_0 in the collective electron theory of ferromagnetism (Stoner 1947) is the ratio of interaction energy to the energy range of unoccupied states in the d-band. Consideration of the latter quantity shows that a fall of ζ_0 as n_d increases in the iron–cobalt alloys need not be ascribed to any marked fall in the interaction energy. On the basis of a number of general arguments considerable increases in the energy range (ΔE) of unoccupied states are to be expected as the iron-content of iron–cobalt alloys is increased.

(*a*) If no change in the relative positions and breadths of the 3d- and 4s-bands took place between nickel and cobalt and between cobalt and iron n_d would increase by a little less than 1·0 in each step (a fraction of the removed electron coming from the 4s-band) and ΔE would show a marked increase.

(*b*) On general grounds it is to be expected that the overall width of the 3d-band will increase through the series Cu→Ni→Co→Fe→Mn→Cr, and for a given number of d-holes ΔE can be expected to be larger in iron than in nickel.

(*c*) Atomic 3d levels move to higher energy relative to 4s ones along the above series of elements, and corresponding relative movements are to be expected in the metallic state. Such movements would lead to increases in n_d of more than 1·0 holes per atom in the steps from nickel to cobalt and from cobalt to iron, and more rapid increases in ΔE than suggested by (*a*); and the n_d values of 0·6 for nickel and 1·75 for face-centred cobalt show the expected trend. (The postulated values of 1·8 and ~3·2 for body-centred cubic cobalt and iron are in accord with such movements.)

(*d*) If the double-peaked structure for the d-band shown by calculations is correct, increases in n_d will produce larger increases in ΔE when n_d is ~2·0 than when n_d is ~0·6, for the Fermi level for $n_d=2{\cdot}0$ is likely to lie at a region of the *a* half-band where the density of states is smaller than for $n_d=0{\cdot}6$. It is significant that the electronic specific heat coefficient of iron is somewhat less than that for nickel, in spite of the contribution made in the former metal (if the present model is correct) by the *p* half-band.

The above arguments have been brought forward to show that, for a given exchange energy, ζ_0 values of less than unity become more probable as the iron content increases. Such values are still more probable if the exchange energy decreases with an increase of the iron content, and the behaviour of the Curie temperature is in accord with a variation of that type.

Acknowledgments

The authors' thanks are due to many colleagues whose assistance contributed to the work described above ; in particular to Dr. J. E. Goldman and Dr. A. Arrott for much stimulating discussion, and to Dr. M. Simnad and the staff of the Metals Research Laboratory for placing metallurgical facilities at their disposal. Grateful acknowledgment for financial support is made to the U.S. International Cooperation Administration, the U.S. Office of Naval Research, and the U.S. Army Signal Corps.

References

Crangle, J., 1955, *Phil. Mag.*, **46**, 499.
Edwards, O. S., 1941, *J. Inst. Met.*, **67**, 67.
Fallot, M., 1936, *Ann. Phys., Paris*, **6**, 305.
Fletcher, G. C., and Wohlfarth, E. P., 1951, *Phil. Mag.*, **42**, 106.
Hume-Rothery, W., and Coles, B. R., 1954, *Advances in Physics*, **3**, 149.
Koster, G. F., 1955, *Phys. Rev.*, **98**, 901.
Köster, W., 1933, *Arch. Eisenhuttenwesen*, **7**, 263.
Myers, H. P., and Sucksmith, W., 1951, *Proc. Roy. Soc.* A, **207**, 427.
Slater, J. C., and Koster, G. F., 1954, *Phys. Rev.*, **94**, 1498.
Stoner, E. C., 1947, *Rep. Progr. Phys.*, **11**, 43.
Sucksmith, W., 1939, *Proc. Roy. Soc.* A, **171**, 525.
Weiss, P., and Forrer, R., 1929, *Ann. Phys., Paris*, **12**, 279.
Wohlfarth, E. P., 1949 a, *Proc. Roy. Soc.* A, **195**, 434; 1949 b, *Phil. Mag.*, **40**, 1095 ; 1951, *Ibid.*, 42, 374.

L. REVIEWS OF BOOKS

Vistas in Astronomy. Volume I. Edited by A. Beer. (London : Pergamon Press.) [Pp. xvi+776.] Price £9 9*s*.

The two volumes of *Vistas* are dedicated to F. J. M. Stratton in honour of his seventieth birthday. The exertions of the Editor and originator of the scheme have brought together contributions from over two hundred astronomers, geophysicists, physicists and mathematicians to produce "a generous and thorough cross-section through the whole of contemporary astronomy and allied sciences". The first volume ranges from matters concerning international organization in astronomy to radio astronomy and solar physics. The contributions vary from autobiographical records to announcements of new discoveries and reviews of particular branches of astronomy. The result is a book possessing a wholly individual character of remarkable vitality. It will be read and treasured long after more orthodox handbooks have served their day, so keeping alive the memory of one whose influence has so widely pervaded the work of his own times. The Editor and Publishers deserve admiring congratulations for a great undertaking carried through to complete success.

W. H. McC.

Numerical Analysis with emphasis on the application of numerical techniques to problems of infinitesimal calculus in single variable. By Z. Kopal. (Chapman and Hall.) [Pp. xiv+556.] Price 63*s*.

The scope of this book is described more exactly by the full title than by the short title "Numerical Analysis", since such topics as the solution of problems in linear algebra and the numerical solution of partial differential equations are not included. The book is a written version of a course of lectures given to students at the Massachusetts Institute of Technology, and the author has preserved his rhetorical questions and other lecture room mannerisms. This accounts for the great and, indeed, somewhat excessive length of the book. It also accounts, however, for the book's most distinguishing virtue, namely that the material is presented with a lively and stimulating commentary. Thus, although the treatment of particular formulae and methods is less concise than in ordinary books on numerical analysis, it is also less superficial. Any practitioner in numerical analysis, on dipping into the book, is likely to find something which will set him thinking, whether it be to extend, to amplify, or perhaps in some cases to refute what Dr. Kopal has said. Of particular value are the bibliographical notes at the ends of the chapters which contain critical reviews of the literature. Coming at a time when the development of automatic digital computers has called into question much of what was fast becoming established doctrine among numerical analysists trained in desk computing techniques, this book will form a valuable addition to the available literature.

M. V. W.

Introduction to Modern Physics. 5th Edition. By F. K. Richtmyer, E. H. Kennard and T. Lauritsen. (New York : McGraw-Hill.) [Pp. xv+666.] Price 56*s*. 6*d*.

A fifth edition of the well-known text book by Richtmyer and Kennard is very welcome. Professor Richtmyer died in 1939 and Professor Lauritsen has joined Professor Kennard in preparing this revised edition. The book has been brought up to date by including an account of the newly discovered phenomena of high energy physics, while the chapters on X-rays and physics of solids have been somewhat cut down.

Solid State Physics. Advances in Research and Applications. Volume 1. Edited by Frederick Seitz and David Turnbull. [Pp. xii+469.] (New York: Academic Press Inc.) Price $10.00.

It is planned to publish two of these review volumes each year until the subject is adequately surveyed and then to publish annually. The present volume, the first of the series, contains the following articles.

Methods of the One-Electron Theory of Solids by J. R. Reitz; Qualitative Analysis of the Cohesion in Metals by E. P. Wigner; The Quantum Defect Method by F. S. Ham; The Theory of Order–Disorder Transitions in Alloys by T. Muto and Y. Takagi; Valence Semiconductors, Germanium and Silicon by H. Y. Fan; and Electron Interaction in Metals by D. Pines.

There is no doubt that the volume will be very useful indeed, covering as it does the important recent advances in the electron theory of solids and much of the work both experimental and theoretical on the semi-conducting properties of silicon and germanium. It is intended that later volumes will pay more attention to the experimental and technical aspects of the subject than this one does.

It remains to ask, what is 'Solid State Physics'? Not, one gathers from the Introduction, crystallography or metallurgy, yet it includes the study of defects in crystal structures and the theoretical study of the binding forces in metals. Certainly a large part of the subject is concerned with conduction in solids. Perhaps it is best to define the subject by naming some of the people who work in it and who so describe their work, physicists who investigate the properties of solids without wishing to bind themselves to the narrower disciplines of metallurgy and crystallography. N. F.M.

BOOK NOTICES

Topological Transformation Groups. By D. Montgomery and L. Zippin. (New York and London: Interscience Publishers.) [Pp. xii+282.] Price $5.50.

The Number-System. By H. A. Thurston. (London and Glasgow: Blackie & Son Limited.) [Pp. viii+134.] Price 30*s.*

Hydrodynamic Stability. By C. C. Lin. (Cambridge: University Press.) [Pp. xi+155.] Price 22*s.* 6*d.*

La Teoria Fisica. By A. M. Dell'Oro. (Padua: Cedam.) [Pp. viii+155.] Price not stated.

Ludwig Boltzmann. By Engelbert Broda. (Vienna: Franz Deuticke.) [Pp. viii+152.] Price (cardboard bound) DM. 9.50, (clothbound) DM. 11.

[The Editors do not hold themselves responsible for the views expressed by their correspondents.]

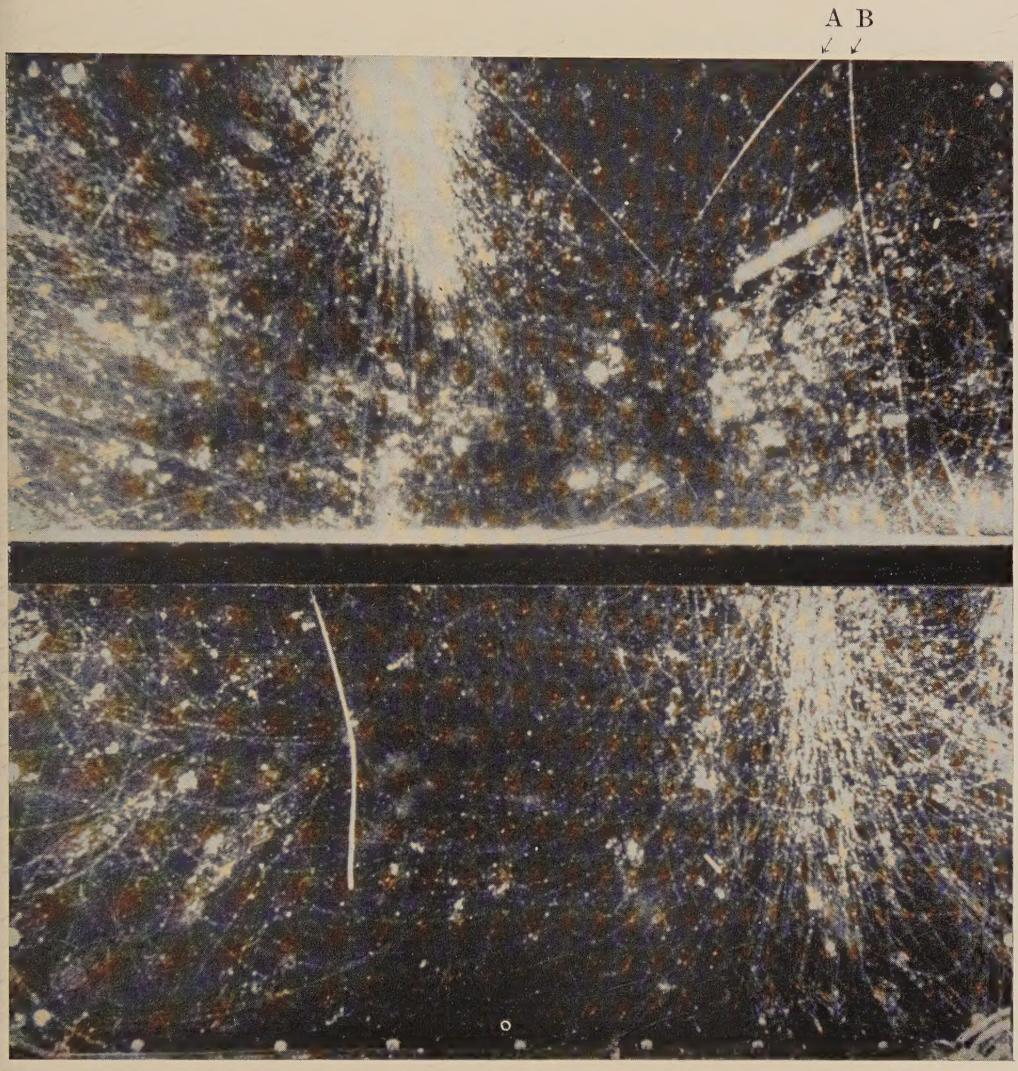

Event SQ 1437. The two tracks marked A and B apparently diverge from a common origin in the lead above the cloud chamber. If this interpretation is correct, both tracks are due to negatively charged particles of mass greater than $700\,m_e$. The measurements made on the tracks are given in the table.

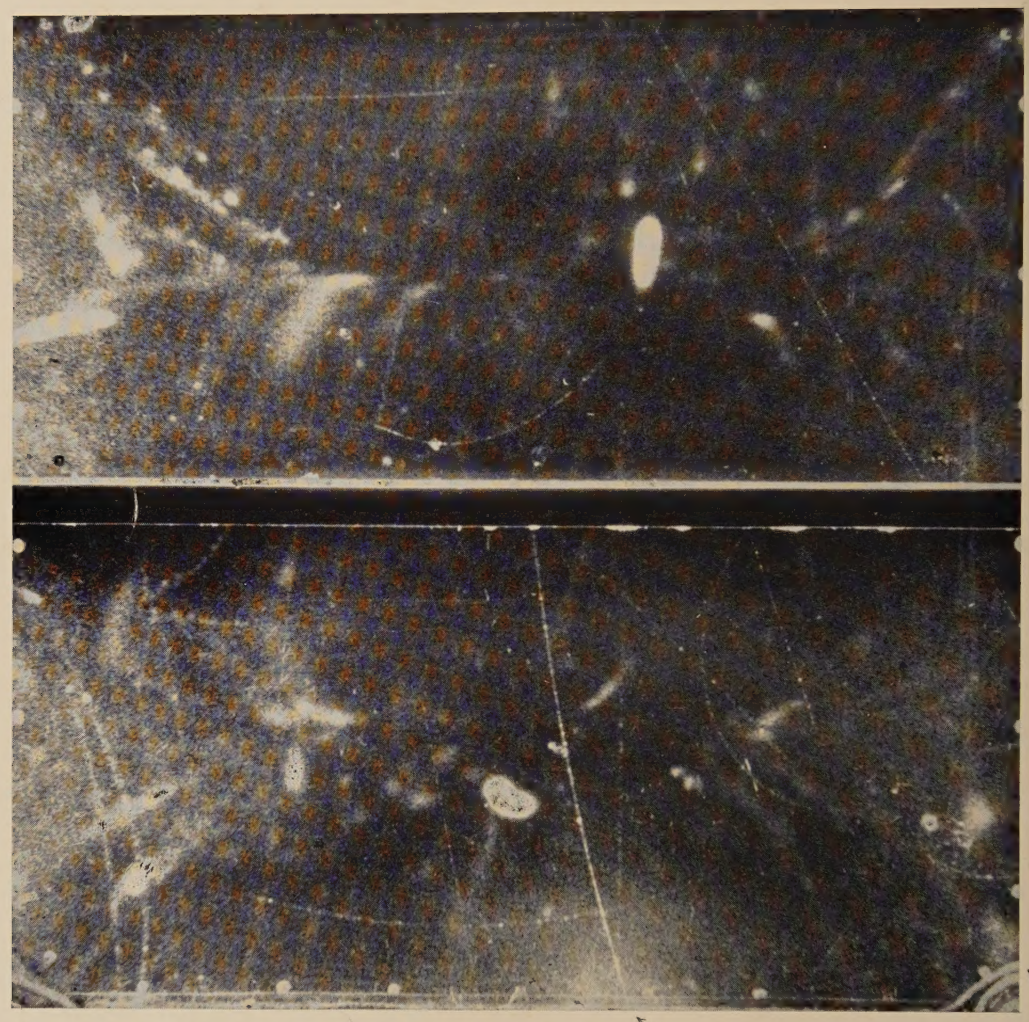

Event SF 992. The two tracks indicated by arrows intersect in the copper plate across the middle of the cloud chamber. The near-vertical, dense track has a curvature corresponding to a momentum of 204 ± 14 MEV/c and its ionization density is estimated to be between $5I_0$ and $8I_0$. From these figures the mass of the particle responsible is between $920\,m_e$ and $1450\,m_e$. The event is interpreted as an upward-moving, positive K-meson which is brought to rest in the plate and decays there. The secondary particle has a momentum of 154 ± 20 MEV/c.